AQUAEXCEL

Aquaculture Infrastructures for Excellence in European Fish Research

Project number: 262336

Combination of CP & CSA
Seventh Framework Programme
Capacities

Deliverable 7.4

Set of methodologies for performance phenotyping in trout, salmon and sea bream

Due date of deliverable: M48

Actual submission date: M48

Start date of the project: March 1st, 2011 **Duration**: 48 months

Organisation name of lead contractor: CSIC

Revision: V2

Project co-funded by the European Commission within the Seventh Framework Programme (2007-2013)	
Dissemination Level	
PU Public	**X**
PP Restricted to other programme participants (including the Commission Services)	
RE Restricted to a group specified by the consortium (including the Commission Services)	
CO Confidential, only for members of the consortium (including the Commission Services)	

Table of contents

Glossary

AQUAEXCEL: Aquaculture Infrastructures for Excellence in European Fish Research

Allostasic load = the process that maintains stability through change of a number of stress mediators, including hormones (e.g. cortisol, catecholamines, pituitary hormones, insulin), immune factors and heat shock proteins.

Apparent availability coefficient (AAC, %) = 100 - (100 x ((% mineral in faeces)/(% mineral in diet) x (% marker in diet)/(% marker in faeces))).

Daily growth index (DGI) = 100*(FBW^1/3 - IBW^1/3)/duration (days)

DM = dry matter (g)

Essential fatty acids (EFA): are those fatty acids that animals must ingest because they cannot synthesize them. They are required for essential biological processes, but do not include the fats that only act as a source of energy. Fish EFA requirements are different from those of mammals, and there are also differences between cold and warm water fish.

Feed efficiency (FE) = wet weight gain (g)/ dry feed intake (g)

Feed intake (FI): DM (g) / fish

Hepatosomatic index (HI) = (100 x liver weight) / fish weight

Mesenteric index (MI) = (100 x mesenteric fat weight) / fish weight

Nutrigenomics: a science that studies the influence of food or food constituents on the transcriptome. In nutrigenomics, nutrients are considered as signals through which cells interpret information about the environment (diet) and respond, according to their necessity, by modifying their metabolic pathways through regulation of gene and protein expression.

Specific growth rate (SGR) = 100 x (ln final body weight - ln initial body weight) / days

Viscerosomatic index (VI) = (100 x viscera weight) / fish weight

Weight gain (WG) (g) = is the increase in body weight after a nutritional trial.

Summary

Objectives: to obtain relevant methods for phenotyping performance of three important farmed fish species (Gilthead sea bream = GSB, Atlantic Salmon = AS, Rainbow trout = RT) exposed to challenging feeding regimes.
Rationale: we have integrated the data coming from nutrigenomics with other biometrical, metabolic and endocrinological data. The experimental trials have concentrated on the effects of the possible nutritional stress derived from including plant ingredients. The effects of vegetable proteins (AS, RT) and/or oils (GSB, RT), protein restriction (GSB, RT), essential amino acids (GSB, RT), minerals (GSB, RT), vitamins, essential fatty acids, phospholipids and phosphorous (GSB) have been studied.
Teams involved: CSIC, INRA, IMR, and UoS
Task: 7.1.3
Geographical areas covered: all Europe

The aim of the current deliverable is to provide methods for phenotyping fish performance under nutritional stress in three teleostean species, gilthead sea bream, Atlantic salmon and rainbow trout. Different experimental models of nutritional stress were used in all experiments using focused candidate genes, focused PCR-arrays and microarray approaches. The data from nutrigenomics has been integrated with other biometrical, physiological and endocrinological parameters to determine "dietary signatures" that characterize each nutritional stressor. In **GSB** three nutritional stressors were applied: high vegetable oil inclusion level (66 VO) (trial 1), fasting (trial 2), and nutrient deficiencies in sulphur amino acids, essential fatty acids, phospholipids, phosphorus, minerals and vitamins (trial 3). The response was studied at the performance, biochemical and molecular level using focused stress-lipid PCR-array (31 genes), OXPHOS PCR-array (88 genes) or focused growth PCR-array (89 genes) in different tissues depending on the trial (liver, heart and/or, muscle). In **AS**, the nutritional stressor was long exposure to high levels of dietary plant-based ingredients (soybean meal, SBM), aiming at immunological and metabolic gene expression changes in liver and intestine using an oligomicroarray. In **RT**, the nutritional challenges consisted of total fish meal replacement with a focus on amino acids and trace minerals, using candidate genes. We aimed at phenotyping effects of dietary changes with brain molecular markers of feed intake (trial 1) and liver/intestine molecular markers of iron homeostasis (trial 2).

In **GSB** trial 1, we showed that the response to confinement stress was highly mediated by the nutritional background, as the rise in plasma cortisol and glucose levels was higher in stressed fish of group 66VO (66VO-S) than in FO group (FO-S), but the former stressed group regained more quickly the cortisol resting values. The molecular study showed that the cell-tissue repair response represented by derlin-1, 75 kDa glucose-regulated protein and 170 kDa glucose-regulated protein was triggered at a lower level in 66VO-S than in FO-S fish. This occurred in concert with a long-lasting up-regulation of glucocorticoid receptors, antioxidant enzymes, enzyme subunits of the mitochondrial respiratory chain, and enzymes involved in tissue fatty acid uptake and β-oxidation. This gene expression pattern allows a metabolic phenotype that is prone to "high power" mitochondria, which would support the replacement of fish oil with vegetables oils, when theoretical requirements in essential fatty acids for normal growth are met by diet.

In trial 2, the analysis of the OXPHOS PCR-array showed that most of the genes were highly regulated by nutrient deprivation in the liver tissue, whereas a moderate or low response was found for the glycolytic skeletal muscle and the highly oxidative cardiac muscle. The direction of the change was also tissue-specific, according to the different metabolic capabilities of liver and muscle tissues. These findings contribute to refining the list of candidate genes for phenotyping any metabolic disturbance in GSB.

In trial 3, the analysis of the growth-chip showed the existence of molecular signatures for nutrient deficiencies, which are tissue-specific. Thus, skeletal muscle seems to

be especially sensitive to deficiencies in vitamins, whereas liver is to deficiencies in EFA and phosphorous.
In **AS**, dietary SBM caused a loss of performance above inclusion levels of 200 g kg^{-1}. Thus the transcriptome study was done only in AS fed 300 g kg^{-1} SBM. The transcriptomic snapshot after 12 weeks showed a higher effect at the local level (distal intestine) than at the liver. The observed response was due to the induced inflammation of the distal intestine and the consequent immune response, which involved the up-regulation of tumour necrosis factor (TNF), MAPK, NF-kB, T cell receptor, NOD-like receptor, apoptosis and cytosolic DNA sensing pathways. In the liver, some innate immune factors were also regulated, such as the complement cascade. The up-regulation of the MASP1 genes suggested that activation of the complement pathway possibly occurred through the lectin pathway which is activated through recognition of patterns of carbohydrate or glycoprotein. By contrast, CD59 decreased suggesting inhibition of the formation of the membrane attack complex which is formed as a result of the complement cascade. At the metabolic level, processes and systems of the organisms such as digestion and absorption of nutrients (vitamins, minerals, proteins and fat) were also significantly affected. In the distal intestine a down-regulation of virtually all pathways from these specific categories (including genes involved in lipid digestion and absorption, primary bile acid biosynthesis and secretion) was observed. Genes involved in digestion and absorption of proteins as well as several pathways of amino acid metabolism were differentially expressed in liver and intestine. The pathways altered in the liver involved aspartate, glutamate, alanine, serine, cysteine, glycine and threonine, non-essential amino-acids, and the complement and coagulation cascades. In addition, in the distal intestine there was a down-regulation of cellular processes such as the lysosome, peroxisome and to a lesser extent the phagosome. On the contrary, all pathways involved in the processing of genetic information and protein synthesis were significantly up-regulated which, together with a number of other pathways such as those regulating cell cycle, pyrimidine metabolism, etc., suggests possible regeneration and proliferation of the damaged tissue.

In **RT** trial 1, the PCR analysis of the brain showed that an imbalance in methionine and / or proteins induced a nutritional stress causing the activation of GCN2/ATF4-signaling pathway, as indicated by the up-regulation of the ATF4 gene. The gene expression of the anorectic neuropeptide CCK was stimulated, which would allow the fish to decrease feed intake and hence to avoid an imbalanced nutritional status harmful for its survival. In trial 2, the PCR analysis of liver and intestine, shows that regulation of Fe absorption and metabolism in RT depends on the dietary ingredient composition (fish- versus plant-ingredient based diets) and on the inclusion of mineral premix. It is suggested that the disturbances in Fe metabolism are secondary effects of hepato-biliary dysfunction in relation to cholesterol and bile metabolism when fed plant-ingredient based diets. Relevant molecular markers for revealing and studying such dietary interactions on the regulation of Fe homeostasis are ferroportin1 and hepcidin in intestine and liver, respectively.

In conclusion these results provide: a) a platform for the identification of candidate genes for molecular phenotyping and b) molecular signatures to which other future nutrigenomic studies might refer to.

1. Introduction

Aquaculture is playing a major role in the global food security program producing approximately fifty percent of the world seafood supply (World Bank, 2013). In an effort to provide the growing population with a consistent supply of high-quality and sustainable seafood, alternative sources of protein to the traditionally used fishmeal (FM) are extremely sought after, particularly for industries involved in farming carnivorous fish species such as Atlantic salmon (*Salmo salar*) or gilthead sea bream (*Sparus aurata*). Over the last two decades, a significant research investment has been made to identify alternative sources of proteins and lipids that could fulfil the requirement of fish, provide a competitive growth rate and good flesh properties and avoid a negative impact on fish welfare. Thus far, vegetable ingredients are the most attractive alternative mainly due to an unrivalled market price and availability. Plant products such as soybean, pea and other legumes, wheat and corn gluten are either already established in commercial feed manufacturing protocols or are proven to be a viable alternative to FM (Gatlin *et al.*, 2007).

Plant products, however, contain chemical substances known as anti-nutritional factors (ANFs), endogenously produced by the plant with different functions including structural, storage or as a defence mechanism (reviewed by Francis *et al.*, 2001;Gatlin *et al.*, 2007; and Krogdahl *et al.*, 2010). Fish are not accustomed to metabolize ANFs and when present in their diet can cause a number of effects primarily associated with the digestive physiology, health and metabolism, ultimately resulting in reduced productivity and impact on fish welfare. In addition, some ANFs can have important health consequences primarily affecting the intestinal mucosa, causing inflammation and increasing the permeability to pathogens and other unwanted substances. Plant ingredients might also lack some nutrients, like the hemes, iron containing heterocyclic molecules which are essential for the function of all aerobic cells. Hemes are expressed ubiquitously in all tissues, serve as the prosthetic group of numerous hemoproteins (eg, hemoglobin, myoglobin, cytochromes, guanylate cyclase, and nitric oxide synthase) and play an important role in controlling protein synthesis, cell differentiation and immune response (Dutra and Bozza, 2014). Finally, the replacement of fish oils by plant derived oils involves changes in the profile of quantitative essential fatty acid (EFA) and phospholipids (PL) and in the ratio of n-3/n-6 HUFA, and this may affect fish health status and resistance to diseases (Oliva-Teles, 2012).

The determination of **nutrient requirements** for a growing number of species is still important, especially when new ways (greater diversity of feedstuffs) to meet these requirements are involved. It follows that the nutritional profile of raw materials as determined by traditional analytical methods, it does not necessarily reflect the value available to the animal for absorption and utilization, but it varies depending on the presence and abundance of ANFs, the interactions of the different nutrients and the particular physiology and rearing conditions of each fish species. At the same time, new methodologies to have true estimates of these requirements, not only based on growth performance, are required. Semipurified and purified diets have started to be utilized to estimate the nutrient requirements of fish, and this has been the approach in this deliverable for GSB. The targeted nutrients have been sulphur amino acids (SAA), EFA (n3 LC-PUFA), PL, phosphorus (P), minerals (Min) and vitamins (Vit). Fish have a requirement for a well-balanced mixture of essential and nonessential **amino acids**. Methionine and cysteine are SAA. Methionine has been the nutrient target for RT for the current study. Adequate amounts of both methionine and cysteine are needed for proper protein synthesis and other physiological functions of the fish. Cysteine is considered dispensable because it can be synthesized by the fish from the indispensable amino acid methionine. When methionine is fed without cysteine, a portion of the methionine is used for protein synthesis, and a portion is converted to cysteine for incorporation into protein. If cysteine is included in the diet, it reduces the amount of dietary methionine needed. It appears that most fish have a SAA requirement value of about 2 to 3%

of protein, whereas catla, chinook salmon, and GSB appear to require higher levels of methionine. When fed a diet deficient in an essential AA fish mostly decrease feed intake (National Research Council, 2011). Mechanisms involved in the reduced feed intake and the central sensing of an essential AA imbalance in fish brain remain unknown. This topic is however considered important taking into account the necessity to replace the fish meal by plant protein with a very different profile in some essential AA such as methionine

Dietary **lipids** have to meet gross lipid requirement in terms of energy provision and qualitative and quantitative essential fatty acid (EFA) requirements. All vertebrate species have absolute dietary requirements for certain PUFA. If a dietary deficiency occurs, the animal stops growing and reproducing, develops various pathologies, and eventually dies (Sargent *et al.*, 2002). The PUFA include members of both the n-6 and the n-3 series typified by linoleic acid, 18:2n-6, and α-linolenic acid, 18:3n-3.

All forms of aquatic animals require inorganic elements or **minerals** for their normal life processes, including formation of skeletal structure, maintenance of colloidal systems, and regulation of acid–base equilibrium. They are also important components of hormones, enzymes, and activators of enzymes. However, the information available on uptake, function, and biological availability of many trace elements in fish is fragmentary and incomplete. Many of them are required in such small quantities that it is difficult to formulate diets to demonstrate a mineral deficiency and to formulate purified diets low in mineral and to maintain water sufficiently free of the test element. The most commonly used measure of nutritional status is the level of trace element in the blood, muscle, liver, and bone. However, those tests that include metabolic function of the element rather than a tissue analysis are more desirable. For many elements such functional tests are not clearly established. Elucidation of techniques that will allow for the identification of subclinical, pathological change in the assessment of nutritional status remains a challenging area for mineral nutrition research (Lall, 2002).

Fish, like all other animals, need a certain amount of **vitamins** for optimal growth and proper health. Recommendations for vitamin requirements must be seen in relation to factors like species, life stage, overall feed composition and farming conditions (Waagbø, 2008). Vitamin requirement data are only available for a limited number of fish species and for a limited number of vitamins. Although vitamin deficiencies are easy to avoid in practical fish diets, they are among the commonest deficiencies observed in commercial aquaculture (Hardy, 2001). In practice, diets are rarely deficient in only one specific micronutrient, and usually the clinical signs and histopathological features are not particularly specific (Roberts, 2002). Deficiencies may result, among other factors, from incorrect dietary supplementation or antagonistic interactions with other dietary compounds. Vitamins are prone to be lost because of exposure to adverse environmental conditions such as high moisture, temperature or light, and water-soluble vitamins may also be lost through leaching in water (Oliva-Teles, 2012). In addition, the use of some plant derived oils instead of fish oils has introduced changes in the content of some vitamins (see Krossøy *et al.*, 2011). It is necessary to define more precisely dietary requirements for vitamins and thus far it has been mostly performed on the basis of each vitamin. However, it has become clear that it is necessary to have a more integrated approach with multiple variables, especially when considering that different vitamins show interactions with each other.

In this scenario, understanding how fish respond to the different nutritional interventions that are being used or probably will be incorporated into the aquaculture industry in the future and how fish utilize different dietary ingredients has been a central topic of research in recent years. When testing these ingredients, a macroscopic physiological response might not necessarily be measurable in experimental setups, however cumulative adverse effects might appear overtime and pathologies or other detrimental physiological conditions might accentuate under long-term or more challenging commercial conditions (Krogdahl *et al.*, 2010). Therefore, it is critical to have sensitive tools able to detect subtle physiological changes and help predict long-term detrimental effects that might decrease fish performance. Among the different methodologies for phenotyping fish performance, this deliverable has focused on **nutrigenomics**, as it can provide a mean to interpret how dietary

ingredients are perceived by fish at tissue level (Muller and Kersten, 2003). In the current study, nutrigenomic studies have utilized candidate genes, focused PCR-arrays and microarray approaches to investigate the physiological response at tissue level and the mechanisms of adaptation to modern diets or to understand mechanisms underlying pathologies such as enteritis. We have tried to make an efficient diagnostic use of nutrigenomic approaches, to determine "**dietary signatures**" that characterize the physiological state of nutritional stressors. For doing so, we have integrated the data coming from nutrigenomics with other biometrical, metabolic and endocrinological data. The experimental trials have concentrated on the effects of the possible nutritional stress derived from including plant ingredients. The effects of vegetable proteins (AS, RT) and/or oils (GSB, RT), protein restriction (GSB, RT), essential amino acids (GSB, RT), minerals (GSB, RT), vitamins, essential fatty acids, phospholipids and phosphorous (GSB) have been studied.

2. Material and Methods

Common ethics statements

All procedures with GSB were approved by the Ethics and Animal Welfare Committee of Institute of Aquaculture Torre de la Sal and carried out in a registered installation (code 36271-42-A) in accordance with the principles published in the European animal directive (2010/63/EU) and Spanish laws (Royal Decree RD53/2013) for the protection of animals used in scientific experiments. In all lethal samplings, fish were decapitated under 3-aminobenzoic acid ethyl ester (MS-222,100 µg/mL) anaesthesia, and all efforts were made to minimize suffering.

All experimental procedures on AS were conducted in compliance with the Animals Scientific Procedures Act 1986 (UK Home Office Code of Practice. HMSO: London January 1997) under Project Licence (No. PPL 60/3969) and approved by the National Legislation on Animal Care of the Norwegian Food Safety Authority under the number ID 3889, in accordance with EU regulation (EC Directive 86/609/EEC) and approved by the Animal Ethics and Welfare Committee of the University of Stirling.

All the RT experiments and sampling procedures follow the guidelines of the National Legislation on Animal Care of the French Ministry of Research (Decree no. 2001-464, May 29, 2001) and the animal ethics committee of INRA (INRA 2002-36, April 14, 2002).

Table 1. Summary of the experimental procedures done with the three fish species.

FISH SPECIES	Trial no.	NUTRITIONAL STRESSOR	Duration	NON LETHAL SAMPLES		LETHAL SAMPLES		
				Plasma	Other	Performance	Gene expression	Other
Gilthead sea bream	1	Vegetable oil x confinement stress	10 wks	Cortisol, glucose*	-	SGR, FGR	Liver (focused lipid PCR-array)	
	2	Fasting	10 days	**	-	BW, organosomatic indexes	Liver, heart, muscle (OXPHOS PCR-array)	**
	3	Nutrient deficiencies (SAA, n3 LC-PUFA, PL, P, Min, Vit)	13 wks	**	--	SGR, FE, organosomatic indexes	Liver, muscle (focused growth PCR-array)	**
Salmon	1	Full fat soy	12 wks	-	-	SGR	Liver, intestine (oligomicroarray)	
Trout	1	Methionine deficiency x low protein level	12 wks	-	-	FI, Growth FCR	Brain (markers of EAA,protein deficiency and regulation of feed intake)	
	2	Vegetable diet x mineral supplementation	12 wks	Fe	Faecal samples: Fe-ACC	FI, FE, Growth FCR, DGI	Liver (markers of Fe metabolism), Intestine (markers of Fe absorption)	WB-Fe, Int, liver: Fe-reductase

* After confinement stress; ** Samples for clinical biochemistry, histopathology and tissue composition were taken, but analysed in the context of another EU project, ARRAINA.

2.1 Gilthead sea bream (CSIC)

Nutritional stress was studied in three different trials. In the first one, fish were fed with two diets with a different amount of fish oil and then exposed to confinement stress. In the second trial, fish were fasted for 10 days. In the third trial, fish were fed diets with different nutritional deficiencies (sulphur amino acids, essential fatty acids, phospholipids, phosphorus, minerals and vitamins). In trial 1, the transcriptomic study was done in liver and using a set of mitochondrial-related genes, as they were found to be very informative of the environmental stress (see D7.3 and D7.1). In the second trial the study was extended to cardiac and skeletal muscle and the number of mitochondrial related genes was also amplified to study in depth the full respiratory chain. In the third trial, the molecular study was done in liver and muscle using a focused growth PCR-array which included molecular markers of growth performance.

2.1.1 Experimental setup (trial 1)

Four hundred and eighty juveniles of GSB (17 g initial body weight) were randomly allocated in eight 500 L tanks (60 fish per tank) and reared from May to June (10 weeks) under the natural photoperiod and temperature conditions of IATS-CSIC (latitude: 40°5´N; 0°10´E). Two groups (4 replicates each) were established by feeding fish to visual satiety with plant protein-based diets with either fish oil (FO diet) or a blend of vegetable oils at the 66% of replacement of fish oil (66VO diet) as the most important source of dietary lipids (for details of diet composition see Benedito-Palos *et al.*, 2007). As expected, no effect of diet composition was found on growth or nutrient utilisation and both dietary groups (65-70 g final body weight) had high growth rates (SGR = 1.8-1.9) and good feed:gain ratios (1-1.1).

Feeding was stopped one day before crowding challenge start. At that point, three replicates from each dietary group (9-10 kg/m^3) remained undisturbed (control fish), whereas the remaining replicate was used as a donor tank of stressed fish, according to the protocol conducted in previous studies (Calduch-Giner *et al.*, 2010; Saera-Vila *et al.*, 2009b) and summarized in Fig. 1. Briefly, for each diet group, seven batches of seven fish from the donor tank were used as stressed fish by transferring all of them at the same time to seven cylinder net baskets of 5-L volume (90-100 kg/m^3), each one suspended in 90-L tanks with a seawater flow of 10-L/min to ensure good water quality (oxygen > 5 ppm; unionised ammonia < 0.02 mg/L). These stressed fish were sampled for blood (1 h, 2 h, 4.5 h and 6.5 h) or blood and liver (3 h, 24 h and 72 h) at fixed times after stressor onset. In parallel, fish from control tanks were sampled for blood and liver at 3 h, 24 h or 72 h.

No mortality was registered during the course of the crowding period. At each sampling time, fish from control (FO-C, 66VO-C) and stressed (FO-S, 66VO-S) groups were netted into a bucket containing 0.1 g/L of 3-aminobenzoic acid ethyl ester (MS-222; Sigma, Saint Louis, MO, USA). Blood was taken from caudal vessels (in less than 2 min for all fish), centrifuged at 3000 *g* for 20 min at 4 ºC, and plasma samples were frozen and stored at -20 ºC until analyses. Prior to tissue collection, fish were killed by cervical section and the liver was then rapidly extracted, frozen in liquid nitrogen and stored at -80 ºC until RNA isolation.

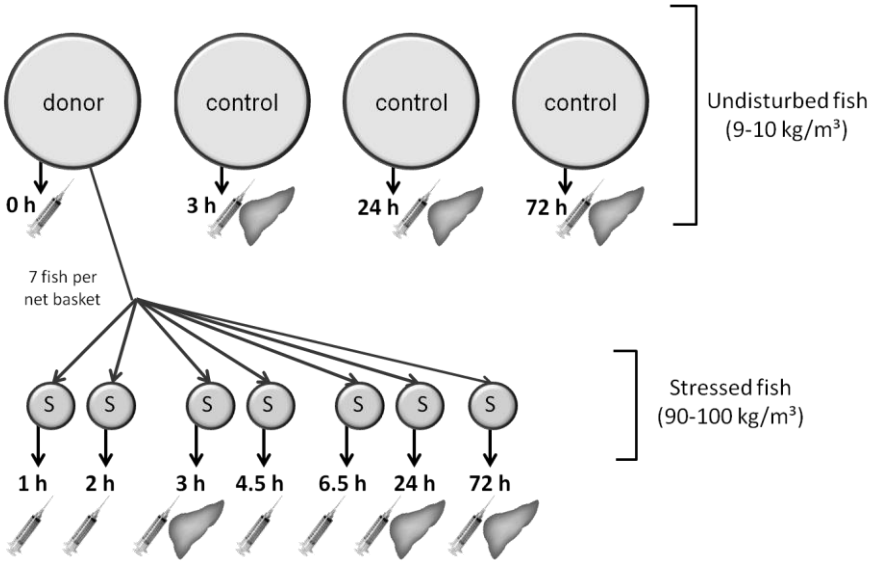

Figure 1. Scheme of the crowding stress protocol for GSB fed FO or 66VO diets in trial 1. Three replicates from each dietary group (9-10 kg/m3) remained undisturbed (control fish), whereas the remaining replicate was used as donor of fish for the zero time and the following samplings. These later fish (S) were stressed by transferring them to cylinder net baskets of 5-L volume (90-100 kg/m3) and sampled for blood or blood and liver within the 72 h after the onset of stressor. Fish from control tanks were sampled for blood and liver at 3 h, 24 h or 72 h.

2.1.2 Experimental set up (trial 2)

Juvenile GSB of Atlantic origin (Ferme Marine de Douhet, Ile d'Oléron, France) were raised in the indoor experimental facilities of IATS-CSIC. After an acclimation period of 3 months, fish with an average body weight of 86 g were distributed into 500 L tanks in 2 groups of 30 fish each. One group of fish continued to be fed with a commercial diet (EFICO YM 4.5, BioMar, Dueñas, Palencia, Spain) twice per day at full ration until visual satiety (CTRL group). The second group remained unfed for ten days. The feeding trial was conducted under natural photoperiod and temperature conditions at the latitude of the IATS (40°5N; 0°10E). Water flow was 20 L/min, the oxygen content of water effluents was always higher than 85% saturation, and unionized ammonia remained below toxic levels (< 0.02 mg/L). At the end of the trial (following overnight fasting), eight randomly selected fish per dietary treatment were anesthetized with 3-aminobenzoic acid ethyl ester (MS-222, 100 µg/mL). Liver, white skeletal muscle (right-hand side) and heart ventricles were rapidly excised, frozen in liquid nitrogen and stored at −80 °C until RNA extraction.

2.1.3 Experimental set up (trial 3)

Seven isoproteic and isolipidic semi-purified diets were formulated to assess specific nutrient deficiencies in sulphur amino acids (SAA), essential fatty acids (n3 LC-PUFA), phospholipids (PL), phosphorus (P), minerals (Min) and vitamins (Vit). The control diet (CTRL) contained all the essential nutrients in adequate amounts. Each diet was allocated to triplicate groups of juvenile GSB (initial mean body weight = 15 g) fed to satiety over an 11-week feeding trial. Diets were produced in a semi-industrial scale (Sparos LDA, Algarve, Portugal). Details on diet formulation and fatty acid (FA) composition are found in Supplemental Tables 15, 16 (Annex 1). All diets contained casein (20%), casein hydrolysate (5%), gelatin (5.8%) and soy protein concentrate (34.5%) and were adequately supplemented with L-threonine (0.02%), taurine (0.3%), betaine (0.3%), glucosamine (0.4%), dextrin (11.2%) and ethoxyquin (0.1%). DL-Methionine was supplemented at 0.4% in all diets except the diet designed to be deficient in sulphur amino acids (SAA diet). FO was added at 13.9% in all diets except in the FA deficient diet (n-3 LC-PUFA diet), in which FO was totally replaced by a blend of vegetable

oils (VO) in order to reduce the EPA (eicosapentaenoic acid) and DHA (docosapentaenoic acid) contents to trace levels. Soy lecithin (2%) was added as the unique source of PL in all diets except in the PL deficient diet. Calcium phosphate (2.2%) was added in all diets except in the P deficient diet. Mineral premix based on available data on mineral requirements of fish (National Research Council, 2011) was included at 2.2% in all diets except in the diet designed to be mineral deficient (Min diet). Vitamin premix, based on National Research Council requirements (2011), was added in all diets at an incorporation level of 2% except in the diet designed to be vitamin deficient (Vit diet).

Following the acclimatisation period, GSB of 15 g initial mean body weight were randomly distributed into 500 L-tanks in triplicate groups of 35 fish each. Fish were fed to visual satiety one (12 h)/two times (9h, 14 h) per day (6 days per week). The trial was conducted under natural photoperiod and temperature conditions at IATS latitude, increasing water temperature from 19 ºC in May to 24ºC at the end of July. Water flow rate was 20 L/min, oxygen content of water effluents was always higher than 85% saturation, and unionised ammonia remained below toxic levels (<0.02 mg/L). At the end of the trial and following overnight fasting (10-12 h in the morning), 12 fish per dietary treatment (four per tank) were randomly selected and decapitated under anaesthesia with 3-aminobenzoic acid ethyl ester (MS-222, 100 µg/mL). Liver and white skeletal muscle were rapidly excised, frozen in liquid nitrogen and stored at −80 °C until RNA extraction.

2.1.4 Biochemical assays (trial 1)

Plasma cortisol levels were measured using an EIA kit (Diagnostic Systems Laboratories, Webster, TX, USA) as reported elsewhere in GSB and other fish species (Bermejo-Nogales *et al.*, 2007; Kumar *et al.*, 2011; Pereira Maduenho and Martinez, 2008). The assay is based on the competition between unlabelled cortisol and cortisol–horseradish peroxidase for a fixed number of antibody-binding sites. The tetramethylbenzidine was used as a chromogen 3solution, and the limit of detection of the assay was 1 ng/ml with ED20 and ED80 values of 100 ng/ml and 2 ng/ml, respectively. The coefficient of variation intra- and inter-assay was lower than 8% and 12%, respectively. Plasma glucose levels were measured by the glucose oxidase method (Thermo Electron, Louisville, CO, USA) as reported elsewhere (Bermejo-Nogales *et al.*, 2007; Saera-Vila *et al.*, 2009b).

2.1.5 Gene expression analysis (trial 1)

A focused PCR-array including 31 stress-responsive genes, selected as markers of lipid and lipoprotein metabolism, antioxidant defence system, cell-tissue repair mechanims, xenobiotic metabolism and stress transcriptional regulation was used. The new sequences can be found in Supplemental Table 1 (Annex 1). Total RNA from *liver* was extracted with the ABI PRISM™ 6100 Nucleic Acid PrepStation (Applied Biosystems, Foster City, CA, USA) with a DNAse step. The RNA yield was 30–50 µg with absorbance measures (A260/280) of 1.9–2.1 and RIN (RNA integrity number) values of 8-10 with the Agilent 2100 Bioanalyzer, which is indicative of clean and intact RNA. Reverse transcription (RT) of 500 ng total RNA was performed with random decamers, using the High-Capacity cDNA Archive Kit (Applied Biosystems) following manufacturer's instructions. Negative control reactions were run without reverse transcriptase and real-time quantitative PCR was carried out with an iCycler IQ Real-time Detection System (Bio-Rad, Hercules, CA, USA) as described earlier (Calduch-Giner *et al.*, 2003). Briefly, RT reactions were conveniently diluted and the equivalent of 660 pg of total input RNA was used in a 25 µL volume for each PCR reaction. PCR-wells contained a 2x SYBR Green Master Mix (Bio-Rad) and specific primers at a final concentration of 0.9 µM were used to obtain amplicons of 50–150 bp in length (Supplemental Table 2, Annex 1). The program used for PCR included an initial denaturation step of 95 ºC for 3 min, followed by 40 cycles of denaturation for 15 s at 95 ºC and annealing/extension for 60 s at 60 ºC. The efficiency of PCR reactions was always higher than 90% and negative controls without sample templates were routinely performed for each primer set. The specificity of the reactions was verified by analysis of melting curves (ramping rates of 0.5

ºC/10 s over a temperature range of 55-95 ºC, yielding a single peak for each sample and gene), linearity of serial dilutions of RT reactions, and electrophoresis and sequencing of PCR amplified products.

PCR reactions were performed in triplicate and the fluorescence data acquired during the extension phase were normalized by the delta-delta Ct method using β-actin as housekeeping gene (Livak and Schmittgen, 2001). Four genes (β-actin, elongation factor 1, α-tubulin and 18S rRNA) were tested for stability using the GeNorm software. The most stable gene in relation to dietary treatment and crowding exposure was β-actin (M score = 0.21) and, thereby, it was used as housekeeping gene in the normalization procedure. When each dietary group was considered individually, fold-change calculations for each gene were referred to the expression ratio between stressed and control fish (values >1 indicates stress up-regulated genes; values < 1 indicates stress down-regulated genes). For multi-gene analysis comparing the mRNA gene expression between stressed fish of the two diet groups, all data values were referred to the expression level of AHR1 in non-stressed fish of the FO diet group (arbitrarily referred as 1).

2.1.6 Gene expression analysis (trials 2 & 3)

RNA from liver, white skeletal muscle and heart (trial 2) or liver and muscle (trial3) was extracted using a MagMAX TM-96 total RNA isolation kit (Life Technologies, Carlsbad, CA, USA). RNA yield was 50–100 µg with 260 and 280 nm UV absorbance ratios (A260/280) of 1.9–2.1, and RIN (RNA integrity number) values of 8–10 were measured on an Agilent 2100 Bioanalyzer, which is indicative of clean and intact RNA. Reverse transcription (RT) of 500 ng total RNA was performed with random decamers using a High-Capacity cDNA Archive Kit (Applied Biosystems, Foster City, CA, USA) according to the manufacturer's instructions. Negative control reactions were run without reverse transcriptase and real-time quantitative PCR was carried out on an Eppendorf Mastercycler Ep Realplex Real-Time PCR Detection System (Eppendorf, Wesseling-Berzdorf, Germany).

For both trials, 96-well PCR-array layouts were designed for the simultaneous profiling of all the markers considered in each assay, under uniform cycling conditions. In trial 2, the array included 88 oxidative phosphorylation (OXPHOS) genes: 33 enzyme subunits and 1 assembly protein of Complex I, 4 enzyme subunits and 2 assembly proteins of Complex II, 12 enzyme subunits and 1 assembly protein of Complex III, 19 enzyme subunits and 3 assembly proteins of Complex IV, and 12 enzyme subunits and 1 assembly protein of Complex V (n=12) (Supplemental Table 3, Annex 1). The GSB transcriptomic database of CSIC-nutrigroup (www.nutrigroup-iats.org/seabreamdb) is highly enriched in mitochondrial-related genes with 926 non-redundant sequences with the Gene Ontology term "mitochondrion." This allowed the unequivocal annotation of 99 sequences (E-values > 1e-15) as components of the KEGG pathway oxidative phosphorylation: 40 enzyme subunits and 1 assembly protein of Complex I, 4 enzyme subunits and 2 assembly proteins of Complex II, 12 enzyme subunits and 1 assembly protein of Complex III, 20 enzyme subunits and 3 assembly proteins of Complex IV, and 15 enzyme subunits and 1 assembly protein of Complex V as diagrammatically represented in Supplemental Fig. 1 (Annex 1). Ninety-seven out of 99 were new GSB sequences with open reading frames of 159–1992 nucleotides in length and a variable number of reads (10–2349) composing the assembled sequences (Supplemental Tables 4-8, Annex 1). All these sequences were uploaded to GenBank with accession numbers KC217558–KC217654. In trial 3, the array included 89 molecular markers of growth performance, identified and validated in the ARRAINA EU project as highly informative markers of growth status and deficiencies in essential nutrients. This set of genes included 31 new sequences for GSB, already represented in the sea bream transcriptomic database of CSIC-nutrigroup, and uploaded to GenBank with the accession numbers KM522771-KM522803 (Supplemental Table 17, Annex 1).

Quantitative real-time PCR (qPCR) was performed using an Eppendorf Mastercycler Ep Realplex real-time PCR system (Eppendorf, Wesseling-Berzdorf, Germany). Housekeeping genes and controls of general PCR performance were included on each array, with all of the pipetting operations performed using the EpMotion

5070 Liquid Handling Robot (Eppendorf). Briefly, RT reactions were diluted to convenient concentrations and the equivalent of 660 pg of total input RNA was used in a 25 µL volume for each PCR reaction. PCR-wells contained a 2x SYBR Green Master Mix (Bio-Rad, Hercules, CA, USA), and specific primers at a final concentration of 0.9 µM were used to obtain amplicons of 50–150 bp in length. See supplemental Tables 9-13 (Annex 1) for primers of trial 2 and supplemental Table 18 (Annex 1) for primers of trial 3. The program used for PCR amplification included an initial denaturation step at 95ºC for 3 min, followed by 40 cycles of denaturation for 15 s at 95ºC and annealing/extension for 60 s at 60ºC. The efficiency of PCR reactions was always higher than 90%, and negative controls without sample templates were routinely used for each primer set. The specificity of reactions was verified by analysis of melting curves (ramping rates of 0.5ºC/10 s over a temperature range of 55–95ºC), linearity of serial dilutions of RT reactions, and electrophoresis and sequencing of PCR amplified products. Fluorescence data acquired during the PCR extension phase were normalised using the delta-delta Ct method (Livak and Schmittgen, 2001). β-actin, elongation factor 1, α-tubulin and 18S rRNA were initially tested for gene expression stability using GeNorm software, and the most stable gene was found to be β-actin (M score = 0.17-0.21); therefore, this gene was used as a housekeeping gene in the normalisation procedure for routine assays.

In trial 2, when genes for a given nutritional condition were individually analysed, fold-change calculations for each gene were in reference to the expression ratio between fasted and CTRL fish (values > 1 indicate fasting up-regulated genes; values < 1 indicate fasting down-regulated genes). For multi-gene analysis comparing mRNA gene expression level, all data values in a given tissue were in reference to the expression level in CTRL fish of NDUFC2 (liver), NDUFA5 (skeletal muscle) or NDUFB2 (heart), for which a value of 1 was arbitrarily assigned in the corresponding tissue. In trial 3, when genes for a given nutritional condition were individually analysed, fold-change calculations for each gene were in reference to the expression ratio between CTRL and nutrient deficient fish (values > 1 indicate CTRL up-regulated genes; values < 1 indicate nutrient deficient down-regulated genes). For multi-gene analysis comparing mRNA gene expression level, all data values in a given tissue were in reference to the expression level in CTRL fish of IGFR2, for which a value of 1 was arbitrarily assigned in the corresponding tissue.

2.1.7 Statistical analysis (trials 1-3)

Effects of nutritional stressors on basic blood biochemistry and liver, muscle or heart gene expression were analysed by Student t-test and/or one-way ANOVA followed by Student-Newman Keuls (SNK) test at a significance level of 5%. All analyses were made using the SPSS package version 20.0 (SPSS Inc., Chicago, IL, USA).

2.2. Atlantic salmon (IMR, UoS)

The nutritional stress was induced by inclusions of dietary soybean meal (SBM) up to a level of 300 g kg-1 (S30), because it has been extensively demonstrated to induce reduced performance and enteropathy in the distal intestine (Baeverfjord and Krogdahl, 1996; Urán *et al.*, 2008, 2009). A control treatment with no SBM, as well as intermediate levels of inclusion were included to span a range of optimal and sub-optimal conditions. Performance parameters were measured and impaired growth was taken as an indicator of pronounced nutritional stress. Analyses were performed in liver and distal intestine only for S30 compared to the control one, as no effects on growth performance were found in the intermediate levels. Distal intestine was chosen for being the site most morphologically and physiologically affected during the development of intestinal pathologies associated with plant ingredients such as SBM (Baeverfjord and Krogdahl, 1996 ;Kortner *et al.*, 2011), while liver for being arguably the most metabolic active tissue.

2.2.1 Experimental set up, diets and sampling

The nutritional trial was conducted at Institute of Marine Research, Matre (IMR, Norway) using AS of the commercial Aquagen strain (Aquagen Ltd, Kyrksæterøra, Norway). The fish were naturally smoltified (1+) in 5 m indoor tanks under natural light. In end of May, the a total of 540 fish were anaesthetized in Finquel, tagged with PIT tags, and equally distributed into 12 white fibre glass tanks each holding 500 liter (95 cm * 95 cm * 60 cm, L * W * H). The tanks were closed with lids, and supplied with two fluorescent light tubes (18 Watt each) and an automatic feeder (ARVO-TEC T Drum 2000, Arvotec, Huutokoski, Finland, www.arvotec.fi). After 2 days of rest, the salinity was gradually increased from freshwater to full salinity (35 ppt) and the temperature adjusted to 12^{o}C (aerated and temperature controlled seawater). Water flow was fixed at 20L/min. Two days before start of the trial, the individual fish were weighted (group mean 175 g) and returned to the tanks. Fish were acclimatized for fed the same acclimation feed (D0, Supplemental Table 1, Annex 2) after transfer to the tanks (4 weeks). Four dietary treatments were investigated and are shown in Supplemental Table 1 (Annex 2). They had progressively higher inclusion of SBM (0 g kg^{-1}, 100 g kg^{-1}, 200 g kg^{-1}, 300 g kg^{-1}) substituting other protein sources (FM, corn, sunflower and horsebeans protein) referred to as diets S0, S10, S20, S30 respectively. Each experimental feed was fed to triplicate tanks. All feeds were formulated to meet the nutritional requirement of salmon (National Research Council, 2011). The nutritional trial lasted for 12 weeks and at the end of this period fish were weighed and liver and intestine samples dissected from 6 individuals in total per dietary treatment (S0 and S30 only). Samples were immediately placed in RNALater (Life Technologies, Paisley, UK) and processed as per manufacturer instructions before being stored at -20°C prior to analyses. Individual weight and length were taken at the end of the trial and specific growth rate (SGR) was calculated.

2.2.2 Transcriptomic analysis

Transcriptomic analysis was conducted using a custom-made 4 x 44K Atlantic salmon oligo microarray (Agilent Technologies, Wokingham, UK; ArrayExpress accession no. A-MEXP-2065) described in detail previously (Tacchi *et al.*, 2011). The salmon custom array and laboratory procedures utilized have been widely used and validated in several previous studies (Martinez-Rubio *et al.*, 2012; Morais *et al.*, 2012a,b). Briefly, total RNA was extracted from individual samples using TRI Reagent essentially according to manufacturer instructions (Sigma-Aldrich, Dorset, UK), and including a high salt precipitation as recommended for polysaccharide-rich tissues such as liver (Chomczynski and Mackey, 1995). RNA quantity, integrity and purity were assessed by agarose gel electrophoresis and spectrophotometry (NanoDrop ND-1000, Thermo Scientific, Wilmington, USA). Equal amounts of RNA from six individual fish livers and intestines were analysed. The same RNA samples were used both for transcriptomics analyses and subsequent RT-qPCR validation. The resulting RNA samples were amplified using TargetAmp™ 1-Round Aminoallyl-aRNA Amplification Kit, (Epicentre Technologies Corporation, Madison, Wisconsin, USA) following recommended procedures and purified with RNeasy Mini Kit (Qiagen, Manchester, UK). Aminoallyl-amplified RNA (aRNA) samples were labelled with Cy3 dye (GE HealthCare Life Sciences, Buckinghamshire, UK) while a pool of all aRNA samples was labelled with Cy5 dye (GE HealthCare Life Sciences) and used as a common reference. Unincorporated dye was removed by purifying the aRNA samples with Illustra AutoSeq G-50 dye terminator columns (GE HealthCare Life Sciences). Successful dye incorporation and sample integrity was assessed for 1 µL aliquots of labelled samples by agarose gel electrophoresis followed by fluorescent detection of aRNA products (Typhoon scanner, GE Healthcare Life Sciences). Cy dye concentration and aRNA quantification was measured by Nanodrop mediated spectrophometry.

Labelled aRNA samples were hybridized to the custom-made array. A dual-label common reference design was adopted, where equal amounts of each individual aRNA sample and the common reference pool were competitively hybridized to one array. The common reference design allowed standardization of inter- and intra-array variability.

Samples were processed with the Gene Expression Hybridization Kit (Agilent Technologies), applied to the arrays and immediately incubated using SureHyb hybridization chambers in a DNA Microarray Hybridization Oven (Agilent Technologies) at 65 °C for 17h. Throughout the experiment samples were always randomized, avoiding samples from the same treatment being overrepresented in a particular batch in order to avoid unintentional biases. Scanning was performed using a GenePix 4200 AL Scanner (Molecular Devices (UK) Lid., Wokingham, UK) and the resulting images analysed with Agilent Feature Extraction Software v.9.5 (Agilent Technologies) to extract the intensity values and identify the features. The foreground intensity was computed as the mean value of pixels, considered a better estimator as being less susceptible to distortion from outlier values (Russell *et al.*, 2009), while background intensities were computed as the median value of pixels. Details of microarray experiment will be submitted to ArrayExpress upon publication and accession number provided.

2.2.3 Data pre-processing and differential expression analysis

Transcriptomic data analysis was performed using R v.3.0.1 and Bioconductor v.2.13 (Gentleman *et al.*, 2004; R Core Team, 2013). Quality control, data pre-processing and identification of differentially expressed features/genes were conducted using the package Limma (Smyth, 2004). Array quality was controlled by visualizing and comparing boxplots of red (R) and green (G) background and foreground intensities, MA plots [$M = \log_2(R/G)$; $A = 1/2\log_2(R*G)$] and spatial heterogeneity to reveal the presence of any technical bias. Following quality control, all arrays were retained for further analyses. Features considered outliers in more than 30 % of the replicates within at least one treatment were excluded from further analyses. Foreground intensities were background-corrected using the normexp approach (maximum likelihood variant “mle”, offset = 50) as previously reported as the most reliable method for two-colour microarrays where background estimates are available (Ritchie *et al.*, 2007; Silver *et al.*, 2009). Data were log-transformed and normalized using the function normalizeWithinArrays (method = “loess”). A second normalization was performed using the normalizeBetweenArrays function (method = “RQuantile”) (Smyth and Speed, 2003). Filtering of control and features expressed just above background were also removed. Features of the array were annotated using BLAST 2.2.29+ (blastx) against the entire non-redundant protein database as well as using the KEGG Automatic Annotation Server to obtain functional annotations (Altschul *et al.*, 1990; Moriya *et al.*, 2007). A total of 92.8% of all probes were returned with a BLAST annotation with e-value < 10 (89.6% with e-value < 0.001), while 59 % of probes were returned with a functional annotation using the KAAS server. Differentially expressed features between treatments were estimated by least squares fitting of linear models on a probe-by-probe basis using the entire pre-processed dataset. The function *lmFit* was used to compute differential expression and statistics were extracted using *ebayes* (trend = TRUE) both functions of the package limma (Smyth, 2004). Features representing the same target gene as implied from KEGG annotation were merged into a unique value obtained by selecting the feature with the highest F-value. A new dataset was therefore generated for further analyses where each gene was only represented by one feature. Merging features resulted in a dataset of 6729 annotated features targeting unique genes.

2.2.4 Data Mining

Hierarchical Clustering. Hierarchical cluster analysis was performed on gene expression values to evaluate overall similarity between each sample analysed using the R package *pvclust* (Suzuki and Shimodaira, 2011). The distance measure used was the “correlation” with 1000 bootstrap replication.

Overview of differential expression. Differentially expressed genes were plotted using the R package *ggplot2* (Wickham, 2009). For figures involving functional information, the KEGG database was used as the preferred classification system. Venn diagrams were generated

using the function *VennDiagram* from the Limma package.

Gene-Set Enrichment Analysis (GSEA). Unique annotated sequences were analysed using the R function *gage* of the package GAGE [Generally Applicable Gene-set Enrichment, (Luo *et al.*, 2009)] to identify mechanistic changes as suggested by coordinated expression changes in gene-sets. Two types of test were performed: *1d*) testing all genes in a gene-set moving towards the same direction; and *2d*) testing genes in a gene-set moving towards both directions simultaneously. Gene-set with *q*-value < 0.1 were considered significant, where the *q*-value represented the *p*-value adjusted for false discovery rate. KEGG classification was used for these analyses and all figures were produced using the package *ggplot2*.

2.2.5 Identification and validation of candidate genes for molecular phenotyping

Validation of microarray expression data was performed by reverse transcriptase RT-qPCR. A total of 12 targets were analysed including 5 genes in the liver and 7 in the intestine (Supplemental Table 2, Annex 2). The selected reference genes were selected based on stability across the analysed treatments from a pool of candidate reference genes (data not shown). The expression of the target genes was normalized using the delta-delta Ct approach (Pfaffl, 2001). Target genes investigated in this study were selected based on the results of the transcriptomic data to represent functions that were greatly affected by the extreme diets S0 and S30. Primers for the target genes were designed using the program PerlPrimer (Marshall, 2004) either to overlap the probe sequence or, where not possible, in proximity of it to also guarantee a proper validation of the microarray results by amplification of the same target sequence. Protocols for reverse transcription and qPCR assays are routinely used and were described in detail previously (Bicskei *et al.*, 2014).

2.3 Rainbow trout (INRA)

Nutritional stress was studied in two different trials. In trial 1, fish were fed either a low protein diet (LP) or a diet deficient in an essential amino acid (EAA), methionine. The objective was to determine how fish react in front of dietary EAA deficiency, either by reducing methionine or by reducing crude protein in the diet, and how this is translated in the expression of anorectic *vs* orexigenic markers involved in the control of food intake and to integrate these data with responses related to AA signalling and feed intake. In trial 2, trout were fed either a FM-FO based diet or a totally plant ingredient based diet, with or without trace mineral (Fe, Cu, Mn, Zn and Se) premix inclusion. Iron levels in whole body and plasma and the responses related to iron absorption, transport or metabolism of trace minerals in liver and intestine were analysed The objective was to determine whether the transition from fish meal based diet to a full plant- based diet affect affects iron metabolism and whether the supplementation of extra iron affects or interacts with the ingredient composition of the diet on Fe absorption or metabolism.

2.3.1 Fish and experimental set up

RT were reared in flow through systems (natural spring water) at the INRA experimental fish farm (Donzacq, France). Water temperature was constant at 17 ± 0.5°C and the water flow rate was set at 50 L min^{-1}. The fish were distributed into 12 experimental units, 350 L (40 fish $unit^{-1}$). Each unit was randomly assigned to one of the four dietary treatments in triplicates. In both trials, the fish were carefully hand fed twice a day to apparent visual satiation for a period of 12 weeks (6 days a week). Feed intake was recorded on a daily basis. Fish were group-weighed on a 3-week basis in order to follow growth parameters. The initial body weight of the RT juveniles was 41 ± 0.7 g and 20 ± 1 g in **Trial 1** and **Trial 2**, respectively.

2.3.2 Experimental diets

Trial 1. Markers of reduced feed intake in RT fed a diet deficient in EAA

The four diets (2 x 2 design) differed in protein level (24% vs 38%, LP and MP) and in methionine (Met) content (Supplemental Table 1, Annex 3). The proteins are provided by soy protein concentrate, wheat and soluble fish protein concentrate (respectively 67.4, 19.1 and 13.5% of the protein blend) and an amino acid mixture which lacks crystalline methionine (Supplemental Table 1, Annex 3). The diets had similar digestible energy contents, but differed in carbohydrate level which compensated for the difference in protein level. At each of the two protein levels (LP and MP), two different levels of Met and cysteine (as % of crude protein) were tested, either deficient (1.4 to 1.5% of Met and about 1% cysteine) in deficient diets 0 (LP-0 and MP-0) or adequate (2.2% of Met and cysteine approximately 1.2%) in adequate diets 1 (LP-1 and MP-1). Diet MP1, covering the needs of protein and Met in RT, served as a control feed. The 2 x 2 design in diet formulation allows comparison the effect of different levels of protein and Met on brain markers involved in the regulation of food intake and amino acid sensing.

Trial 2. Markers of iron homeostasis

Two basal diets, named as M0 and V0 were formulated (Supplemental Table 2, Annex 3). The M0 diet was based on fishmeal (FM) and fish oil (FO); while the V0 diet was made entirely of plant derived ingredients. Essential trace minerals (Fe, Cu, Mn, Zn and Se) were supplemented to the basal diets, as a premix at 1% inclusion level, to provide diets M1 and V1, respectively (see Supplemental Table 2, Annex 3).

2.3.3 Fish, tissue and faecal samplings

At the end of the 12 week growth trial fish were group-weighed to determine the final growth. Anaesthetised (benzocaine, 30 mg $L^{-1)}$ fish were sampled for trial 1: the hypothalamus and remaining part of the whole brain (n=9 fish per treatment, 18-h starved) and for trial 2: liver and anterior intestine (without caeca). Samples were rinsed in 0.9 % NaCl to remove any blood (in liver), food or faecal remains (in intestine) and immediately frozen in liquid nitrogen and stored at -80 °C until further analysis. For trial 2**,** a pooled sample of 6 fish from each experimental unit was taken for final Fe analysis. Further, 3 more fish from each experimental unit were randomly withdrawn, anaesthetised and sampled for blood from the caudal vein using heparinised syringe. The blood was centrifuged (3000 *g* for 5 min) and the plasma was stored at -20 °C. After the tissue sampling, 25 fish of each tank were used for the determination of the Fe apparent availability coefficient (AAC). The fish were fed a single meal (86 g $tank^{-1}$) and 9h after the meal, faecal samples were collected by the method of stripping. The samples were collected over ice, frozen immediately and stored at -20°C until Fe analysis.

2.3.4 Gene expression analysis

Gene expression of candidate bio-markers was studied in brain (Trial 1) or liver and intestine (Trial 2). Full gene names and details of the primer sequences are presented in Supplemental Tables 3 and 4 (Annex 3), respectively.

Total RNA was extracted from liver and anterior intestine samples (n=9 per treatment) using Trizol reagent (Invitrogen, Cergy-Pontoise, France). For quantitative RT-PCR, complementary DNA was generated from 1 µg total RNA using SuperScript® III reverse transcriptase (Invitrogen) with a mix of $oligo(dT)_{15}$ and random primers (Promega, Charbonnières, France). RT was performed in duplicate for each sample and the quantitative PCR analyses were performed in LightCycler 480 II thermocycler (Roche) using LightCycler 480 SYBR Green I Master mix (Roche Diagnosis, Indianapolis, IN, USA). Total reaction volume was 6µL, with 2µL of cDNA (RT product) and 4 µL of master mix added with 0.4mM of each primer. Relative quantification of target gene transcripts were normalized using

Elongation Factor 1α (EF1α) as the reference gene, following the method of Pfaffl (2001).

Concentrations of Fe in the diets, whole fish, faeces and plasma were analysed using inductively coupled plasma-mass spectrometry (ICP-OES) at USRAVE-INRA, Bordeaux, France (Trial 2).

2.3.5 Statistical analysis

Two-way ANOVA was used to analyse data for main dietary effects (2 x 2 designs). In the case of a significant interaction, one-way ANOVA (Tukeys' multiple comparison) was performed.

3. Results

3.1 Gilthead sea bream (CSIC)

3.1.1 Plasma cortisol and glucose kinetics (trial 1)

Plasma cortisol levels in control fish remained almost unchanged during the course of the stress challenge, though overall cortisol titres were 3-fold higher in 66VO-C fish (20-35 ng/mL) than in FO-C fish (3-11 ng/mL). In both dietary groups, plasma cortisol levels rapidly increased after crowding exposure, and the peak of cortisol was 2- to 3- fold higher in fish fed the 66VO diet (66VO-S group) than in the FO stressed fish (FO-S group) (Fig. 2A). A recovery of cortisol resting values was found at 24 h after the induction of crowding stress in 66VO-S fish, whereas persistently high plasma cortisol levels were observed in FO-S fish.

Glycaemia remained almost unchanged in control fish (60-80 mg/dL) with no effects of diet composition on the measured values. In both dietary groups, plasma glucose levels increased rapidly after crowding exposure with a maximum at 1-3 h and a recovery towards control values at 24 h (Fig. 2B). However, the magnitude of response was dependent on the nutritional background and the peak of glycaemia (> 200 mg/dL) in 66VO-S fish was significantly higher ($P < 0.05$) than in FO-S fish (130-150 mg/dL).

3.1.2 Hepatic gene expression (trial 1)

The time course of the liver transcriptional response was analysed with a focused lipid PCR-array at 3, 24 and 72 h after crowding exposure and fold-changes in mRNA transcript levels were referred to the control group of non-stressed fish for each diet and sampling time (Fig. 3). Overall, the strongest up-regulated changes in mRNA transcript levels were found 24 h after confinement, which was particularly evident for some cell- and tissue-repairing genes (derlin-1, DER-1; estrogen receptor-associated Hsp40 co-chaperone, ERdj3; 94 kDa glucose-regulated protein, GRP-94; and 170 kDa glucose-regulated protein, GRP-170), antioxidant enzymes (glutathione peroxidase 4, GPX4; peroxiredoxin 3, PRDX3; superoxide dismutases, Cu-Zn-SOD and Mn-SOD), nuclear receptors (estrogen receptor alpha, ER-α; glucocorticoid receptor, GCR) and transcription factors (cyclic AMP response element-binding protein 2, CREB-2; hypoxia inducible factor-1 alpha, HIF-1α). Most gene markers of lipid and lipoprotein metabolism (carnitine palmitoyltransferase 1A, CPT1A; hydroxyacyl-CoA dehydrogenase, HADH; heart-FA binding protein, H-FABP; hepatic lipase, HL; hormone-sensitive lipase, HSL; lysosomal acid lipase, LAL) were also strongly up-regulated at 24 h after crowding exposure, though in the case of lipoprotein lipase (LPL) the maximum response was attained earlier (3 h after crowding exposure). Likewise, aryl hydrocarbon receptor 1 (AHR1) was transiently up-regulated at 24 h after crowding exposure, whereas other xenobiotic gene markers (cytochrome P450 1A1, CYP1A1; glutathione S-transferase 3, GST3) were mostly down-regulated within the 72 h after the onset of stressor disturbance.

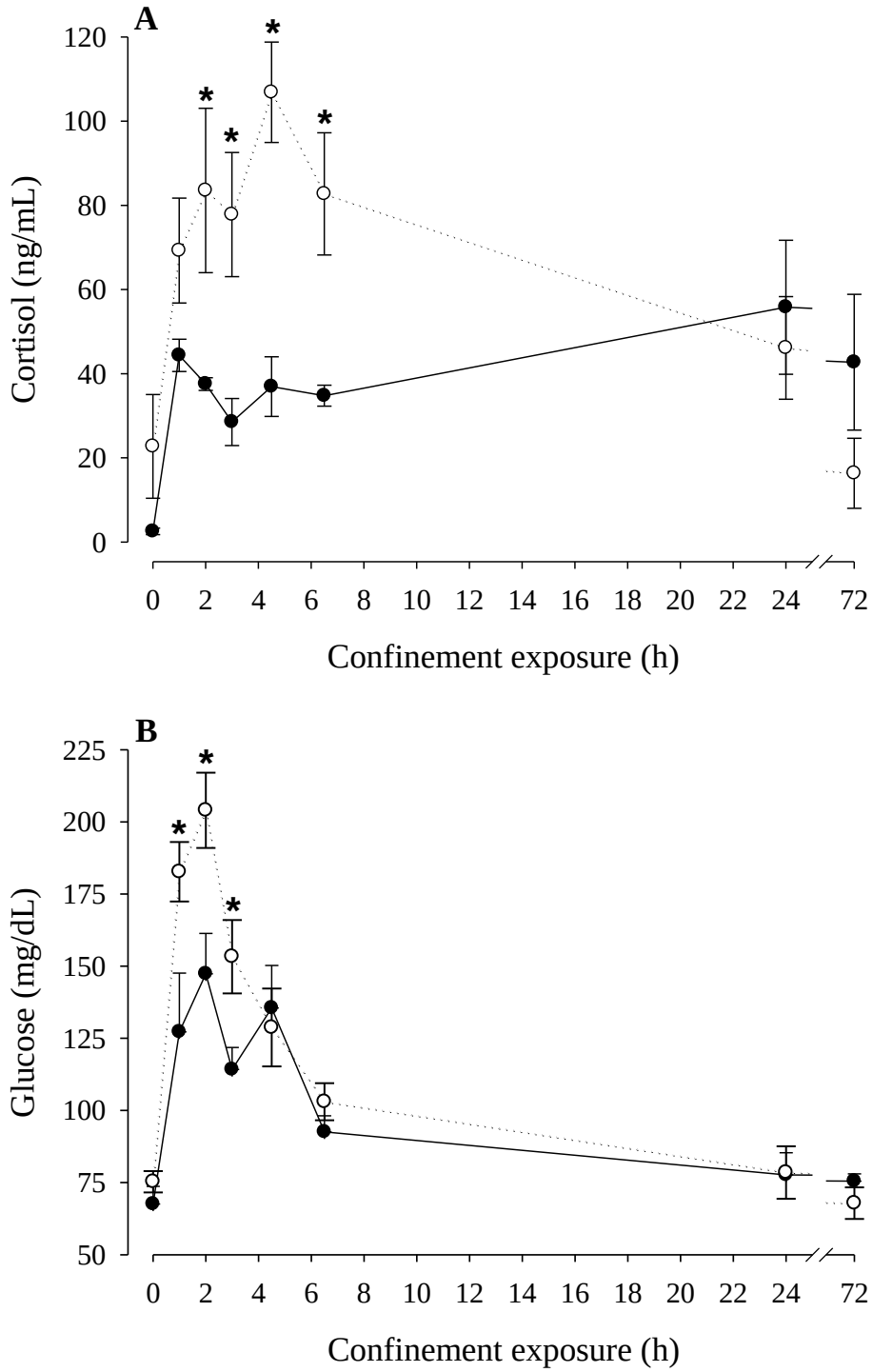

Figure 2. Effect of nutritional background on the time course of plasma cortisol (A) and glucose (B) stress responses in stressed GSB of the 66VO diet group (white circles) and FO diet group (black circles), in trial 1. Data are the mean ± SEM (n = 7). *, denotes significant differences (P < 0.05) between stressed fish of the two dietary groups at a given sampling time. Control values are shown as two inserts. †, denotes significant differences between control and stressed fish at 3 h , 24 h and 72 h after crowding exposure.

The stress-transcriptional response was also modulated by the nutritional history and overall the magnitude of change was quantitatively and qualitatively higher in the FO diet group (Fig. 3A) than in 66VO fish (Fig. 3B). Thus, with the exception of glutathione peroxidase 1 (GPX1), the expression profile of all the measured genes was transcriptionally regulated by stress confinement in at least one sampling time in FO-S fish. In contrast, in 66VO-S fish, up to 5 genes, including cytochrome c oxidase subunit IV isoform 1 (Cox4a), enoyl-CoA hydratase (ECH), uncoupling protein 1 (UCP1), catalase (CAT) and GST3 did not vary significantly at any sampling time when data were referred to the corresponding diet control group.

When gene expression levels from the two stressed groups of fish were plotted against each other (FO-S *vs* 66VO-S), the results rendered a gene expression pattern changing over time from a down- to up-regulated adjustment in stressed fish of the 66VO diet. Hence, at 3 h after the onset of the stressor disturbance, CAT, Cox4a, CYP1A1, Cu-Zn-SOD, DER-1, PRDX3 and glutathione reductase (GR) were significantly down-regulated in 66VO-S fish in comparison to the FO-S group (Fig. 4A). At 24 h after crowding exposure, differentially expressed genes were either down- (DER-75; 75 kDa glucose-regulated protein, GRP-75; GRP-170 and Cox4a) or up-regulated (ECH, ER-α, HADH, and GCR) (Fig. 4B) in 66VO-S fish, whereas later on (72h) all the differentially expressed genes (GR, Cox4a, GCR, HADH, PRDX3, LPL; peroxiredoxin 5, PRDX5) were up-regulated in 66VO-S fish in comparison to FO-S group (Fig. 4C).

Figure 3. Effect of nutritional background on the hepatic expression of stress-relevant genes at 3 h (black bars), 24 h (grey bars) and 72 h (white bars) after the onset of initial disturbance in GSB, in trial1. Data are the mean ± SEM (n = 7). β-actin was used as a housekeeping gene. Each gene expression value in stressed fish of the FO diet group (A) and 66VO diet group (B) was referred for a given sampling time to each diet-control value. Data in control fish were used as arbitrary reference values (values >1 indicates stress up-regulated genes; values < 1 indicates stress down-regulated genes). Asterisks indicate statistically significant differences (P < 0.05) with respect to diet-control group at each sampling time.

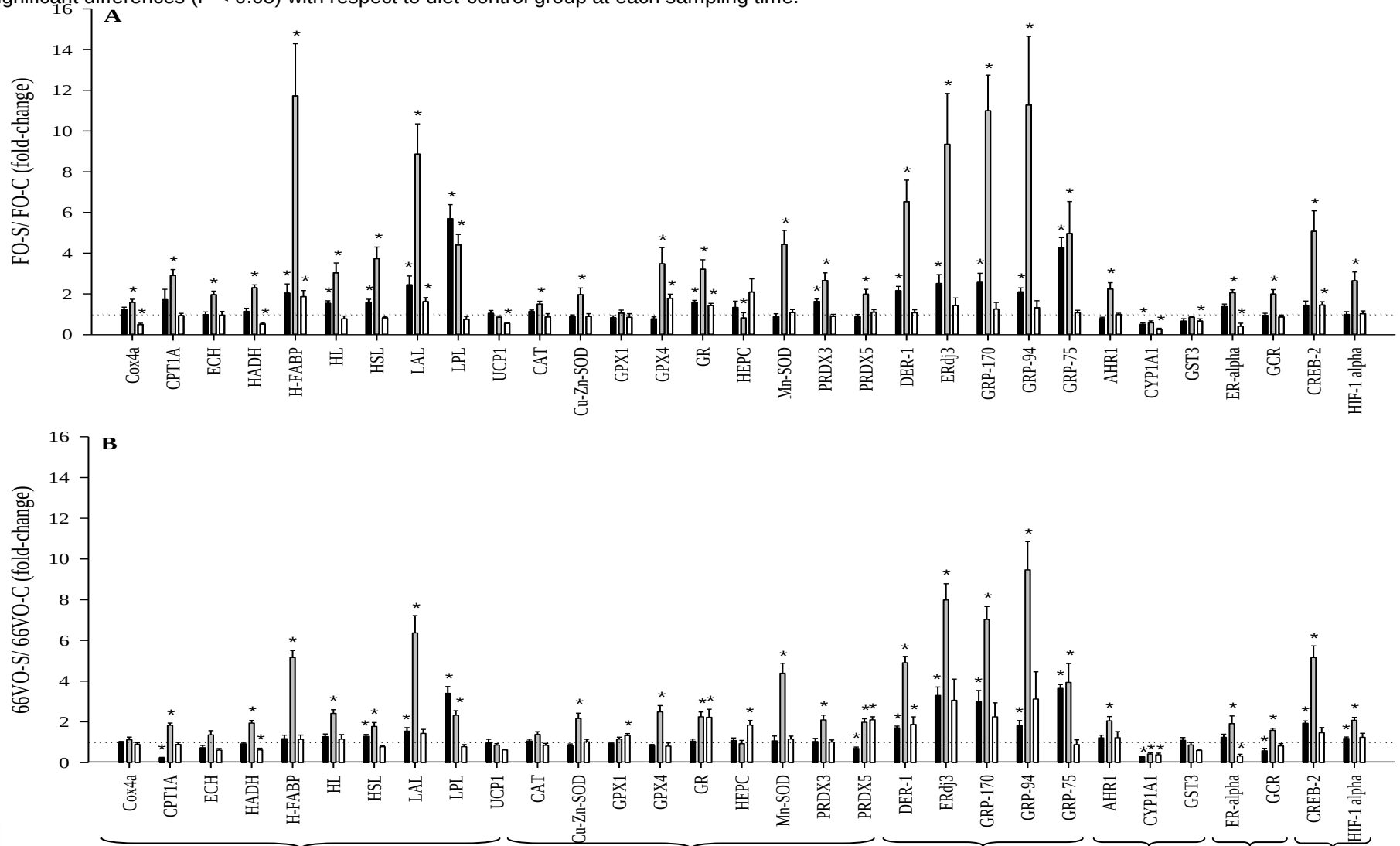

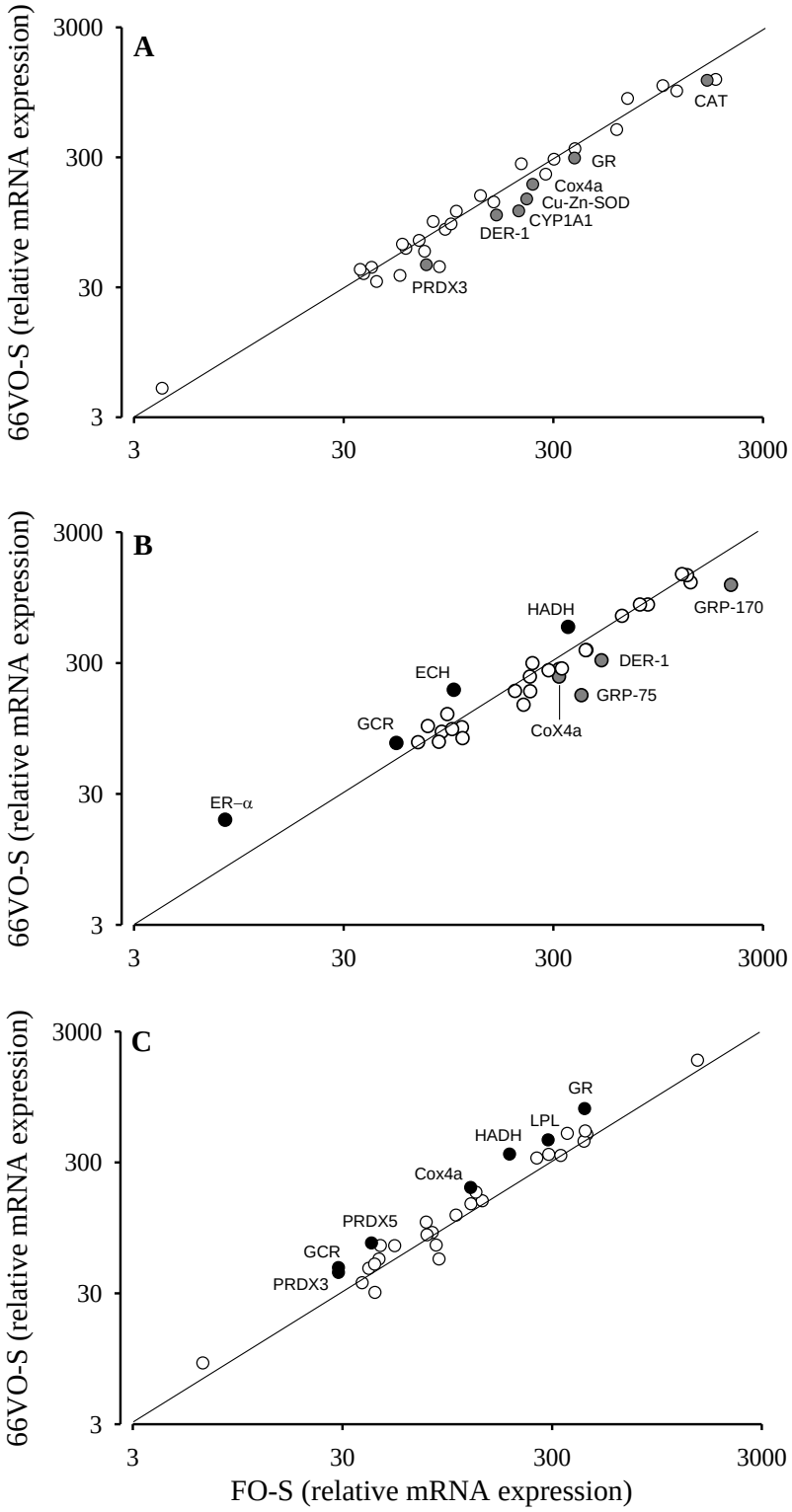

Figure 4. Gene expression values in stressed GSB of the two dietary groups (66VO, FO) in trial 1 plotted against each other in different scatterplots for each sampling time at 3 h (A), 24 h (B) and 72 h (C) after the onset of initial disturbance. Data are the mean of 7 fish. Standard error is not plotted to simplify the graphical representation. β-actin was used as a housekeeping gene and regardless of dietary group all data values were referred to the expression level of AHR1 in control fish of the FO diet group. Black circles, up-regulated genes ($P < 0.05$) in stressed fish of the 66VO diet; gray circles, down-regulated genes ($P < 0.05$) in stressed fish of the 66VO diet; white circles, non-differentially regulated genes.

3.1.3 Growth performance (trial 2)

As shown in Table 2, continuously fed fish (CTRL) grew efficiently with an 18–20 % increase in body weight, while fasted fish lost 6–8 % of body weight mass over the course of the 10-day fasting period. The viscera weight and liver weight of fasted fish were significantly lower than those of CTRL fish, and the resulting viscerosomatic and hepatosomatic indexes decreased from 8.5% to 5.4% and from 2.1% to 0.6%, respectively.

Table 2. Growth and biometric parameters of fed (CTRL group) and fasted GSB. Each value is the mean ± SEM of the 8 sampled fish for transcriptional analysis. Initial average weight for the entire population was 86 ± 0.08 g. For abbreviations see the glossary.

	CTRL	Fasted	*P* [a]
Final body weight (g)	109.48 ± 3.42	79.93 ± 1.82	*<0.001*
Viscera (g)	9.35 ± 0.49	4.34 ± 0.23	*<0.001*
Liver (g)	2.31 ± 0.13	0.52 ± 0.03	*<0.001*
VSI (%)	8.52 ± 0.23	5.41 ± 0.19	*<0.001*
HSI (%)	2.10 ± 0.06	0.64 ± 0.02	*<0.001*
DM intake (g/fish)	17.25	-	

[a] *P* values result from Student-t test.

3.1.4 Growth performance (trial 3)

Data on growth, somatic indexes and body composition are shown in Table 3. As a general rule, nutrient deficient diets reduced significantly feed intake, growth rates and feed efficiency in fish fed P and n-3 LC-PUFA diets. This resulted in a weight gain of 50% (n/3 LC/PUFA), 60-75% (P, Vit) and 80-85% (PL, Min, SAA) of CTRL fish. Mesenteric fat index (MSI) was markedly reduced in Vit fish. The same was observed in PL and n-3 LC-PUFA groups, although there were no statistically significant differences. Conversely, MSI was significantly increased in P fish. Hepatosomatic index (HIS) was also altered by dietary treatments, and it was largely increased in n-3 LC-PUFA fish. The opposite was found in Min fish and in a lower extent in Met and Vit fish.

Table 3. Effect of nutrient deficiencies on growth performance of GSB fed to visual satiety from May to July (13 weeks) in GSB trial 3. Data on body weight (BW), feed intake (FI), growth indices and body composition are the mean (SEM) of triplicate tanks. Data on viscera, mesenteric fat (MF) and liver weight are the mean (SEM) of 20 fish. Different superscript letters in each row indicate significant differences among dietary treatments (SNK test, P<0.05).

	Diet							
	CTRL	SAA	n-3 LC-PUFA	PL	P	Min	Vit	P-value[1]
Initial BW (g)	15.1(0.06)	15.1(0.21)	15.2(0.14)	15.0(0.25)	15.1(0.11)	15.0(0.04)	15.2(0.08)	0.977
Final BW (g)	85.5(1.58)^{a}	72.5(1.41)^{b}	51.2(0.17)^{d}	71.7(1.80)^{b}	60.2(0.66)^{c}	71.5(2.12)^{b}	66.1(0.65)^{bc}	*<0.001*
FI (g)	65.9(1.46)^{a}	54.7(1.36)^{b}	37.9(0.68)^{d}	49.6(2.16)^{bc}	51.4(0.91)^{bc}	51.6(1.73)^{bc}	46.9(0.59)^{c}	*<0.001*
Viscera (g)	6.39(0.27)^{a}	5.34(0.23)^{b}	4.40(0.21)^{d}	5.80(0.19)^{ab}	5.79(0.18)^{b}	5.54(0.20)^{abc}	4.90(0.16)^{cd}	*<0.001*
MF (g)	1.14(0.13)^{a}	0.92(0.12)^{abc}	0.58(0.09)^{c}	0.79(0.08)^{bc}	1.27(0.11)^{a}	1.04(0.11)^{ab}	0.49(0.06)^{c}	*<0.001*
Liver (g)	1.09(0.06)^{a}	0.80(0.03)^{c}	0.98(0.04)^{ab}	1.01(0.05)^{ab}	0.87(0.02)^{bc}	0.77(0.02)^{c}	0.79(0.03)^{c}	*<0.001*
VSI (%)	7.12(0.20)^{bc}	7.03(0.22)^{bc}	7.81(0.20)^{b}	7.43(0.16)^{bc}	8.95(0.23)^{a}	7.10(0.19)^{bc}	6.92(0.16)^{c}	*<0.001*
MSI (%)	1.27(0.13)^{b}	1.19(0.14)^{bc}	0.98(0.12)^{bc}	0.99(0.10)^{bc}	1.97(0.16)^{a}	1.32(0.13)^{b}	0.70(0.08)^{c}	*<0.001*
HSI (%)	1.23(0.04)^{bc}	1.05(0.02)^{cd}	1.76(0.08)^{a}	1.29(0.04)^{b}	1.36(0.04)^{b}	0.99(0.02)^{d}	1.10(0.04)^{cd}	*<0.001*
SGR (%)	1.97(0.02)^{a}	1.82(0.04)^{b}	1.38(0.01)^{d}	1.77(0.05)^{b}	1.57(0.01)^{c}	1.77(0.03)^{b}	1.67(0.01)^{b}	*<0.001*
FE (%)	1.07(0.01)^{a}	1.08(0.01)^{a}	0.95(0.02)^{b}	1.10(0.01)^{a}	0.88(0.01)^{c}	1.09(0.01)^{a}	1.08(0.01)^{a}	*< 0.001*

[1]Result values from one-way analysis of variance. See the glossary for abbreviations.

3.1.5 Gene expression profiling (trial 2)

Complete data on liver, white skeletal muscle and heart gene expression are shown in Supplemental Table 14 (Annex 1). As a general rule, fasting produced a down-regulated response of OXPHOS in the liver tissue, which was statistically significant for 80% of the genes present in the array (72 out of 88). In contrast, a statistically significant up-regulated response was found for 29 and 10 genes in white skeletal muscle and the heart, respectively. Overall, in each tissue the magnitude of change paralleled the number of differentially expressed genes, and the multiplier factor for the average fold-change of differentially expressed genes was 0.5 in the liver, 1.7 in white skeletal muscle and 1.5 in the heart.

For a better understanding of expression data, differentially expressed genes with a fold-change cutoff of 1.25 and 0.8 were compiled and graphically represented for each tissue in. In the liver (Fig. 5), the magnitude of change was of the same order within and among all the components of the respiratory chain, encoded either by mtDNA or nDNA. Thus, 30 out of 34 sequences of Complex I, including catalytic (ND2, ND5, NDUFS2, NDUFS4, NDUFS5, NDUFS7, NDUFV1-3), regulatory (NDUFA1-9, NDUFA12, NDUFB2-6, NDUFB9-11, NDUFC1) and assembly factors (NDUFAF2), were significantly down-regulated with fold-changes of 0.3 –0.7. Complex II was also consistently and significantly down-regulated (4 out of 6 sequences) with fold-changes of 0.4–0.5 for catalytic (SDHA), regulatory (SDHC, SDHD) and assembly factors (SDHAF2). Two catalytic (CYB, UQCRFS1) and 8 regulatory (UQCRC1-2, UQCRH, UQCRB, UQCRQ, UQCR10, UQCR11-A, UQCR11-B) subunits of Complex III (10 out of 13) were significantly down-regulated with fold-changes of 0.4–0.7. Complex IV was also extensively down-regulated (17 out of 22 subunits) with fold-changes varying between 0.2 and 0.7 for catalytic (COXI-III), regulatory (COX4a,-b, COX5a2, COX5b2, COX6a2, COX6b1a-b, COX6c1, COX7a1-2, COX7b-c, COX8b) and assembly (SURF1) factors. Finally, 5 catalytic (ATP5A1, ATP5B, ATP5C1, ATP5D, ATP5E) and 6 regulatory (ATP5F1, ATP5G1, ATP5I, ATP5J2, ATP5L, ATP5O) elements of Complex V (11 out of 13) were significantly down-regulated by nutrient intervention with fold-changes of 0.3–0.6.

As shown in Fig. 6, 12 nuclear-encoded subunits of Complex I with catalytic (NDUFS4, NDUFS7), regulatory (NDUFA1, NDUFA4, NDUFA6-7, NDUFB5, NDUFB9-10, NDUFC2) and assembly (NDUFAF2) functions were consistently up-regulated (fold-change 1.3–2.3) by fasting in white skeletal muscle, but we failed to detect consistent changes in catalytic mitochondrial-encoded elements. Complex II was entirely encoded by nDNA and a consistent up-regulation was found for catalytic (SDHB) and regulatory (SDHC, SDHD) subunits with fold changes of 1.4–1.6. It was the same for Complex III and IV with a significant up-regulation of 12 nuclear transcripts encoding for catalytic (UQCRFS1), regulatory (UQCRC1-2, UQCRH, UQCRQ, UQRC10, COX5A1-2, COX8B) and assembly factors (UQCC, SCO1, SURF1) with fold-changes varying between 1.4 and 2.8, but again no consistent changes were found for the mitochondrial-encoded subunits. Less evident were the transcriptionally mediated effects on Complex V, and a consistent up-regulation with fold changes of 1.5 was only found for the nuclear-encoded ATP5A1 and ATP5O.

In the heart (Fig. 7), the number of differentially regulated genes of OXPHOS was drastically reduced to 10 with overrepresentation of nuclear-encoded assembly factors (Complex I, NDUFAF2; Complex II, SDHAF1-2; Complex IV, SURF1) and mitochondrial-encoded elements (Complex III, CYB; Complex IV, COXI, COXII, COXIII) with fold-changes of 1.3–1.4 and 1.6–1.8, respectively.

Liver, fasting down-regulated response
72 out of 88 are differentially regulated genes

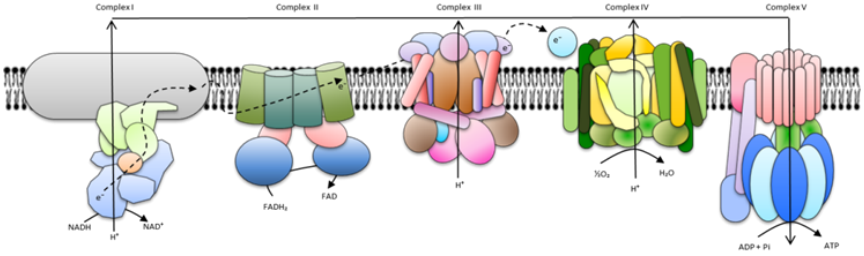

Complex I

ND2	**0.37**	NDUFB2	0.49
ND5	**0.31**	NDUFB3	0.70
NDUFA1	0.51	NDUFB4	0.47
NDUFA2	0.57	NDUFB5	0.57
NDUFA3	0.44	NDUFB6	0.54
NDUFA4	0.61	NDUFB9	0.57
NDUFA4-L2	0.50	NDUFC1	0.64
NDUFA5	0.47	NDUFS2	0.36
NDUFA6	0.72	NDUFS4	0.48
NDUFA7	0.69	NDUFS5	0.58
NDUFA8	0.63	NDUFS7	0.49
NDUFA9	0.45	NDUFV1	0.48
NDUFA12	0.52	NDUFV2	0.51
NDUFB10	0.52	NDUFV3	0.53
NDUFB11	0.50	*NDUFAF2*	*0.47*

Complex II

SDHA	0.47
SDHC	0.45
SDHD	0.42
SDHAF2	*0.42*

Complex III

CYB	**0.53**
UQCRFS1	0.57
UQCRC1	0.64
UQCRC2	0.51
UQCRH	0.67
UQCRB	0.56
UQCRQ	0.50
UQCR10	0.40
UQCR11-A	0.69
UQCR11-B	0.63

Complex IV

COXI	**0.50**
COXII	**0.38**
COXIII	**0.40**
COX4a	0.69
COX4b	0.47
COX5a2	0.44
COX5b2	0.44
COX6a2	0.34
COX6b1a	0.56
COX6b1b	0.58
COX6c1	0.39
COX7a1	0.45
COX7a2	0.43
COX7b	0.19
COX7c	0.39
COX8b	0.35
SURF1	*0.66*

Complex V

ATP5A1	0.48
ATP5B	0.31
ATP5C1	0.37
ATP5D	0.55
ATP5E	0.40
ATP5F1	0.51
ATP5G1	0.38
ATP5I	0.54
ATP5J2	0.38
ATP5L	0.63
ATP5O	0.35

Figure 5. Fold-change of differentially expressed genes (P< 0.05) in the liver tissue of fasted GSB, trial 2. Fish were fed with a commercial diet (Control, CTRL group) or remained unfed for ten days (fasted group). Data of fold-change are relative to the CTRL group. The intensity of green boxes represents the degree of down-regulation. Mitochondrial-encoded catalytic subunits are in bold and red. Nuclear-encoded catalytic subunits are in red. Nuclear-encoded regulatory subunits are in black. Nuclear-encoded assembly factors are in blue and italics.

White skeletal muscle, fasting up-regulated response
29 out of 88 are differentially regulated genes

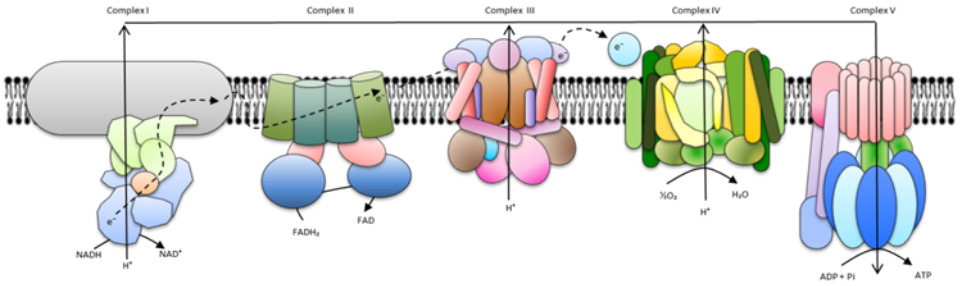

Complex I

NDUFA1	1.35
NDUFA4	1.28
NDUFA6	1.45
NDUFA7	1.72
NDUFA8	1.29
NDUFB5	1.68
NDUFB9	1.46
NDUFB10	1.45
NDUFC2	1.54
NDUFS4	1.43
NDUFS7	1.60
NDUFAF2	*2.30*

Complex II

SDHB	1.56
SDHC	1.52
SDHD	1.43

Complex III

UQCRFS1	1.39
UQCRC1	1.98
UQCRC2	1.95
UQCRH	1.53
UQCRQ	1.46
UQCR10	1.70
UQCC	*2.03*

Complex IV

COX5A1	1.87
COX5A2	1.90
COX8B	1.44
SCO1	*2.78*
SURF1	*1.93*

Complex V

ATP5A1	1.55
ATP5O	1.56

Figure 6. Fold-change of differentially expressed genes (P< 0.05) in the white skeletal muscle of fasted GSB, trial, 2. Fish were fed with a commercial diet (Control, CTRL group) or remained unfed for ten days (fasted group). Data of fold-change are relative to the CTRL group. The intensity of red boxes represents the degree of up-regulation. Nuclear-encoded catalytic subunits are in red. Nuclear-encoded regulatory subunits are in black. Nuclear-encoded assembly factors are in blue and italics.

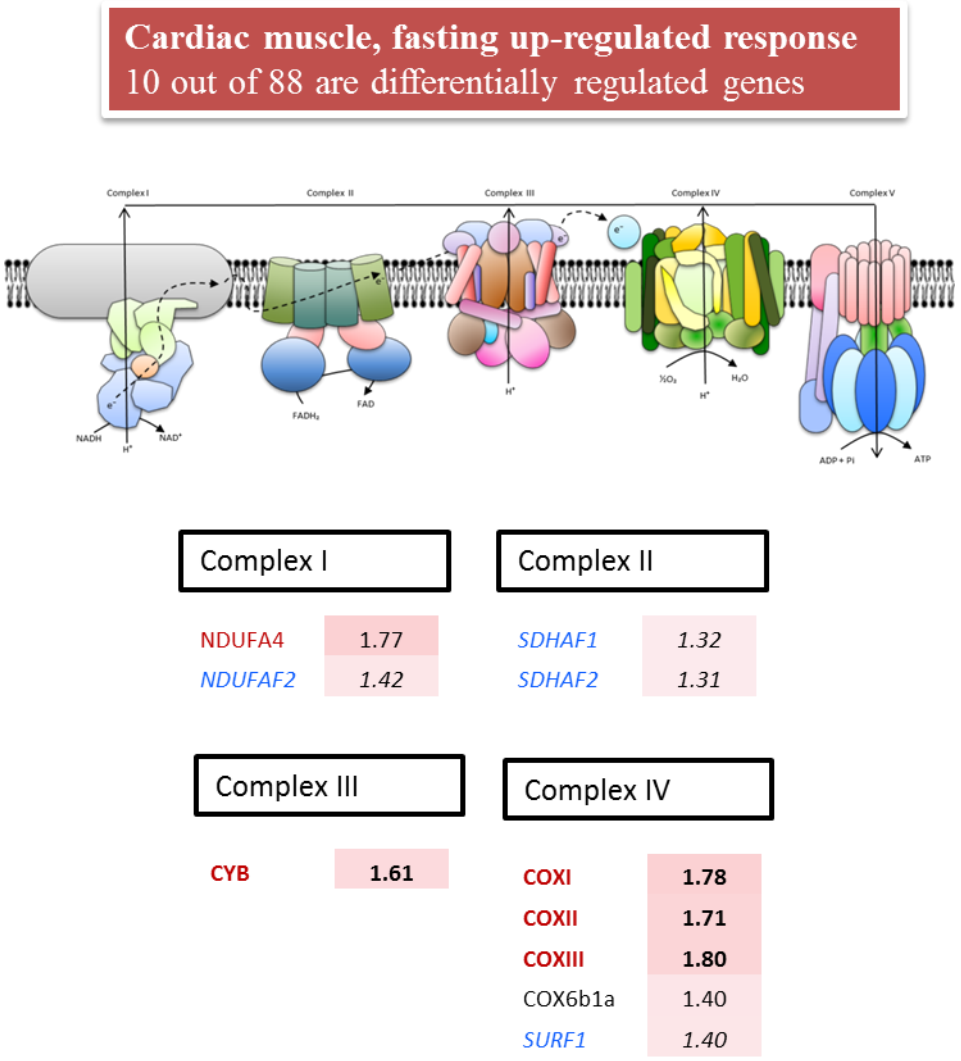

Figure 7. Fold-change of differentially expressed genes (P< 0.05) in the cardiac muscle of fasted GSB, trial 2. Fish were fed with a commercial diet (Control, CTRL group) or remained unfed for ten days (fasted group). Data of fold-change are relative to the CTRL group. The intensity of red boxes represents the degree of up-regulation. Mitochondrial-encoded catalytic subunits are in bold and red. Nuclear-encoded catalytic subunits are in red. Nuclear-encoded regulatory subunits are in black. Nuclear-encoded assembly factors are in blue and italics.

3.1.6 Gene expression profiling (trial 3)

The effect of nutrient deficiencies on the relative mRNA expression of growth-related genes in liver and muscle are shown in supplemental Tables 19 and 20 (Annex 1), respectively. In the liver tissue, up to 74 genes included in the array had detectable levels. Among them, 21 were differentially expressed in response to a given nutrient deficiency. Relative expression of GHR-I, IGF-I, IGF-II, IGFBP4 and IGFALS were consistently down-regulated in n-3 LC-PUFA and P groups in comparison to CTRL fish, which highly reflected the poorest growth performance of fish fed these nutrient deficient diets. IGFBP2, another related marker of GH/IGF system, was exclusively down-regulated in n-3 LC-PUFA fish. Conversely, the expression of a proliferative cell marker (PCNA) was significantly up-regulated in the Vit group with a clear opposite trend in n-3 LC-PUFA group. Markers of protein-breakdown were also differentially affected by dietary intervention with the highest expression of MET in Vit and Min fish groups and the lowest in SAA fish. Likewise, CAPN1 was down-regulated in n-3 LC-PUFA and P fish. CTSD was only down-regulated in the group of LC-PUFA fish, although a similar trend was found in SAA, PL, Min and Vit groups. Conversely, the highest

expression of CTSL was found in PL fish and the lowest in the P group. The relative expression of molecular chaperones was also affected by the nutritional status with the highest expression of GRP-170 and GRP-94 in Min fish, and the lowest in LC-PUFA and/or P fish groups. Similarly, the lowest expression of DER-1 was found in the LC-PUFA fish and the highest in PL, Min and Vit fish with intermediate values in the other three experimental groups. The expression of IL-receptors was also altered with a down-regulated expression of IL-1R1 and IL-6RB in LC-PUFA and P fish, which was especially evident when comparisons were made with the Vit group. Otherwise, markers of energy sensing (SIRT4), oxidative phosphorylation (SCO1) and mitochondrial respiration uncoupling (UCP1) were overexpressed in P fish, whereas key limiting enzymes on mitochondrial FA transport (CPT1A) were up-regulated in LC-PUFA fish with the lowest expression in P fish.

Most of the genes present in the growth array were found at detectable levels in white skeletal muscle (82 out of 89). Like liver, up to 22 genes were differentially expressed in response to different nutrient stressors, although the most responsive genes and the resulting molecular signature were highly tissue-specific. Hence, GHR-I and GHR-II were up-regulated in the skeletal muscle of fish PL and P deficient diets, respectively. By contrast, IGFR2 was consistently down-regulated in P fish but not in PL fish, and the expression of IGF-II was intriguingly up-regulated in Vit fish. Most muscle myogenic factors, including MyoD2, MSTN, MEF2A and FST were differentially regulated by nutritional intervention, with an opposite trend for MyoD2 in SAA, P and Min fish (up-regulation) in relation to Vit fish (down-regulation). MST and MEF2A were consistently up-regulated in P fish and n-3 LC-PUFA fish, respectively. By contrast, FST was down-regulated in either PUFA or PL fish. Muscle proteases were also affected in a large extent by dietary intervention and CAPN3 was mostly down-regulated in SAA fish. CAST was primarily up-regulated in P fish, whereas the up-regulation of CTSB and CTSD was highly specific of Vit fish. Likewise, some markers of protein-ubiquitination pathway (UCHL3) were significantly up-regulated in this fish group of fish. Muscle inflammatory/anti-inflammatory markers were also highly responsive to dietary vitamin deficiencies with a consistent up-regulation of IL-1R1, IL-1R2 and IL-6RB as well as IL-10, IL-10RA and IL-10RB in Vit fish, which was linked to up-regulation of SIRT3, SCO1 and UCP2. By contrast, the LXRα was significantly down-regulated in SAA fish but not in the other experimental groups.

The above different molecular signatures for a given tissue a nutrient deficiency is reinforced by the results of PCA. Thus, in the liver, the most divergent groups are fish fed P and n-3 LC-PUFA diets (Fig. 8), but interestingly fish fed the Vit deficient diet clearly emerged as the outlier group in the case of muscle tissue (Fig. 9).

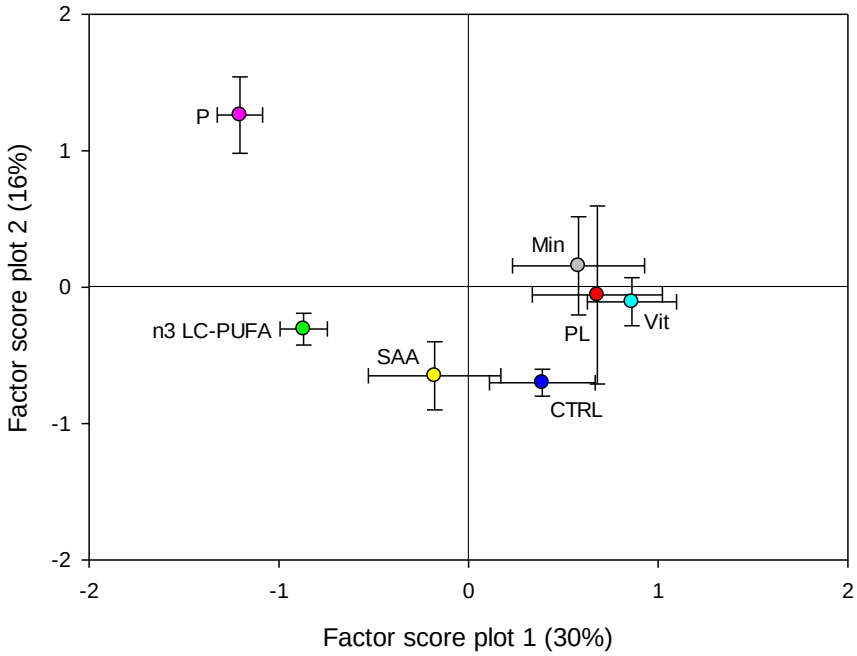

Figure 8. PCA scores resulting from the analysis of the gene expression of liver of GSB fed the different nutrient-deficient diets in trial 3.

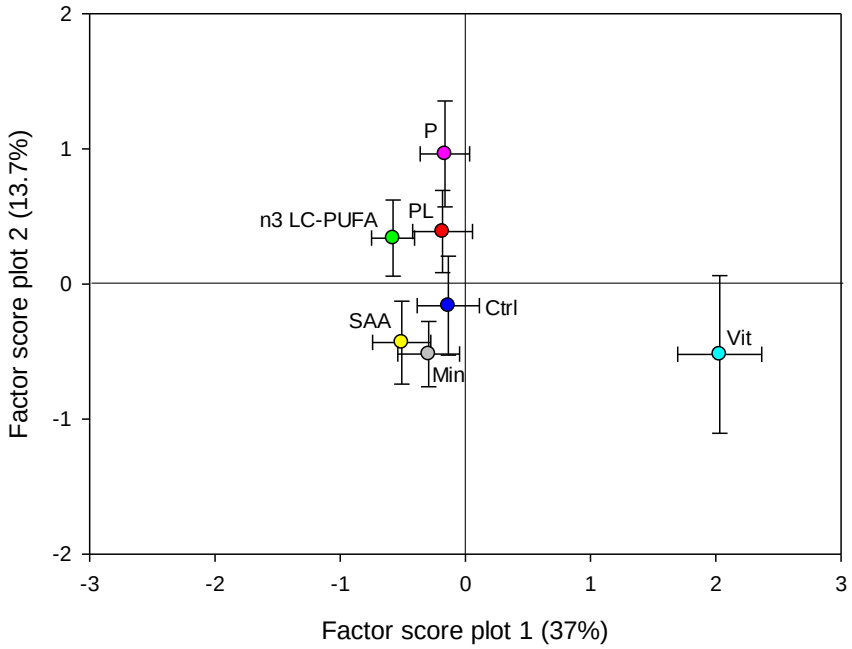

Figure 9. PCA scores resulting from the analysis of the gene expression of white skeletal muscle of GSB fed the different nutrient-deficient diets in trial 3.

3.2 Atlantic salmon (IMR, UoS)

3.2.1 Growth performance

Dietary SBM inclusions up to a level of 200 g kg^{-1} (i.e. feed S10 and S20) did not result in a significant loss of performance and had a growth rate comparable with that of S0. Alternatively, S30 (300 g kg^{-1} SBM inclusion) induced a significant growth retardation (Table 4).

Table 4. Growth performance and somatic indexes of Atlantic salmon

Diet	Initial wt (g)	Final wt (g)	SGR
S0	175 ± 27	424 ± 78^{a}	1.03 ± 0.22^{a}
S10	170 ± 25	422 ± 76^{a}	1.03 ± 0.21^{a}
S20	176 ± 28	405 ± 67^{a}	0.96 ± 0.16^{b}
S30	175 ± 25	378 ± 67^{b}	0.87 ± 0.18^{c}

Mean ± SD of 45 fish x 3 replicates per diet. Weight (wt). Data were analysed by nested ANOVA. SGR calculations were based on individual fish growth rates. Different letters denote statistical significance ($P < 0.05$). Values not sharing similar letters within each column are significantly different.

3.2.2 Transcriptome analysis: Overview

Hierarchical clustering performed on the gene expression data indicated the existence of a clear structure in the dataset with four main clusters (Fig 10). The first clear separation was between the liver (red shaded, Fig 10) and the intestine (blue shaded, Fig 10) that formed two independent clusters fully supported by statistical values (100). Within each tissue cluster the dietary treatments S0 and S30 also induced a clearly identifiable gene expression response. The response of the intestine was fully supported by statistical bootstraps (100), whereas that of the liver received a weaker, but still significant support (63-68).

The analysis of differential expression computed by Limma reflected the structure observed by hierarchical clustering indicating a marked response in the intestine where a total of 2331 gene were differentially expressed ($P < 0.01$) and a less pronounced but still evident response in liver where 259 genes were differentially expressed ($P < 0.01$). The difference between the two tissues was immediately evident in that the intestine had generally greater (by fold changes) and more significant (by P values) response compared with that of the liver (Fig. 11a & b).

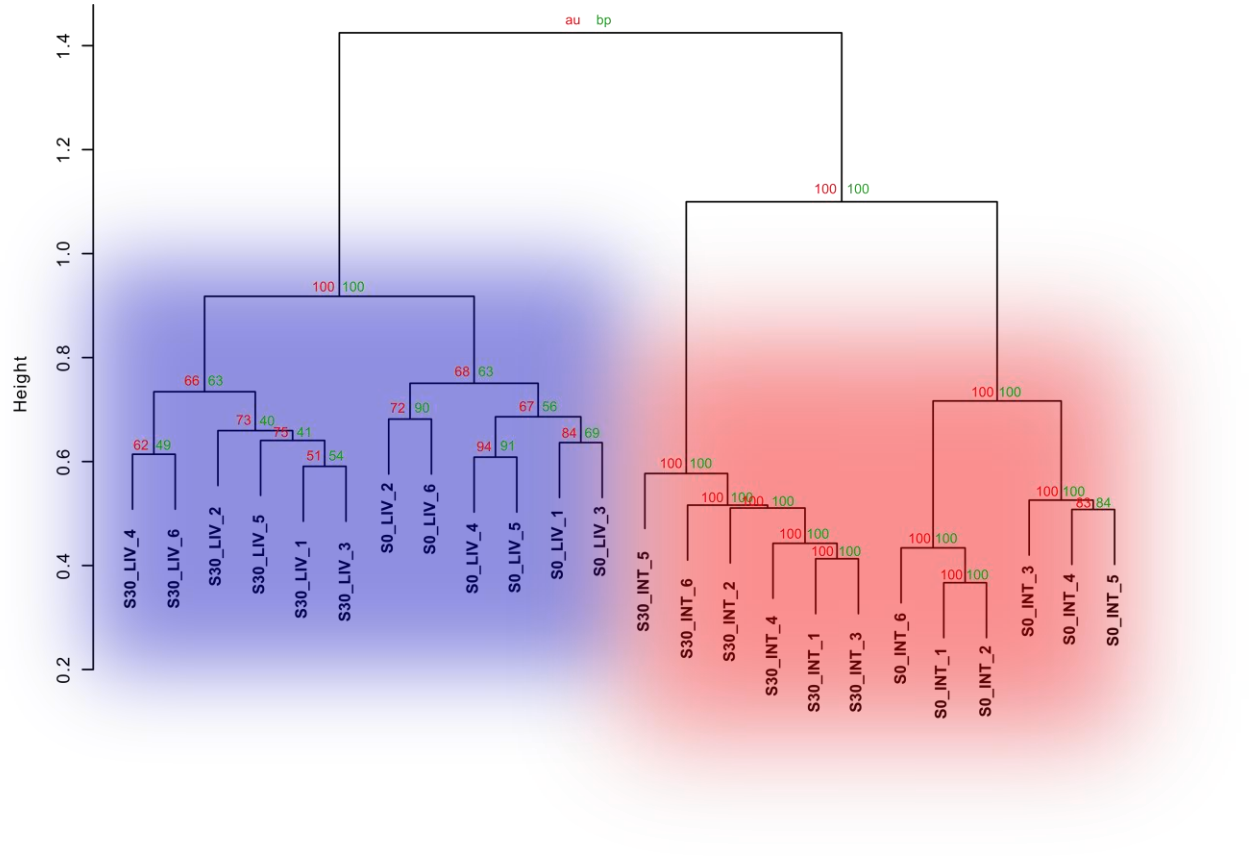

Figure 10. Hierarchical clustering of gene expression samples. Two types of *p*-values are provided: AU (Approximately Unbiased) is computed by multiscale bootstrap resampling (1000 rep) and reported in red and BP (Bootstrap Probability) is computed by normal bootstrap resampling is reported in green. INT is intestine and LIV is liver.

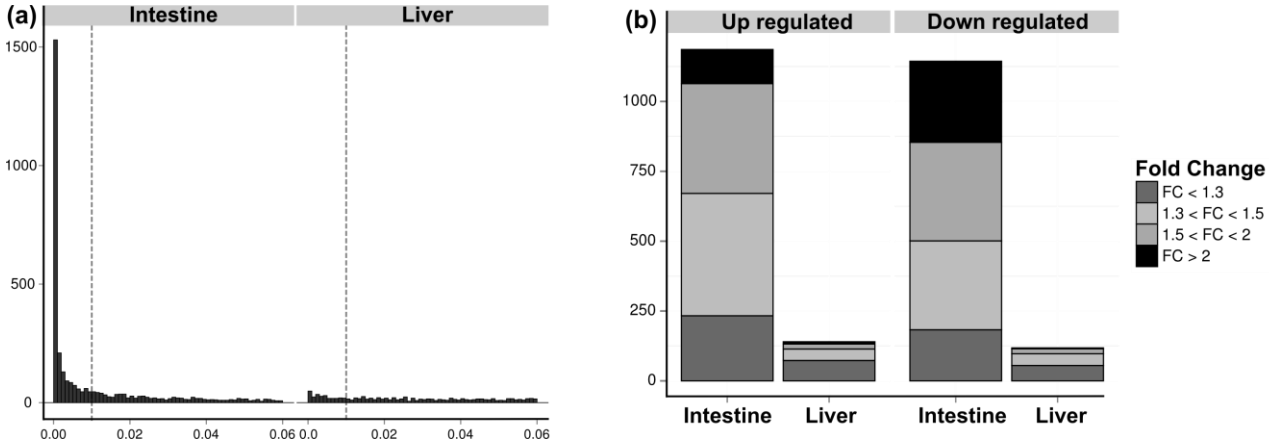

Figure 11. Histograms plotting the results of differential expression analysis in liver and intestine in S30 compared to S0. Figure 2a plots the number of differentially expressed genes based on *p* value and shows that a larger number of genes with a $P < 0.01$ (the dashed line depict the *p* value = 0.01) were present in the intestine. Figure 2b only plots genes with $P < 0.01$. FC is fold change.

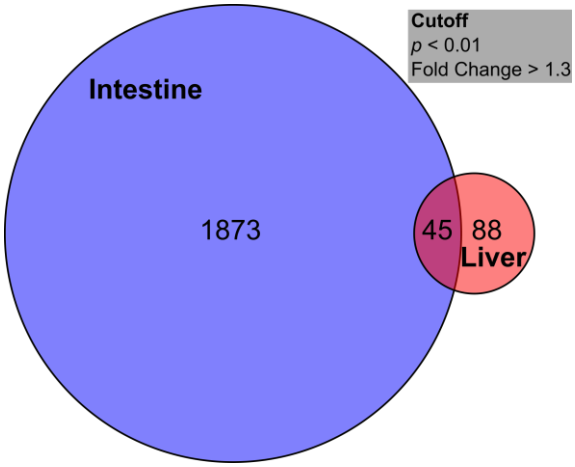

Figure 12. Venn diagram comparing the response of liver and intestine. The overlapping area indicates the genes differentially expressed in both tissues. Only genes that had a fold change > 1.3 and *P* < 0.01 in both tissues are shown. The common 45 genes are presented in Table 3.

A total of 45 genes were significantly affected (*P* < 0.01) in both tissues, while the remaining represented a tissue-specific response (Fig. 12). Of those genes affected in both liver and intestine, 31 were regulated towards the same direction (either up or down regulated in both tissues) while 13 were regulated in opposite directions (Table 5). Expression was always reported compared to the S0 treatment. Amongst genes whose transcript abundance increased in both liver and intestine there was an over-representation of ribosomal subunits (L5, L21, L11, L3, S3A), enzymes involved in ribosome biogenesis such as ribonucleases P/MRP protein subunit RPP25, casein kinase II subunit alpha, proteins involved in RNA processing such as translation initiation factor 5 and cleavage and polyadenylation specificity factor subunit 5, the spliceosome component U5 snRNP protein and factors involved in protein processing such as ER degradation enhancer, mannosidase alpha 3 (Table 4). In addition, the bile salt-stimulated lipase and complement component C7 also increased in both tissues. Alternatively, down-regulated genes were mostly coding for proteins involved in metabolic processes such as lipid metabolism (glycerol kinase, elongation of very long chain fatty acids protein 5, very long chain-3 hydroxyacyl-dehydratase), sugar metabolism (GDP-L-fucose synthase) and glycan metabolism (alpha-1,6-mannosyl-glycoprotein beta-1,2-N-acetylglucosaminyltransferase).

Table 5. Genes differentially expressed ($P < 0.01$) in both liver and intestine of AS.

			LIVER		INTESTINE	
Probe Name	*KOID*	*Description*	*logFC*	*P.Value*	*logFC*	*P.Value*
Ssa#S18863091	K02377	GDP-L-fucose synthase	-1.01	0.0028	-4.15	< 0.0001
Ssa#STIR17220	K15985	cAMP-dependent protein kinase inhibitor alpha	-0.68	0.0013	-1.22	< 0.0001
Ssa#STIR09972	K00736	alpha-1,6-mannosyl-glycoprotein beta-1,2-N-acetylglucosamir	-0.54	0.0035	-1.17	< 0.0001
Omy#S19713672	K00864	glycerol kinase	-0.53	0.0050	-1.10	< 0.0001
Ssa#STIR19155	K03940	NADH dehydrogenase (ubiquinone) Fe-S protein 7	-0.53	0.0076	-0.75	0.0004
Ssa#S18889774	K11251	histone H2A	-0.53	0.0066	-0.79	0.0002
Ssa#S18892283	K10244	elongation of very long chain fatty acids protein 5	-0.52	0.0039	-1.12	< 0.0001
Ssa#STIR02057	K10703	very-long-chain (3R)-3-hydroxyacyl-dehydratase	-0.50	0.0013	-1.22	< 0.0001
Ssa#CL8Contig2	K00522	ferritin heavy chain	-0.40	0.0063	-0.85	< 0.0001
Ssa#STIR14547	K04644	clathrin light chain A	-0.37	0.0031	-0.51	0.0001
Ssa#STIR09213	K11428	histone-lysine N-methyltransferase SETD8	-0.30	0.0034	-0.28	0.0057
Ssa#STIR24145	K06109	Ras-related protein Rab-13	-0.29	0.0074	-0.46	< 0.0001
Ssa#S48420585	K02977	small subunit ribosomal protein S27Ae	-0.23	0.0099	-0.24	0.0064
Ssa#S30295137	K09850	Ras association domain-containing protein 1	0.26	0.0084	0.27	0.0063
Ssa#STIR03252	K14525	ribonucleases P/MRP protein subunit RPP25	0.33	0.0023	0.55	< 0.0001
Ssa#S30282579	K12859	U5 snRNP protein, DIM1 family	0.34	0.0090	0.40	0.0024
Ssa#CX727575	K02932	large subunit ribosomal protein L5e	0.35	0.0091	0.59	< 0.0001
Ssa#S35581780	K02889	large subunit ribosomal protein L21e	0.35	0.0049	0.57	< 0.0001
Ssa#TC80353	K03262	translation initiation factor 5	0.36	0.0019	0.35	0.0027
Omy#CR372283	K02868	large subunit ribosomal protein L11e	0.38	0.0016	0.51	< 0.0001
Ssa#S35675551	K02984	small subunit ribosomal protein S3Ae	0.39	0.0051	0.53	0.0003
Ssa#S19097184	K00940	nucleoside-diphosphate kinase	0.40	0.0064	0.60	0.0001
Ssa#S18892246	K12298	bile salt-stimulated lipase	0.41	0.0004	0.30	0.0058
Ssa#S35660727	K03996	complement component 7	0.41	0.0061	0.52	0.0009
Ssa#STIR22184	K10086	ER degradation enhancer, mannosidase alpha 3	0.43	0.0076	0.43	0.0072
Ssa#S32004762	K03097	casein kinase II subunit alpha	0.47	0.0007	0.58	< 0.0001
Ssa#CL26Contig2	K02936	large subunit ribosomal protein L7Ae	0.52	0.0003	0.70	< 0.0001
Ssa#S35514366	K08765	carnitine O-palmitoyltransferase 1	0.65	0.0023	0.74	0.0007
Omy#S18928540	K09414	heat shock transcription factor 1	0.77	< 0.0001	0.45	0.0038
Omy#S34313815	K14397	cleavage and polyadenylation specificity factor subunit 5	0.90	0.0002	0.96	< 0.0001
Ssa#STIR38249	K01594	sulfinoalanine decarboxylase	1.03	0.0060	2.56	< 0.0001
Ssa#STIR15782	K11262	acetyl-CoA carboxylase / biotin carboxylase	-0.84	0.0015	0.70	0.0068
Ssa#STIR24420	K00222	delta14-sterol reductase	-0.61	0.0028	0.64	0.0017
Ssa#STIR14033	K01507	inorganic pyrophosphatase	-0.53	0.0042	1.08	< 0.0001
Ssa#TC99926	K01875	seryl-tRNA synthetase	-0.47	0.0043	0.82	< 0.0001
Ssa#DW469980	K04440	c-Jun N-terminal kinase	-0.25	0.0062	0.30	0.0015
Ssa#STIR13401	K10577	ubiquitin-conjugating enzyme E2 I	0.32	0.0057	-0.39	0.0011
Ssa#DY727734	K07292	hepatocyte nuclear factor 4-alpha	0.36	0.0035	-0.51	0.0001
Ssa#S35672064	K10574	ubiquitin-conjugating enzyme E2 B	0.38	0.0059	-0.48	0.0008
Ssa#S35702211	K06624	cyclin-dependent kinase inhibitor 1B	0.55	0.0034	-0.81	< 0.0001
Ssa#S24638283	K08550	estrogen receptor alpha	0.63	0.0082	-0.77	0.0015
Ssa#STIR20675	K12408	cholest-5-ene-3beta,7alpha-diol 3beta-dehydrogenase	0.68	0.0055	-1.40	< 0.0001
Ssa#STIR16390	K01103	6-phosphofructo-2-kinase / fructose-2,6-bisphosphatase	0.75	0.0004	-2.99	< 0.0001
Ssa#STIR10702	K04630	guanine nucleotide-binding protein G(i) subunit alpha	1.52	0.0018	-4.41	< 0.0001

Up-regulated genes are highlighted in red, while down regulated genes in green. Colour intensity is relative to the magnitude of change. All expression values are reported as $\log_2$ fold change (logFC) relative to the control treatment FM. KOID = KEGG identifier.

To profile the specific response of each tissue, gene-set enrichment analysis was used to identify mechanistic changes of group of genes (sections 3.3 and 3.4). A large number of gene-sets were significantly affected ($q < 0.1$) in the intestine, while liver was only marginally affected, clearly reflecting the results herein observed in terms of differentially expressed genes.

3.2.3 Transcriptomic analysis: Distal Intestine

A global response affected the distal intestine, involving genes regulating a number of different processes (Fig. 13a & b). Major biological processes affected in the intestine identified by either *1d* and *2d* analyses included metabolism (e.g. lipid, amino acid and energy metabolism), organismal systems (e.g. digestion and absorption, immune and endocrine system) and cellular processes. Amongst the highly significantly regulated gene-

sets (q < 0.0001) identified through *2d* test (*2d* allows genes to change in both directions simultaneously) there were the cellular organelles lysosome and phagosome, PPAR signalling pathway of the endocrine system, fat and vitamin digestion and absorption pathways, antigen processing and presentation (immune system) and a number of pathways of metabolism including glycan degradation, amino sugar and nucleotide sugar degradation, retinol metabolism, arginine/proline metabolism, alanine/aspartate/glutamate metabolism and glutathione metabolism (Fig. 13a). A number of other pathways, mostly metabolic, were differentially expressed below the q = 0.0001 cut-off (Fig. 13a). The *1d* test (testing that all genes are moving towards the same direction) is also helpful to identify the overall trend of expression within specific pathways. As expected, the majority of gene-sets that tested significant in the *2d* test were also significant with the *1d* test. However, the *1d* test revealed the presence of a number of genetic information processing gene-sets (e.g. ribosome, proteasome, spliceosome, RNA transport, etc.) amongst the up-regulated and highly significantly different gene-sets (Fig. 13b). Amongst gene-sets with increased expression in response to the S30 treatment were those regulating functions such as cell growth and death, cell cycle, apoptosis and MAPK signalling (Fig. 13b). Amongst the down-regulated pathways there were those of metabolism that significantly decreased in response to S30 compared to the control (S0). Other down-regulated processes included digestion and absorption of proteins, fats, vitamins and minerals. Finally, down-regulation of organelles/cellular compartments such as lysosome and peroxisome was also detected (Fig. 13b).

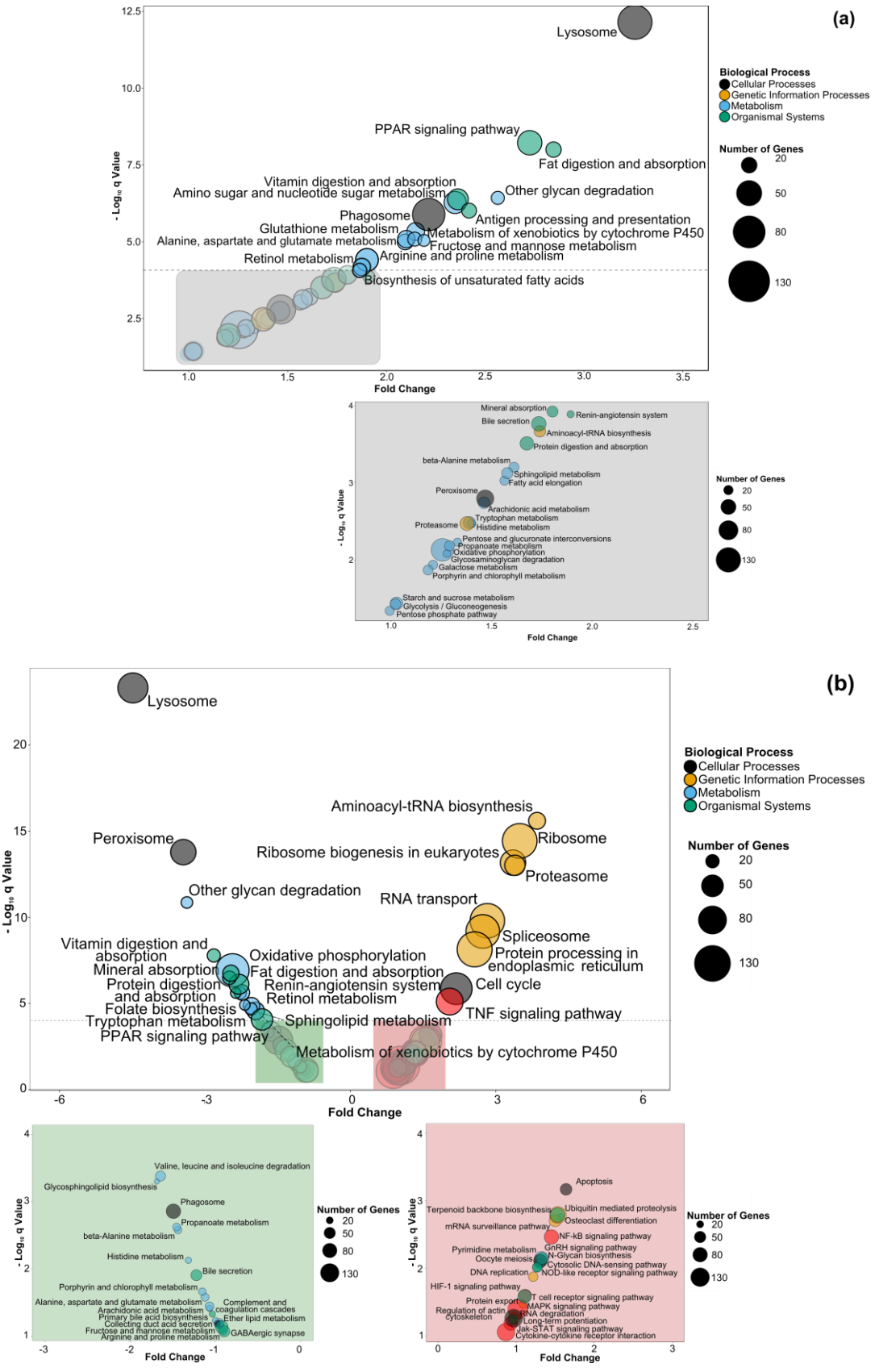

Figure 13a & b. Bubble graph plotting GAGE results from the *2d* test (a) and *1d* test (b) in the intestine of AS. The x-axis plots the fold change (mean statistics) while the y-axis plots the Log_{10} transformed *q*-value. The size of the bubbles is proportional to the number of genes used by the algorithm to test the gene-set. Colours of bubbles refer to the biological process (KEGG classification).

The dashed line denotes the cutoff of “highly significant gene-sets” (q < 0.0001). Figures are not on the same scale.

An overall increased expression of a number of pathways and their underlying genes involved in the immune response were observed. Fig. 14 summarizes propose a model for the response observed involving the pathways and genes differentially expressed in S30 compared with S0 in the distal intestine (Fig. 13a &b). The immune response involved the up-regulation of a number of pathways, notably the TNF signalling pathway (p < 0.0001), NOD-like receptor interaction, NF-kB signalling pathway and cytosolic DNA sensing pathway, Jak-STAT signalling pathway, cytokine-cytokine receptor interaction and T cell receptor signalling pathway (gage *1d* test, Fig. 13b).

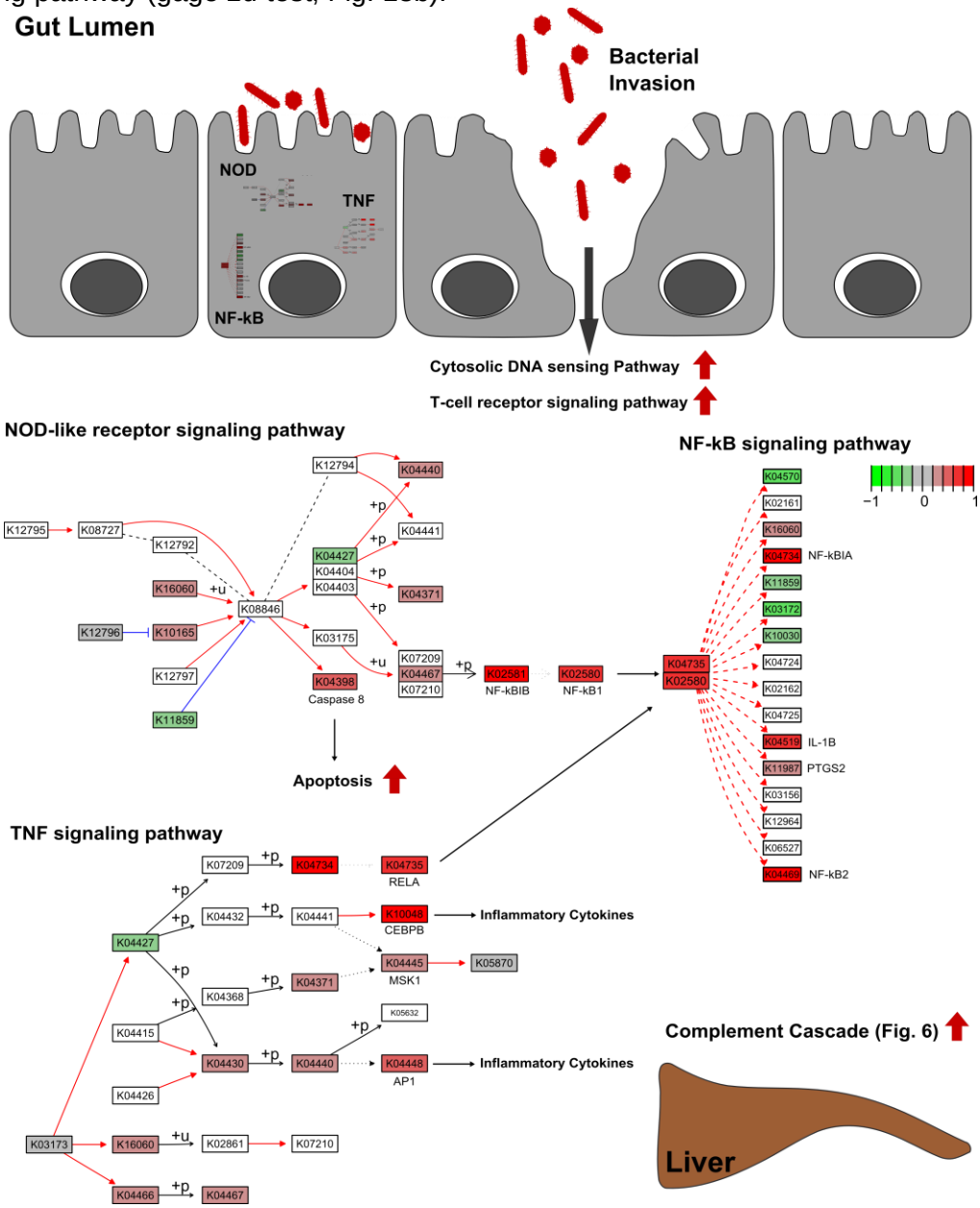

Figure 14. Differentially expressed genes detected in the distal intestine of AS fed 300 g kg^{-1} SBM inclusions compared with control diet (0 g kg^{-1}). The figure shows the model proposed from present results occurring in the distal intestine of fish undergoing nutritional stress. NF-kB1is nuclear factor NF-kappa p105 subunit, NF-kBIB is NF-kappa-B inhibitor beta, IL-1B is Interleukin 1 beta, PTGS2 is prostaglandin-endoperoxide synthase 2, BIRC2_3 is baculoviral IAP repeat-containing protein 2/3, CEBPB is CCAAT/enhancer-binding protein beta, RELA is NF-kappa-B p65 subunit, AP1 is transcription factor AP-1, MSK1 is ribosomal protein S6 kinase alpha-5. Gene abbreviation is reported

only for certain key genes. KEGG identifier is also reported. For clarity, only selected cascades of the pathways are shown. Red arrows indicate activation, blue arrow inhibition, dotted arrows indirect effect, +p indicates phosphorylation, +u indicates ubiquitination.

3.2.4 Transcriptomic analysis: liver

Compared with the distal intestine, liver was only marginally affected by the S30 treatment (Fig. 15a & b). Gene sets significantly affected in this tissue involved processes such as lipid (steroid biosynthesis), amino acid (glycine/ serine/threonine metabolism, alanine/aspartate/glutamate metabolism), energy (oxidative phosphorylation) and vitamin metabolism (retinol metabolism). Immune and endocrine functions were also significantly perturbed (complement and coagulation cascades, PPAR signalling pathway), together with the PI3K-Akt pathway.

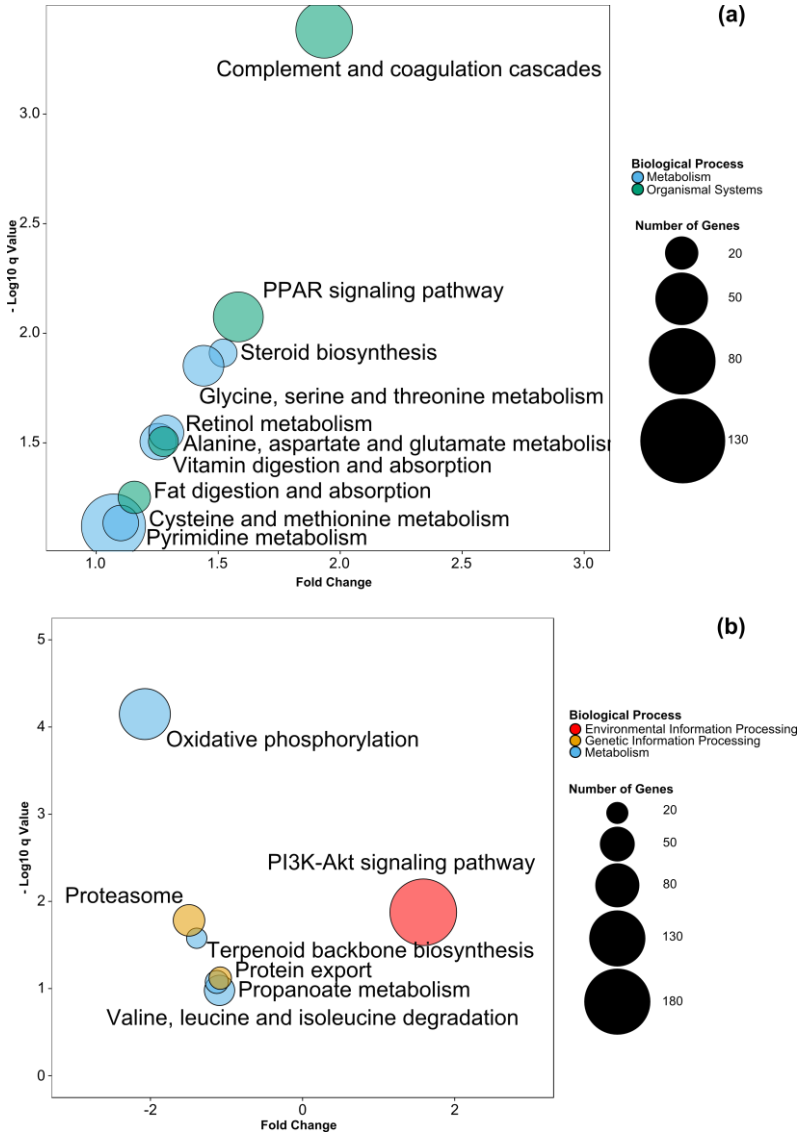

Figure 15. Bubble graph plotting GAGE results from the *2d* test (a) and *1d* test (b) in the liver of AS. The x-axis plots the fold change (mean statistic) while the y-axis plots the Log_{10} transformed *q*-value. The size of the bubbles is proportional to the number of genes used by the algorithm to test the gene-set. Colours of bubbles refer to the biological process (KEGG classification). Figures are not on the same scale.

The most significantly affected gene-set in the liver was the complement and coagulation cascades. The array included a number of genes that participate in this pathway and they were all up-regulated, including complement component 3 (C3), C5, C6 and C7, complement component receptor type 2 and the mannan-binding lectin serine protease 1 (MASP1) (Fig. 16). In contrast, the CD59 antigen was down-regulated.

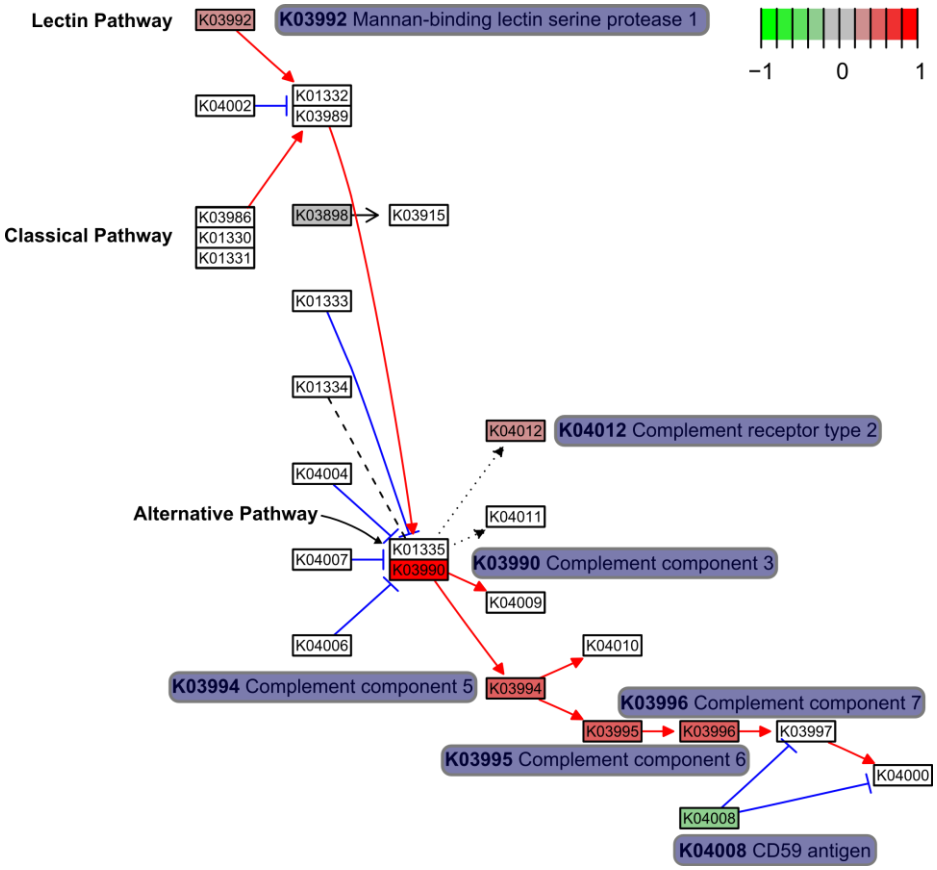

Figure 16. Complement cascade generated with the R package *pathview* (Luo and Brouwer, 2013). Red arrows indicate activation, blue arrow inhibition and dotted arrows indirect effect. Highlighted in blue are the names of the differentially expressed genes and the corresponding KEGG identifier.

3.2.5 Identification of markers for molecular phenotyping

The genes presented in Table 6 were chosen as representative of affected functions identified after transcriptome analysis for molecular phenotyping. These genes were amplified by RT-qPCR.

Table 6. Selection of genes with key functions to represent good candidate for molecular phenotyping and nutrigenomic profiling in AS.

Tissue	KEGG ID	Gene Name	LogFC	*p* Value	Cellular function
Liver	K01312	Trypsin	1.12	0.0000	*Digestive enzyme overproduced by pancreatic tissue in fish fed ingredients containing trypsin inhibitors*
Liver	K01597	Diphosphomevalonate decarboxylase	-0.63	0.0002	*Enzyme of to the family of lyases, participate in the biosynthesis of steroids*
Liver	K00164	2-oxoglutarate dehydrogenase E1 component	0.61	0.0001	*Key enzyme participating into the citric acid cycle, lysine degradation and tryptophane metabolism*
Liver	K12298	Bile salt-stimulated lipase	0.41	0.0004	*Enzyme produced by the pancreatic tissue participating in the digestion of fats*
Liver	K01435	Biotinidase	-0.85	0.0006	*Involved in the recycle of the B vitamin biotin, a water-soluble vitamin involved in the metabolism of fats, carbohydrates and proteins*
Intestine	K08847	Receptor-interacting serine/threonine-protein kinase 3	1.28	0.0000	*Essential for programmed cell death process in response to death-inducing TNF-alpha family members*
Intestine	K04364	Growth factor receptor-binding protein 2	-0.76	0.0000	*Involved in signal transduction/cell communication*
Intestine	K06503	Transferrin receptor (p90, CD71)	0.68	0.0011	*Transferrin receptor maintains cellular iron homeostasis*
Intestine	K05482	Interleukin 18	1.08	0.0000	*Proinflammatory cytokine*
Intestine	K09869	Aquaporin-8	-4.96	0.0000	*Water channel protein*
Intestine	K14619	Transcobalamin-2	-2.36	0.0000	*Binds cobalamin once it has been uptaken by enterocytes of the distal intestine and the "Intrinsic Factor-Vitamin B12" complex has been degraded*
Intestine	K08751	Fatty acid-binding protein 2, intestinal	-2.23	0.0000	*Lipid binding protein*

3.3 Rainbow trout (INRA)

3.3.1 Trial 1. Markers of reduced feed intake in rainbow trout fed a diet deficient in (essential) amino acids (methionine and total protein)

Fig. 17 shows the growth performance during the 12-week of feeding. Trout fed diet MP1 had the highest final weight (117 ± 3 g), followed by the MP0 group (79 ± 18 g), then the LP1 group (54 ± 6 g), while the group fed LP0 with food (42 ± 3 g) has not grown over the 12 weeks. These results confirm the negative effect of the low protein content and of a methionine deficiency on growth performance of RT, as indicated by the 2-way ANOVA: protein effect (P <0.001) and methionine effect (P < 0.01). Fig. 18 shows the food intake of the fish, expressed in gram per unit metabolic body weight, so after correcting for differences in growth. The two-way ANOVA showed a significant effect of protein and methionine level on the amount of feed intake (P < 0.05) in both cases.

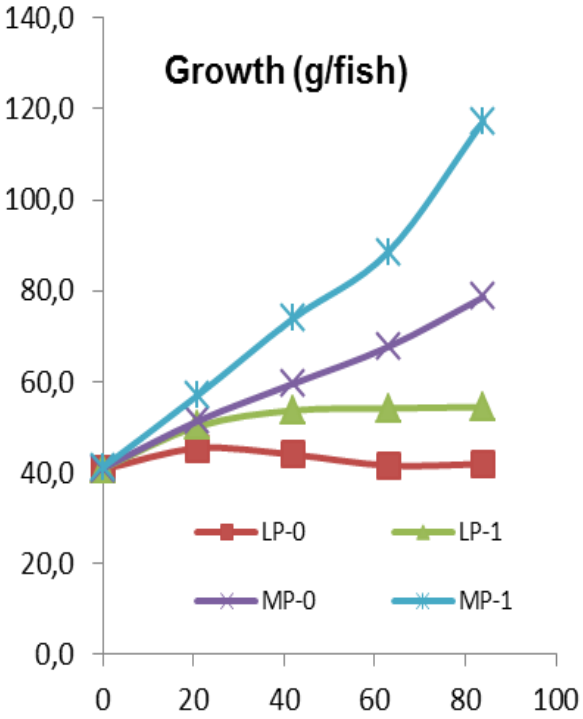

Figure 17. Growth of the trout (g) fed the different diets for 12 weeks in trial 1.

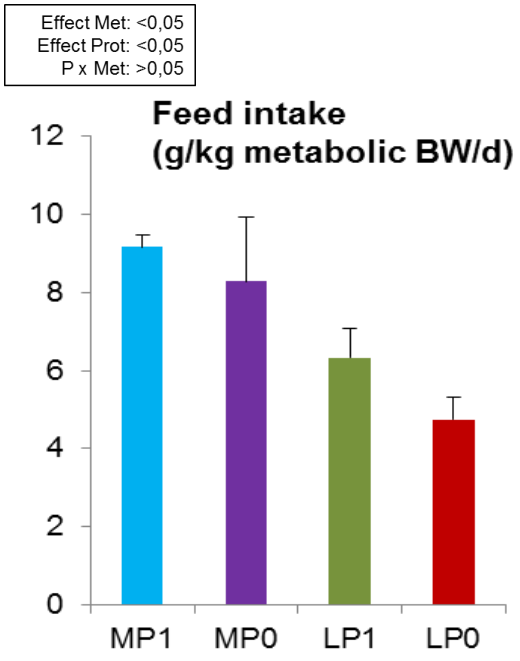

Figure 18. The amount of daily feed intake in trout fed the different diets in trial 1.

The relative mRNA expression of genes involved in the central detection of an essential amino acid deficiency and in the control of food intake is shown in Fig. 19A and 19B. Both the low amount of dietary methionine and protein increased the gene expression of ATF4 in the trout brain, confirming its transcriptional regulation (Figure 19A). In contrast, methionine deficiency had no significant effect on the mRNA level of the ASNS gene (Fig. 19A), which was found to be increased only by the dietary protein intake. The two analysed subtypes of somatostatin receptor family, SSTR1B and SSTR2, showed increased expression in brain of trout fed the low protein diet. There was no significant effect of methionine content on SSTR2, whereas SSTR1B gene expression was stimulated by the two dietary factors.

Regarding the expression of feeding peptides, our results show a significant increase

in the expression of the NPY gene level when the dietary protein supply is deficient. However there was no significant effect of the methionine content of its expression (Fig. 3A). The gene expression of CCK-N and CCK-T in the trout brain was significantly increased by both dietary deficiencies, protein and methionine (Fig. 19B)

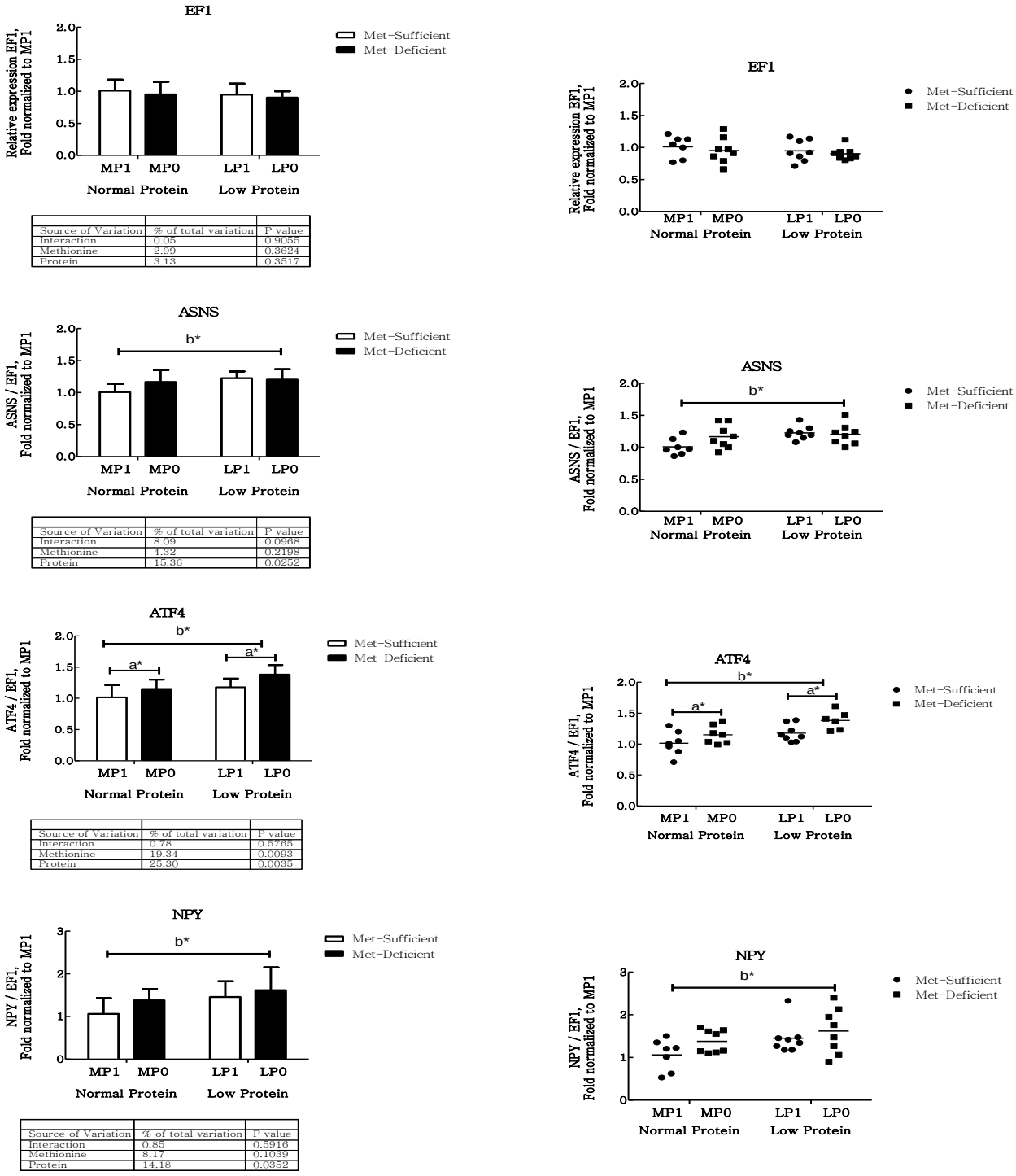

Figure 19A. Expression of markers of amino acid sensing (ASNS, ATF4 genes) and feed intake (NPY gene) in the brain of RT as a function of the diets fed, in trial 1. EF1α served as housekeeping gene a*: significant effect related with Methionine level (adequate vs deficient) b*: significant effect related with protein level (adequate *vs* deficient).

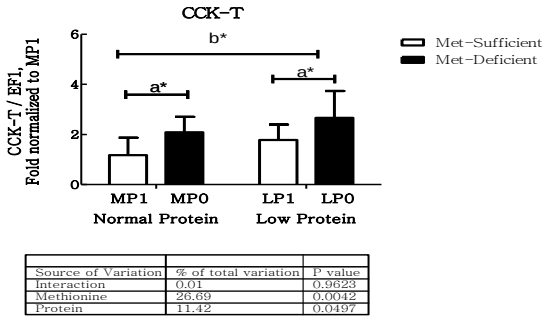

Source of Variation	% of total variation	P value
Interaction	0.01	0.9623
Methionine	26.69	0.0042
Protein	11.42	0.0497

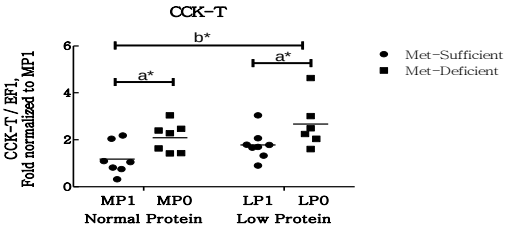

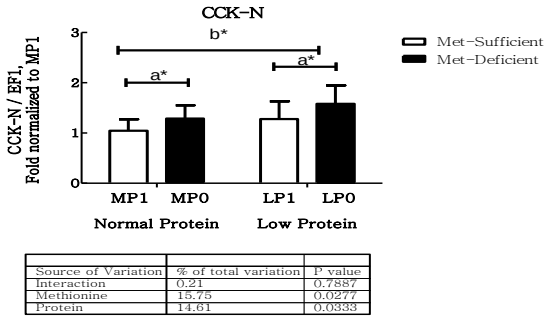

Source of Variation	% of total variation	P value
Interaction	0.21	0.7887
Methionine	15.75	0.0277
Protein	14.61	0.0333

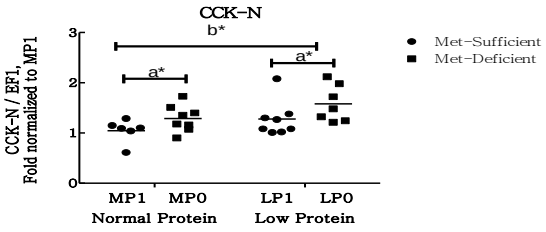

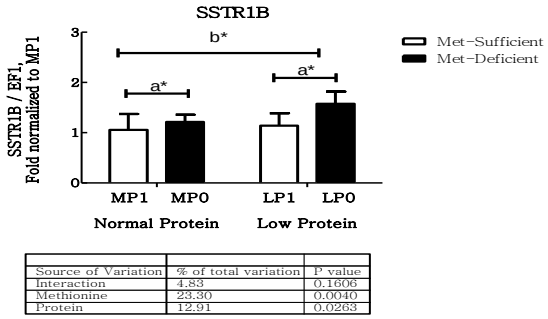

Source of Variation	% of total variation	P value
Interaction	4.83	0.1606
Methionine	23.30	0.0040
Protein	12.91	0.0263

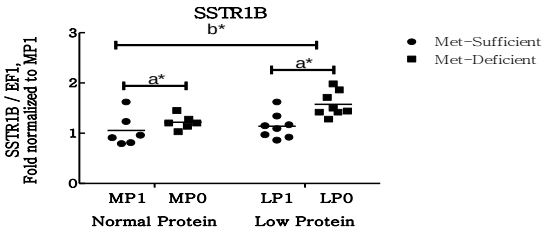

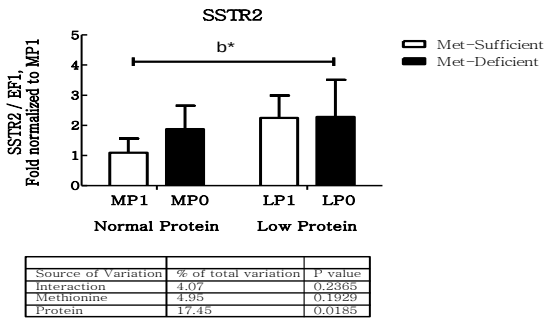

Source of Variation	% of total variation	P value
Interaction	4.07	0.2365
Methionine	4.95	0.1929
Protein	17.45	0.0185

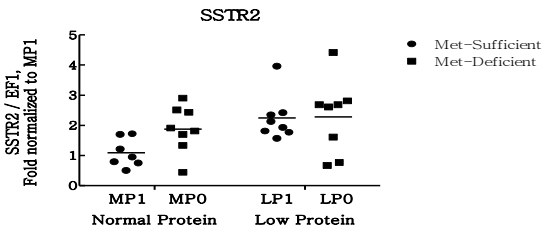

Figure 19B. Expression of markers of feed intake (CCK genes) and of two subtypes of the somatostatin receptor (SSTRB) in the brain of RT as a function of the diet, in trial 1. EF1α served as housekeeping gene a*: significant effect related with Methionine level (adequate *vs* deficient) b*: significant effect related with protein level (adequate *vs* deficient).

3.3.2 Trial 2. Markers of iron homeostasis

Feed intake and growth related parameters (Table 7) of fish fed the M diets were significantly higher than those of V diet fed groups. No effect of premix supplementation was observed on these growth-related parameters.

Table 7: Growth performance of RT fed after 12 weeks in trial 2.

	M0	M1	V0	V1	Basal diet	Premix	Diet x Premix
FI (g/fish)	127.6 ± 1.7	131.2 ± 2	113.7 ± 6	115.9 ± 4	< 0.001	0.12	0.76
FBW (g)	187.9 ± 6	190.8 ± 6	143.7 ± 13	145.3 ± 6	< 0.001	0.5	0.89
WG (g)	168.3 ± 5.3	171.1 ± 4	123.8 ± 12	126 ± 5.4	< 0.001	0.46	0.76
DGI	3.6 ± 0.1	3.6 ± 0.04	3 ± 0.15	3 ± 0.07	< 0.001	0.57	0.98
FE	1.4 ± 0.03	1.4 ± 0.03	1.2 ± 0.04	1.1 ± 0.03	< 0.001	0.54	0.73

Initial body weight (IBW) = 19.8 ± 0.8 g; FBW = final body weight. Data are expressed as mean ± SD of n = 3 observations. For abbreviations see the glossary.

Apparent availability coefficient (AAC, Table 8) of Fe was significantly affected by change in basal diet and premix supplementation. The basal diet affected the circulating levels of plasma Fe, being higher with V diet than with diet M. Final body composition of Fe tended to be higher in V fish than in M fish. Premix inclusion increased final Fe body concentration.

Table 8. Analysed dietary Fe concentration (mg/kg DM), Fe-apparent availability coefficient (AAC, %) and Fe concentration in the plasma (µmol L^{-1}) and whole body (WB) (mg kg^{-1} fresh weight) of RT Data are expressed as mean ± SD. P-value indicates statistical significance as obtained through two-way ANOVA.

	M0	M1	V0	V1	Basal diet	Premix	Diet x Premix
Diet Fe	161.6	212.9	153.8	205.4			
AAC-Fe	39.2 ± 3.1^{d}	3.7 ± 0.9^{a}	13.4 ± 1.9^{c}	10.1 ± 1.2^{b}	0.027	0.007	0.012
Plasma Fe	11.1 ± 2	8.5 ± 2.8	13.6 ± 4.1	14.3 ± 2.9	0.006	0.52	0.23
WB-Fe	14.4 ± 0.3	22.5 ± 5.6	17.9 ± 0.6	21.4 ± 2.5	0.06	0.02	0.38

Of the two apical metal reductases assayed in intestine and liver, ferric reductase activity in the intestine alone was significantly affected by change in basal diet, being 2-fold higher in V diet fed groups. Premix inclusion did not affect the activity (Table 9).

Table 9. Ferric reductase activity (unit per mg protein)

	Tissue	M0	M1	V0	V1	Basal diet	Premix	Diet x Premix
Ferric reductase	Intestine	0.71 ± 0.33	0.8 ± 0.36	1.87 ± 0.66	1.89 ± 0.89	0.00	0.81	0.88
	Liver	3.52 ± 0.94	4.17 ± 3.25	6.4 ± 4.73	3.59 ± 1.31	0.32	0.35	0.14

Data presented as mean ± SD of n=9 (two-way ANOVA).

The relative mRNA expression of genes involved in the transport and metabolism of iron is shown in Fig. 20. In liver, HAMP expression, encoding for hepcidin, was increased in fish fed diet M and premix inclusion (Fig. 20C), the induction being stronger in the group M compared to group V. The expressions of HO1 (Fig. 20A) and FPN1 (Fig. 20B) were significantly higher in V diet fed fish compared to M diet fed fish and the effect of premix inclusion was not

significant. In the intestine, expression of DMT1 isoforms namely, Nramp-β (Fig. 20D) and Nramp-γ (Fig. 20E) were not significantly different among the groups and the expression of FPN1 was reduced in M-groups and by the inclusion of premix (Fig. 20F).

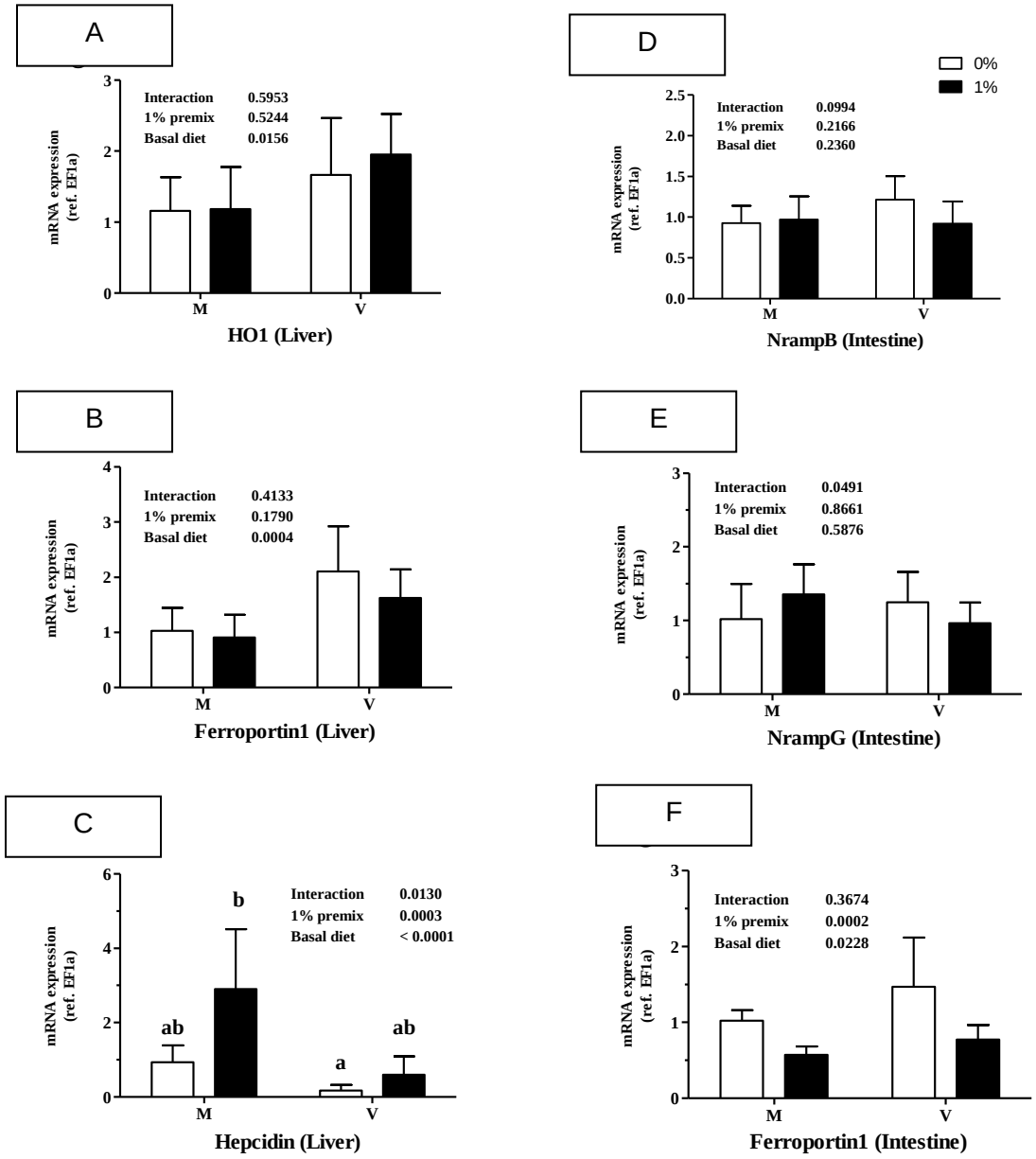

Figure 20. Transcription of selected transporters and regulators of iron metabolism in the liver and intestine of RT in trial 2, expressed relative to elongation factor 1alpha (EF1a). (i) Liver: hemeoxygenase1 (A); ferroportin1 (B); hepcidin (C). (ii) Intestine: Nramp-β, (D) and Nramp-γ (E); ferroportin (F). M= marine ingredient based diet and V= vegetable ingredient based diet stand; with un-supplemented diet (0% (white bars) or mineral premix supplemented diet (1%) (black bars). Each bar represents mean ± SD of n=9 samples. The significance (*P* value, 2-way ANOVA) of the main effects (basal diet and premix inclusion) is indicated for each parameter. Different letters above the bars indicate significant differences between the four treatments, in case of a significant interaction between the main effects

4. Discussion

In the current deliverable we have provided “dietary signatures” in terms of nutrigenomics that could be used for phenotyping nutritional stress for the three studied fish species. The relevance for each species is discussed separately, as different dietary interventions were applied for each of them.

Gilthead sea bream

In the **first GSB trial**, we confirmed and extended the idea pointed out by Ganga *et al.* (2011) that dietary oils largely mediate cortisol kinetics, as the magnitude and duration of cortisol response when GSB were exposed to confinement stress differed depending on the previous diet. Growth performance parameters did not differ between FO and 66VO fish, but their subsequent stress response was different. Stressed fish fed the 66VO diet showed a high and well-defined cortisol peak, accompanied of a high hyperglycemic response which highlights an overactive glucocorticoid system in fish fed a blend of vegetable oils as the most important source of dietary lipids. Whether this differential response is indicative of a different stress susceptibility is, thereby, open to discussion. However, given that both FO and 66VO diets support a normal growth in GSB, it is likely that the nutritional-mediated effects in cortisol kinetics are adaptive rather than maladaptive, serving to assure in each physiological condition the most efficient management of the “allostatic load”, immune factors and heat shock proteins (McEwen, 2002; Sterling and Eyer, 1998). In other words, fish, and GSB in particular, might conveniently adjust the stress response to a specific nutritional background and risk of oxidative stress, which is primarily the result of the tissue FA unsaturation index that experiences an overall decrease with the replacement of fish oil with vegetable oils (Benedito-Palos *et al.*, 2010). Supporting this, total glutathione levels are reduced in GSB fed high levels of vegetable oils (Saera-Vila *et al.*, 2009a), but intriguingly these fish also show a concurrent increase of the glutathione reduced/oxidized (GSH/GSSG) ratio, which is recognized as a reliable marker of a reduced risk of oxidative stress.

The gene expression profiling of the liver has previously been approached for GSB with a microarray (Calduch-Giner *et al.*, 2010) for crowding stress showing three major steps leading to i) rapid enhancement of energy supply, ii) strong activation of tissue repair and remodeling processes and iii) re-establishment of redox balance with increased scavenging of reactive oxygen species (ROS) and a general decline of ROS production. In the current study, using a more focused PCR-array, such temporal gene expression pattern was exemplified by the strong activation 24 h after stressor disturbance of the cell-tissue repair response that assists mitochondria and ER protein-folding and misfolding. This transcriptional feature was especially evident in the FO diet group not only when the gene expression values of stressed fish were referred to the control dietary group, but also when the expression data of the two stressed groups was referred to each other in separate scatter plots for each sampling time. According to this, the repair-response of DER-1, GRP-170 and GRP-75, also termed mortalin or mitochondrial HSP70, was triggered at a lowest level in stressed fish of the 66VO diet group. Of note, DER-1 elicits ER-associated degradation (Lilley and Ploegh, 2004), whereas GRP-170 (Chen *et al.*, 1996; Park *et al.*, 2003) is a molecular ER chaperone that assists the folding of nascent chains and help to achieve an active conformation for mature proteins. GRP-75 is found in ER, cytosol and cytoplasmic vesicles, though it is primarily of mitochondrial origin and its expression is triggered by glucose deprivation, oxidative injury, ionizing radiation, calcium ionophores and hyperthyroidism (Wadhwa, 2002; Wadhwa *et al.*, 2002). It also performs a broad spectrum of cellular functions ranging from stress response, intracellular trafficking, antigen processing, and cell differentiation and proliferation that makes GRP-75 and its yeast homologue (SSC1p) life-essential (Craig *et al.*, 1989; Kaul *et al.*, 2007). This also applies to fish species and GRP-75-deficient mutants of zebrafish have serious blood developmental defects (Craven *et al.*, 2005). In the same line, experimental evidence indicates that both protein and mRNA GRP-75 expression is highly inducible by acute and chronic stressors in the liver

tissue of GSB (Bermejo-Nogales *et al.*, 2008). Besides, the hepatic expression of this protein remains specially elevated in the liver tissue of common dentex (Bermejo-Nogales *et al.*, 2007), a closely related sparid fish with stressful behaviour, low larval survival and increased susceptibility to opportunistic pathogens (Company *et al.*, 1999; Pujalte *et al.*, 2003; Sitjà-Bobadilla *et al.*, 2007).

As reported for GRP-75, there are many lines of evidence supporting a key role of many other mitochondrial-related genes in acute and chronic allostatic states leading to explain the differences in stress susceptibility among individuals and animal species (Manoli *et al.*, 2007). Strong support for this notion comes from inbreeding selection of rat strains with "low power" versus "high power" mitochondria, which demonstrates that most stressful and health risk factors segregate with low expression levels of genes required for mitochondrial biogenesis and oxidative phosphorylation (Wisløff *et al.*, 2005). Likewise, the prophylactic role of calorie restriction and exercise is due, at least in part, to the induction of antioxidant enzymes, heat shock proteins, and mitochondrial oxidative phosphorylation (Arumugam *et al.*, 2006; Mattson and Kroemer, 2003). Extrapolation of these results to other animal models is always difficult, but it is noteworthy that mitochondrial antioxidant enzymes, including the recently characterized GSB PRDX3 and PRDX5 (Pérez-Sánchez *et al.*, 2011), were long-lasting up-regulated in stressed fish of the 66VO diet group. This gene expression pattern was accompanied by the up-regulation of markers of β-oxidation (HADH), tissue FA uptake (LPL) and oxidative phosphorylation (Cox4a), which is prone to a phenotype of "high power" mitochondria also challenged by the finding that the cell-repair machinery seems to be triggered at a reduced level in stressed fish fed the 66VO diet.

Other important stress-responsive genes are CREB-2 (Chin, 2008; Karpinski *et al.*, 1992) and HIF-1α (Tekin *et al.*, 2010), and their up-regulation at 24 h after the onset of stressor disturbance might orchestrate the overall and strong activation of the transcriptional machinery at this specific steady state. However, the stress responsiveness of these two upstream transcriptional regulatory factors was not differentially regulated by dietary oils, and other factors would contribute to explain the above differences in stress transcriptomics. In this context, it is noteworthy that the modulation of mitochondrial activity by glucocorticoids is considered biphasic with an initial induction of mitochondrial biogenesis and enzymatic activities of selected subunits of the respiratory chain complexes, whereas chronic exposure to high glucocorticoid levels causes respiratory chain dysfunction, increased ROS production, mitochondrial structural abnormalities, apoptosis and cell death (Adzic *et al.*, 2009; Alesci *et al.*, 2006; Manoli *et al.*, 2007). The mechanisms by which GCRs interact with the nuclear and mitochondrial transcription machinery remain largely unknown, especially in fish, though important progress has been made in last years in this field (Aluru and Vijayan, 2009; Schaaf *et al.*, 2009). In our experimental model, the expression of GCRs was consistently up-regulated in stressed fish of the 66VO diet group in comparison to those of the FO diet group (24 h and 72 h after the onset of stressor disturbance). Therefore, although we have no data on the expression of protein GCRs, this transcriptional measure also supports that fish fed high levels of vegetable oils are prone to have an overactive glucocorticoid system with an enhanced hyperglycemic response when facing stressors.

In summary, the stress response is highly mediated at the nutritional level in GSB. If the observed changes in stress kinetics and responsiveness are beneficial or detrimental for fish fed vegetal oils is not easy to answer due to the technical limitations of our experimental approach to ultimately asses the cellular stress response at the tertiary level. However, taken as a whole the fish performance, the risk of oxidative stress and the mRNA expression profile of gene markers of mitochondrial activity and cell-tissue repair response, it appears that the response to crowding stress in fish fed the 66VO diet is prone to be a permissive rather than a constraining factor for the replacement of fish oil with vegetable oils when the theoretical requirements in essential fatty acids for normal growth are met by diet. The precise mechanism remains still elusive, but it can be argued that fish fed vegetable oils allow a strong glucocorticoid response, whereas fish fed fish oil lead a lower but perhaps more persistent response in order to avoid tissue damage in a tissue-cell milieu with a higher risk of oxidative stress. The practical implications for the aquaculture industry are obvious since

growth performance is becoming a more restrictive factor than stress susceptibility when facing the replacement of fish oil with alternative oils in a warm marine fish highly cultured in all the Mediterranean area.

In the **second GSB trial**, we further extend the utility of the mitochondrial related gene markers already seen in trial 1 and in the D7.1 by concentrating on the oxidative phosphorylation (OXPHOS). It is the metabolic pathway in which mitochondria use their structure, enzymes, and energy released by the oxidation of nutrients to produce ATP. Mitochondrial OXPHOS provides over 90% of the ATP produced by mammalian cells, and, therefore, the number of mitochondria and their level of activity vary with the tissue and cell type reflecting the energy requirements (Barbour and Turner, 2014; Schaefer *et al*., 2013). This also applies to fish, and the expression profile of selected markers of mitochondrial dynamics and apoptosis, mitochondrial protein import, folding and assembly, and mitochondrial biogenesis and oxidative metabolism mirror the intensity and severity of natural and husbandry stressors in farmed GSB (Bermejo-Nogales *et al*., 2014b). Previous studies on GSB indicate that the mitochondrial “allostatic load” is altered by dietary oils in crowded stressed fish (Pérez-Sánchez *et al*., 2013), and overall we consider that stressful and health risk factors segregate with the low expression levels of genes required for mitochondrial biogenesis and OXPHOS as previously reported in higher vertebrates (Wisløff *et al*., 2005). Furthermore, experimental evidence in GSB (Bermejo-Nogales *et al*., 2011, 2014a) and other fish species (Coulibaly *et al*., 2006; Jastroch *et al*., 2005) indicates that hypoxia and nutrient (metabolic fuel) overflow activate the futile cycle of energy production via the increased expression of uncoupling respiratory proteins (UCP1–3) to match the antioxidant defence system. However, as pointed out before, the fine regulation of OXPHOS is not yet established, and the present study provides new and valuable insights into how GSB mitochondria are modulated in a tissue-specific manner to cope with the altered metabolic needs upon starvation. This includes the uploading to public repository databases of almost a complete set of OXPHOS genes (97 new GSB sequences), which allowed a new and powerful genomic resource to be developed for a comprehensive transcriptomic profiling of the mitochondrial respiratory chain in a marine farmed fish species of a high added value.

Complex I is the largest among the mitochondrial respiratory chain and varies from 14 subunits in prokaryotes to 45 subunits in mammals (Carroll *et al*., 2006; Gabaldon *et al*., 2005; Hirst *et al*., 2003). In the present study, we unequivocally annotated up to 40 new enzyme subunits, including among them four mtDNA-encoded subunits (ND1, ND2, ND5, ND6), six iron-sulphur proteins (NDUFS2-7), three flavoprotein subunits (NDUFV1-3), 14 regulatory subunits of the alpha subcomplex (NDUFA1-13, NDUFA4-L2), 11 regulatory subunits of the beta subcomplex (NDUFB1-11) and the two subunits of the NDUFC complex (NDUFC1 and NDUFC2), in addition to the essential assembly factor NDUFAF2/mimitin (Ogilvie *et al*., 2005). Two assembly factors (SDHAF1-2) and four nDNA-encoded enzyme subunits of Complex II with either catalytic (SDHA-B) or regulatory (SDHC-D) properties were also recognized and properly annotated (Sun *et al*., 2005). Likewise, Complex III is composed of 12 enzyme subunits and all of them, with the exception of cytochrome b (CYB), are encoded by nDNA (Zara *et al*., 2009). Importantly, all these enzyme subunits are conserved in GSB, and together with two enzyme isoforms of the regulatory subunit UQCR11 (UQCR11-A, UQCR11-B) they have been identified as actively transcribed genes in a typical marine fish.

Complex IV is composed of a variable number of enzyme subunits (4–13) (Ludwig *et al*., 2011; Pierron *et al*., 2012), and the catalytic core represented by the mtDNA-encoded COXI, COXII and COXIII is already found in our transcriptomic GASB database. This enzyme complex is the most studied, and early studies in sheep, dogs, rabbits, rats, mice and humans share a characteristic gene expression pattern on the basis of the species (Linder *et al*., 1995), tissue (Huttemann *et al*., 2001) and developmental stage (Parsons *et al*., 1996). In the present study, up to 20 enzyme subunits of Complex IV were annotated, including 16 conserved vertebrate paralogs of COX4 (COX4a, COX4b), COX5a (COX5a1, COX5a2), COX5b (COX5b1, COX5b2), COX6a (COX6a1, COX6a2), COX6b (COX6b1,

COX6b2), COX6c (COX6c1, COX6c2), COX7a (COX7a1, COX7a2), COX8 (COX8a, COX8b) and five fish species-specific subunits annotated as COX6b1a, COX6b1b, COX6c1, COX7b and COX7c (Little *et al*., 2010). Additionally, we annotated for the first time in a non-model fish species the assembly factors COX15, SCO1 and SURF1, which are essential for the normal function of the enzyme complex (Soto, 2012). Indeed, COX15 converts heme O into heme A by hydroxylation, which is then incorporated during early assembly into Complex IV, and any mutation in COX15 leads to the arrest and degradation of the complex (Antonicka *et al*., 2003). Likewise, SCO1 is involved in cellular copper homeostasis, and mutations in SCO1 cause a neonatal hepatopathy and ketoacidotic coma (Leary *et al*., 2007). In humans and flies, mutations in SURF1 are generally lethal, but paradoxically SURF1 knockouts are associated with prolonged longevity and neuroprotection in mice (Dell'Agnello *et al*., 2007).

Complex V comprises a catalytic sector (F1), a membrane sector (F0) and a long stalk connecting F1 to F0. Out of a total of 15 subunits, two (ATP6 and ATP8) are encoded by mtDNA and the remaining by nDNA (Collinson *et al*., 1994; Haberstzer *et al*., 2013), and all of them, including the F1-stator (ATP5A1, B, C), the rotor (ATP5D, E, ATP5G) and the proton translocation of the F0 sector, comprising the membrane stator (ATP6, ATP8), the stator-peripheral stalk (ATP5F1, ATP5H, ATP5J2, ATPO, OSCP) and the dimerization subunits (ATP5I, ATP5L), were properly annotated. The ATPAF2 assembly factor, required for the correct function of Complex V (Ghezzi and Zeviani, 2012), was also identified, which confirms and extends the notion that catalytic, regulatory and assembly factors of OXPHOS have been highly conserved through the evolution of fish and higher vertebrate species with a differential and tissue-specific regulation in fish exposed to different metabolic stressors as reported below.

From a functional point of view, it is noteworthy that in our fasting model most of the components of our OXPHOS array were significantly down-regulated in the liver tissue. The magnitude of change was of the same order of magnitude for all the enzyme complexes (Complex I–V), and importantly this massive response included catalytic enzyme subunits, encoded either by mtDNA (ND2, ND5, CYB, COXI-III) or nDNA (NDUFS2, NDUFS4, NDUFS5, NDUFS7, NDUFV1-3, SDHA, UQCRFS1, ATP5A1, ATP5B, ATP5C1, ATP5D, ATP5E), and nuclear-encoded regulatory enzyme subunits (NDUFA1-9, NDUFA12, NDUFB2-6, NDUFB9-11, NDUFC1, SDHC, SDHD, UQCRC1-2, UQCRH, UQCRB, UQCRQ, UQCR10, UQCR11-B, COX4a,-b, COX5a2, COX5b2, COX6a2, COX6b1a-b, COX6c1, COX7a1-2, COX7b-c, COX8b, ATP5F1, ATP5G1, ATP5I, ATP5J2, ATP5L, ATP5O) and nuclear-encoded assembly factors (NDUFAF2, SDHAF2, SURF1) as well. This consistent response substantiates a reduced energy demand as the result of the fasting inhibition of hepatic lipogenesis, which is considered a major energy-demanding process in the liver tissue (Rui, 2014). Hence, we found herein a marked loss of adipose tissue mass and liver size, which is concurrent with a strong down-regulation of a vast array of hepatic lipogenic enzymes, including fatty acid elongases (ELOVL4, ELOVL5, ELOVL6) and desaturases with Δ6 (FASD2) and Δ9 (SCD1a and SCD1b) activities (Benedito-Palos *et al*., 2014). In the present study, additional evidence for all this is supported by the observation that the expression of COX4 subunit isoforms was dampened by fasting at both the mRNA and protein level. Fasting or caloric restriction also down-regulate OXPHOS and the TCA cycle in the liver tissue of pigs (Lkhagvadorj *et al*., 2010), mice (Bauer *et al*., 2004) and chickens (Désert *et al*., 2008). A similar trend was reported for the liver of European eels after exposure to environmental pollutants (Pujolar *et al*., 2012, 2013), although reliable results were reduced to regulatory enzyme subunits due to the poor representation of assembly factors and catalytic enzyme subunits of OXPHOS in the arrays used for the gene expression profiling.

In fish, switches in muscle energy demand or oxidative capacities are often related to intensity training (Anttila *et al*., 2010) or long fasting spawning migrations (Miller *et al*., 2009; Mommsen, 2004). However, nutrient availability by itself is a major factor driving switches in muscle protein turnover and mitochondrial activity as reported earlier in GASB (Calduch-Giner *et al*., 2014) by microarray gene expression profiling of glycolytic and aerobic muscle

tissues in fish fed to maintenance ration. This is consistent with the up-regulation of OXPHOS in white skeletal muscle and the heart, although both in this and previous studies in pigs (Da Costa *et al*., 2004) and mice (Suzuki *et al*., 2002) the response of skeletal and cardiac muscle tissues to food deprivation and/or restriction is not only opposite to, but also weaker than, in the liver. This notion was substantiated herein by the magnitude of fold-change and the number of differentially expressed genes, which was reduced from 72 in the liver to 29 and 10 in skeletal muscle and cardiac muscle, respectively. Furthermore, it should be noted that the response of skeletal muscle was mostly mediated by regulatory and assembly factors encoded by mitochondrial DNA, whereas that of cardiac muscle was mostly due to catalytic and assembly factors encoded by mitochondrial and nuclear DNA. In humans, a differential response of mitochondrial complexes has also been found with age in skeletal muscle, with a decrease in gene transcripts for several components of complexes I, IV and V, and no major changes for complexes II and III (Welle *et al*., 2003; Zhan *et al*., 2006). The physiological significance of these findings is far from being fully established, although they can be viewed as a different tissue-metabolic plasticity of glycolytic and highly oxidative muscle tissues, which was encompassed in a complex manner by the nuclear and mitochondrial genomes. As reported for liver, changes in mRNA gene expression fit well with the Western blotting of COX4, although further research is needed to assess with commercial and customized antibodies the concurrent protein changes of the most transcriptionally regulated OXPHOS subunits in front of a wide range of physiological challenges.

In summary, the molecular identity of almost all the components of the mitochondrial respiratory chain has been established for the first time in a non-model fish species. This yielded 97 new GSB sequences, all of them manually curated and uploaded to GeneBank. This allowed the development of a powerful PCR-array, which has been used with success for the simultaneous expression profiling of 88 OXPHOS genes with catalytic, regulatory and assembly properties. Most of them are becoming highly regulated genes by nutrient deprivation in the liver tissue, whereas a moderate or low response was found for the glycolytic skeletal muscle and the highly oxidative cardiac muscle, respectively. The direction of change is also tissue-specific, according to the different metabolic capabilities of liver and muscle tissues. These findings contribute to refining the list of candidate genes for phenotyping any metabolic disturbance in farmed fish and GSB in particular. Whether this is fish species-specific remains to be resolved, although we suspect that it is part of the highly conserved metabolic features through the evolution of fish and high vertebrate species, which is prone to conserve the complex interactions of mitochondrial and nuclear genomes.

In the **third GSB trial**, the gene expression profile of a panel of selected markers of growth performance and muscle growth was reported for most common nutrient deficiencies in marine fish, as the result of a high replacement of marine ingredients by alternative terrestrial plants. Liver and withe skeletal muscle were chosen as target tissues and the number of differently expressed genes varied from 2-5 genes up to more than 20 in fish fed FM-free diets formulated for deficiencies in FA, P and vitamins. Therefore, the magnitude of change at the molecular level was close related with the overall impairment of fish performance which was also higher in these groups of fish as shown in Fig. 21.

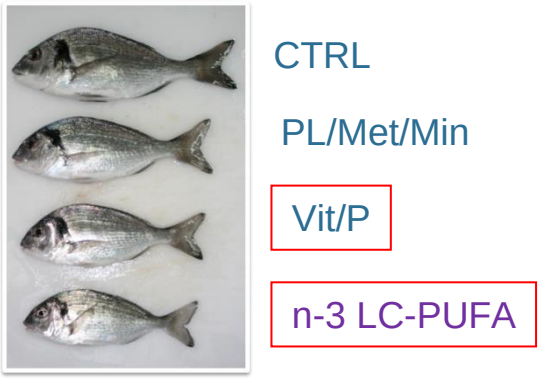

Figure 21. Representative images of GSB of trial 3, in which the effects of nutrient deficiencies are visible.

The nutritionally-mediated changes in molecular signatures also reflected the different tissue metabolic capabilities, and importantly the liver appeared highly sensitive to nutrient deficiencies in P and LC-PUFA, whereas skeletal muscle was especially sensitive to vitamin deficiencies. Hence, as summarized in Fig. 22, markers of GH/IGF system were down-regulated in the liver with the impairment of growth performance (systemic response) with no change or up-regulation in muscle as part of a compensatory response at the local tissue level. Conversely, the expression of myogenic factors was mostly restricted to muscle tissue, although interestingly the expression pattern as a whole of MyoD2, MSTN, MEF2A and FST was able to discriminate among different nutrient deficiencies. Markers of protein breakdown (calpain/calpastatin system; lysosomal proteases; proteasome-ubiquitination pathway) were also highly informative of nutrient deficiencies, especially when considered together liver and muscle tissues. Likewise, it is noticeable that the hepatic up-regulation of molecular chaperones of endoplasmic reticulum (DER-1, GRP170, GRP94) emerged as a good criteria of diagnosis of mineral deficiencies other than phosphorous. By contrast, the selected markers of inflammatory and anti-inflammatory response, including ILs and IL-receptors, were especially informative of nutrient deficiencies in skeletal muscle. Furthermore, this was especially evident for vitamin deficiencies addressed as a whole with a half inclusion level of the vitamin mixture in the deficient diet. Otherwise, it is noticeable that muscle mitochondrial markers of energy sensing (SIRT3), OXPHOS and respiration uncoupling were specially sensitive to changes in vitamin supply, and further studies are running in the framework of National and EU projects (ARRAINA) to determine how these molecular markers in combination with more conventional measures of histopathological scoring, haematology and basic blood biochemistry can be used as new and integrative tools for the re-evaluation of micronutrient requirements with the use of alternative raw materials and feed additives for the improvement of overall health and performance.

	SAA	PUFA	PL	P	Min	Vit
GHR-I		⌄		⌄		
GHR-II						
IGF-I		⌄		⌄		
IGF-II		⌄		⌄		
IGFBP2		⌄				
IGFBP4		⌄		⌄		
IGFALS		⌄		⌄		
PCNA		⌄				⌃
MET	⌄				⌃	⌃
CAPN1		⌄		⌄		
CTSD	⌄	⌄	⌄		⌄	⌄
CTSL			⌃	⌄		
GRP170		⌄			⌃	
GRP94		⌄		⌄	⌃	
DER-1		⌄	⌃		⌃	⌃
IL-1R1		⌄	⌃	⌄		⌃
IL-6RB		⌄		⌄		
SIRT4				⌃		
CPT1A		⌃		⌄		
SCO1				⌃		
UCP1				⌃		

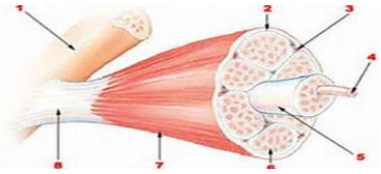

	SAA	PUFA	PL	P	Min	Vit
GHR-I			⌃			
GHR-II				⌃		
IGF-II						⌃
IGFR2				⌄		
MyoD2	⌃			⌃	⌃	⌄
MSTN				⌃		
MEF2A		⌃				
FSTN		⌄	⌄			
CAPN3	⌄				⌄	
CAST				⌃		
CTSB						⌃
CTSS						⌃
UCHL3	⌄					⌃
GRP170		⌄				⌃
IL-1β	⌄		⌃		⌄	
IL-1R1						⌃
IL-1R2						⌃
IL-6RB						⌃
IL-10						⌃
IL-10RA						⌃
IL-10RB						⌃
SIT3						⌃
SC01						⌃
UCP2		⌄	⌄			⌃
LXRα	⌄	⌄	⌄		⌄	

Figure 22. Corollary of significant changes found in the expression of relevant genes in the liver (left) and white muscle (right) of GSB fed with different semipurified diets in trial 3 in comparison with the control diet. Chevrons in red indicate up-regulation, in green down-regulation. The size of the chevron indicates the intensity of the change.

Salmon

The present study reported a molecular snapshot of the hepatic and intestinal (distal) physiology of AS undergoing long-term exposure to dietary plant-based ingredients causing nutritional stress. The results herein presented aimed to provide an experimental model to describe dietary signatures to support future nutrigenomic studies profiling the nutritional response to plant-based diets in fish. These results also represent a platform for the identification of candidate molecular markers. Dietary SBM caused a loss of performance above inclusion levels of 200 g kg^{-1}, but not below this level of inclusion. It was not the scope of this study to determine the performance of salmon fed dietary SBM, since this ingredient at levels of inclusion above 200 g kg^{-1} has been previously proved to cause reduced growth, nutritional stress and degraded health (growth data reviewed in Collins *et al.*, 2013; health effects reviewed in Krogdahl *et al.*, 2010). We solely sought to reproduce the same effects and generate an experimental model for nutritional stress to achieve the main aims of this study. The experimental model was in fact reproduced, including two sub-optimal inclusion levels (100 g kg^{-1} and 200 g kg^{-1}) that did not show significant growth retardation compared with the control and represented interesting biological material to further test identified molecular biomarkers.

The transcriptome response observed in salmon fed 300 g kg^{-1} SBM was greater in the distal intestine than in the liver. These results were expected due to the inflammation of the distal intestine and the consequent immune response that has generally been observed after feeding similar levels of dietary SBM (Baeverfjord and Krogdahl, 1996; Bakke-McKellep *et al.*, 2007; Urán *et al.*, 2008, 2009). The immune response detected in the distal intestine in the present study confirmed the nutrigenomic results of recent works investigating the early onset of SBM-induced enteritis (Sahlmann *et al.*, 2013) and that caused by pea protein concentrate (PPC) supplemented with soyasaponin (Kortner *et al.*, 2012) and significantly overlapped with the immune response developing during human inflammatory bowel disease (Maloy and Powrie, 2011). The inflammation is a consequence of the disruption of the epithelial barrier that in a healthy fish intestine provides a defence mechanism against exposure to exogenous substances or bacterial invasion. In fish, and specifically in salmon a T and B cell mediated response is evident in the very early days of the enteritis onset (Sahlmann *et al.*, 2013), however the profile presented in this study is more likely to mirror a late, chronically inflamed stage similar to that described in salmon fed PPC and soya saponin (Kortner *et al.*, 2012). In fact, genes and pathways affected by the SBM-induced nutritional stress in the intestine were, with few exceptions, the same as those reported by Kortner and colleagues for the PPC and soya saponin induced enteropathy. The observed response in the intestinal tissue clearly involved the tumour necrosis factor (TNF) signalling pathway (highly significantly up-regulated), which is critical in triggering the release of pro-inflammatory cytokines and also the activation of a number of intracellular pathways eventually leading to apoptosis and cell survival (Chu, 2013). Downstream targets of the TNF pathway including MAPK and NF-kB signalling pathways and the pathway regulating apoptosis were also significantly affected in our study. Further indications of an ongoing immune response included the up-regulation of cytokine-cytokine receptor interaction, T cell receptor signalling pathway, NOD-like receptor signalling pathway and cytosolic DNA sensing pathway. An exhaustive immunological view of the intestinal transcriptome profile developing during the development of enteritis can be found in the above-mentioned articles and was outside the scope of this manuscript (Kortner *et al.*, 2012; Sahlmann *et al.*, 2013).

Results in the liver suggest that this organ exerted immune functions in support of the innate immune response. This was evident from the up-regulation of several genes of the complement cascade. The complement cascade plays a crucial role in mediating the non-specific defence against pathogens in the blood and the liver is the major site of production of the proteins participating in this process (Jain *et al.*, 2014). The up-regulation of the MASP1 genes suggested that activation of the pathway possibly occurred through the

activation of the lectin pathway that is activated through recognition of patterns of carbohydrate or glycoprotein present on the pathogens. Notably, the CD59 antigen abundance decreased suggesting an inhibition of the formation of the membrane attack complex which is formed as a result of the complement cascade. Activation of proteins of the complement cascade was not reported in the liver of AS fed 200 g kg^{-1} (Skugor *et al.*, 2011). Since the array utilized in that study (NCBI GEO accession GPL6154) contained probes targeting several complement component proteins, it can be hypothesized that level of SBM inclusions around 200 g kg^{-1} possibly cause an inflammation process localized in the intestine and that does not involve the activation of the complement component in the liver.

Metabolic processes and systems of the organisms such as digestion and absorption of nutrients (vitamins, minerals, proteins and fat) were also significantly affected. In the distal intestine a down-regulation of virtually all pathways from these specific categories following the SBM-induced nutritional stress were observed. These results confirmed those previously reported in salmon and strengthened the theory that tissue malfunction follows severe inflammation in the distal intestine (Kortner *et al.*, 2012; Sahlmann *et al.*, 2013). However, studies from other fish species reported that impaired metabolism could also develop independently from an evident immune response which suggested that some of the effects on metabolism might be possibly associated with the nutritional properties of the SBM or the plant products in general (Murray *et al.*, 2010). Lipid metabolism and in particular sterol, is particularly affected by the use of plant proteins, and we observed a down-regulation of genes involved in lipid digestion and absorption, primary bile acid biosynthesis and secretion. This was in agreement with what previously observed in salmon fed 200 g kg^{-1} SBM where mechanisms of lipids and bile uptake were impaired possibly due to the inflammation of this tissue (Kortner *et al.*, 2013). The presence of certain ANFs such as soyasaponin might interfere with the formation of micelles in the intestine and hence inhibit lipid absorption (Gu *et al.*, 2014; Kortner *et al.*, 2013). Kortner and colleagues (2013) also reported an increase of hepatic cholesterol metabolism, sharply in contrast with the current study where a marked down-regulation was observed. It cannot to be excluded that salmon might respond differently to various regimes of inclusions and, most importantly, depending on the severity of the immune response. The inflammation associated with the enteropathy is also known to impact the correct functioning of the intestine and affect the primary digestive role of this organ and consequent nutrient absorptions. A generally lower level of nutrients was in fact detected in fish after administration of plant-based diets suggesting an impaired capacity to absorb and transport nutrients into the circulatory system (Santigosa *et al.*, 2011; Zhang *et al.*, 2013).

Plants also contain a variety of protease inhibitors that are involved in defence mechanisms against herbivores (Hartl *et al.*, 2011). Protease inhibitors are tightly linked and co-extracted with proteins and are often abundant in protein concentrates from plant products. When included in animal's diet these inhibitors can affect feed digestibility supposedly by interfering with endogenous proteases such as trypsin, chymotrypsin, elastase, etc., causing an over-secretion of these enzymes and loss of endogenous resources which in turn can lead to decreased growth (Sarwar Gilani *et al.*, 2012). The results confirmed that genes involved in digestion and absorption of proteins as well as several pathways of the amino acid metabolism were differentially expressed in liver and intestine. The pathways altered in the liver involved aspartate, glutamate, alanine, serine, cysteine, glycine and threonine, non-essential amino-acids. This suggested that endogenous amino acid synthesis might have up-regulated to counteract the nutritional deficiency. Significantly increased expression of the trypsin gene was also observed in the liver. Since fish liver is made of several cell types, including pancreatic, this result indicated that the "hyperactive pancreas" syndrome with over-secretion of digestive enzymes in response to soy ANFs might be also present in fish (Sarwar Gilani *et al.*, 2012).

Two main trends were observed in the expression data concerning cellular and other processes. In the distal intestine there was a down-regulation of cellular processes such as the lysosome, peroxisome and to a lesser extent the phagosome. The main role of these organelles is the degradation of various cellular metabolites as well as the digestion of

invading pathogens. Lysosome and peroxisome in the distal intestine were the most significantly down-regulated pathways and clearly followed the tendency of most metabolic and digestive processes indicating that their abundance was similarly affected by the malfunction and inflammation of this tissue. On the contrary all pathways involved in the processing of genetic information and protein synthesis were significantly up-regulated which suggests, together with a number of other pathways such as those regulating cell cycle, pyrimidine metabolism, etc., suggesting regeneration and proliferation of the damaged tissue.

Rainbow trout

In **trial 1**, the dietary protein and methionine deficiency highly affected the food intake and hence the growth of the RT, in the order MP1>MP0>LP1>LP0. In order to better understand the molecular mechanisms associated with the reduced feed intake, we analysed in trout brain the gene expression of markers potentially involved in the sensing of AA and in the regulation of feed intake.

Both the low amount of dietary methionine and protein increased the ATF4 gene expression confirming, for the first time in fish, the activation of GCN2--ATF4 pathway in trout brain challenged to a low dietary amino acid supply, similar to findings in mammals (Maurin *et al.*, 2005, Gietzen *et al.*, 2007, Anthony and Gietzen, 2013). As a target of the transcriptional activity of ATF4 (Balasubramanian et al, 2013), ASNS expression is expected to follow the same trend, as seen in its reponse to low dietary protein. The lack of an effect of the methionine deficiency on ASNS expression may be due to the short-term effect of this mechanism. Indeed, in mammals (Kilberg *et al*., 2009) ATF4 activation of ASNS in case of a deficiency in amino acids was observed during the first 6 hours after treatment. Thereafter, a decrease in the activity of the promoter was observed.

SSTR1B and SSTR2 encode two subtypes of the somatostatin receptor family (G protein-coupled receptors). Their specificity has not been well characterized in fish, but the two receptors are present in the brain as demonstrated in *Epinephelus coioides* (Haiyan *et al*., 2010). In our study, we observed a significant increase in the expression of SSTR2 gene by dietary protein deficiency and by both, protein and methionine deficiency on SSTR1B expression. Studies in RT, revealed that the expression of SSTR receptors in the brain is regulated by nutritional status (Nelson and Sheridan, 2005). However, their role in the regulation of appetite has not been examined. Somatostatin, a hormone secreted by the hypothalamus, is known to reduce food intake in mammals. In case of dietary valine-deficiency, one study in mice showed increased expression of somatostatin in the hypothalamus, in line with decreased feed intake. Furthermore, the same effect was observed during administration of a high dose of somatostatin in the brain of rat fed a diet deficient in threonine (Nakahara *et al*., 2012).Thus, overexpression of somatostatin receptor our study may be related to an increased secretion of somatostatin following intake of the diet deficient in protein and/or methionine. As such, increased somatostatin as reflected by overexpression of SSTR, may be a valid candidate marker in trout brain of the decreased feed intake in fish confronted with a diet deficient in methionine but also in protein.

We observed a significant increase in the expression of the NPY gene level in brain of trout fed the low protein diet, without effect of the methionine content on its expression. The lack of effect of the deficiency in essential amino acids on the brain expression of NPY in our study is consistent with the absence of induction of NPY into the hypothalamus of rats fed with a diet deficient in an valine, another essential amino acid (Nakahara *et al*., 2012). Neuropeptide Y acts as a neurotransmitter in the brain. It is produced in different places and is thought to have several functions including increased food intake (orexigenic effect). The increased expression of NPY by the low protein supply, as observed here, is however not associated with a higher food intake. A lack of correlation between the amount of food ingested and NPY mRNA confirms earlier data obtained in trout (Figueiredo Silva *et al*., 2012). In rodents, NPY has been suggested to participate in the anticipation of the metabolic impact of the meal, instead of stimulating food intake per se (Drazen *et al*., 2005).On the

other hand, CCK (cholecystokinin) is a neuropeptide that signals satiety (anorectic effect). In our study, diets deficient in protein and methionine significantly stimulated the expression of CCK-T and CCK-N genes. This correlates with the decrease in intake in fish fed these diets. However, even in mammals, the mechanisms by which a neuropeptide or anorectic neurotransmitter is regulated by the long-term feeding of a diet deficient in an essential amino acid remain largely unknown (Nakahara *et al*., 2012). Nevertheless, our findings that a dietary methionine deficiency induces in the trout brain an increase of markers involved in anorectic (e.g. CCK) rather than a reduction of markers involved in orexigenic (e.g. NPY) responses is in line with findings in rodents (Nakahara *et al*., 2012). These showed that anorexia induced by a diet deficient in valine cannot be completely "abolished" by brain administration of orexigenic peptides such as ghrelin, NPY and AGRP (Goto *et al*., 2010).

In conclusion, results of PCR analysis in RT brain showed that an imbalance in methionine and / or proteins induced a nutritional stress causing the activation of GCN2/ATF4-signaling pathway, as indicated here using ATF4 gene expression as a marker. The gene expression of the anorectic neuropeptide CCK was stimulated which would allow the fish to decrease feed intake and hence to avoid an imbalanced nutritional status harmful for its survival.

In **trial 2,** as expected, the growth of the RT fed an all plant based diet in this study was considerably lower than with the fishmeal based diets. The lack of a positive effect of adding the trace mineral premix on growth indicates that the trace minerals level in the non-supplemented basal diet was sufficient to support growth in both diet groups. When further studying the changes related to hepatic iron metabolism, we clearly detected the effect of the lack of heme in plant proteins, a vital component present in fish meal. Apart from being a good source of Fe, degradation of heme supplies biliviridin, the precursor of bile pigment bilirubin. Activity of heme-oxygenase (HO) in macrophages is essential for catabolizing heme to produce biliverdin and free iron (Poss and Tonegawa, 1997). Hepatic ferroportin1 (FPN1) expression is needed for the cellular export of Fe recycled from heme (Donovan *et al.*, 2005). In vertebrates, the export of Fe from enterocyte or macrophage to plasma by FPN1 transporter is transcriptionally regulated by cellular Fe levels and by hepcidin, which exerts an inhibitory action on FPN1 export (Ganz and Nemeth, 2012). Hepcidin is encoded by HAMP gene in the liver of mammals as also documented in RT (Alvarez *et al.*, 2013). In our study, we noted a down-regulation of hepcidin together with increased expression of HO1 and FPN1 in the liver of V diet fed fish, which suggests increased heme degradation in V diet compared with M diet fed fish. The premix inclusion also up-regulated the expression of HAMP expression in liver, but did not modify that of HO1 and FPN1. This suggests that factors other than dietary Fe supply may regulate the hepatic expression of HO1 and FPN1, possibly in relation with cholesterol metabolism. In RT, plant ingredients such as soybean meal may negatively affect cholesterol metabolism and bile status (Iwashita *et al.*, 2009; Kaushik *et al.*, 1995; Yamamoto *et al.*, 2007). As such, increasing the degradation of endogenous heme-pool, as suggested by the higher HO/FPN1 in our study, could be an adaptive strategy to meet the physiological demand for bile salts essential in cholesterol biosynthesis, when fed plant ingredient based diets devoid of heme. On the other hand, such higher endogenous heme-degradation can lead to increased Fe supply to the plasma, saturating the Fe binding capacity of plasma transferrin and hence increase the non-transferrin bound Fe which is stored in the liver. Like in mammals, body iron stores in fish are known to regulate intestinal Fe absorption and homeostasis (Standal *et al.*, 1999). Accordingly, the heme-degradation induced systemic Fe overload in V-fish, as indicated by higher plasma and whole body Fe levels, may explain the lower AAC of Fe in the V0 vs M0 fed fish, despite similar dietary Fe concentrations. These findings suggest that disturbances in hepatic metabolism when fed plant ingredient based diets have an impact on mechanisms regulating Fe homeostasis in RT.

The dietary interventions also affected the regulation of intestinal iron absorption. The proportion of Fe absorbed from the diet, which is the major source of Fe to fish, has been

found to decrease with increasing dietary levels (Standal *et al.*, 1999), as reflected here by the lowered Fe AAC values following premix addition. Divalent metal transporters (DMT1 or Nramp) are known to facilitate cellular transport of Fe^{2+} across intestinal apical membranes and a brush border ferric reductase (FR) activity exists for the reduction of non-heme Fe^{3+} to Fe^{2+}, the substrate for DMT1 (Carriquiriborde *et al.*, 2004; Cooper *et al.*, 2006). In line with the observations by Carriquiriborde *et al.* (2004), the mineral premix did not stimulate intestinal FR activity in our study probably since the added Fe was already supplied in the Fe^{2+} form as ferrous sulphate, ($FeSO_4.7H_2O$). The activity of FR also indicated that the available Fe supply from M diets was higher than in V diets and as in mammals, FR independent mechanism might exist for heme-Fe uptake in RT when fed fish meal based diets. *In vitro,* iron uptake in the anterior intestine of RT is considered to occur via simple diffusion while carrier mediated transport occurs in the mid- and posterior intestinal segments (Kwong and Niyogi, 2008). In trout, gastro-intestinal expression of Nramp (DMT) genes were initially induced at day 7 on exposure to high dietary Fe but decreased at day 14 (Kwong *et al.*, 2013). Such a phenomenon may explain the lack of differential expression in intestinal DMT isoforms (Nramp-β and Nramp-γ) after 12 weeks of feeding as in the present study. Moreover, DMTs are also transporters of several other divalent metal ions, such as Cu^{++} or Zn^{++} affecting the apical uptake of Fe by DMTs in trout intestine (Carriquiriborde *et al.*, 2004; Kwong and Niyogi, 2009). Given this non-specific nature of DMTs, it is likely that a more specific and critical step exists in regulating intestinal Fe absorption. In this respect, it is important to better understand the role and physiological importance of ferroportin and hepcidin in systemic Fe regulation in fish. In mammals and also in zebrafish, ferroportin-assisted basolateral extrusion of Fe was identified as the rate limiting step of intestinal iron absorption (Andrews, 2000; Fraenkel *et al.*, 2005) and as described earlier, it is regulated by hepatic hepcidin or intracellular Fe levels. Transcriptional suppression of intestinal FPN1 by Fe overload induced hepcidin over-expression in rats *in vivo* (Yeh *et al.*, 2004). Such opposite expression pattern and regulation of hepatic HAMP and intestinal FPN1 was seen in our study in response to changes in basal diet and premix inclusion. This might possibly be the effect of excess Fe supplemented to M diet in the form of Fe SO_4 when Fe in M0 diet was sufficient to meet the requirement of RT. In contrast, the suppression of liver HAMP might be have been to avoid systemic Fe overload in plasma derived from the degradation of heme in the hepatic macrophages, as explained previously. Enterocytes of the intestinal epithelium are sloughed off and replenished regularly. Consequently, the Fe accumulated in the intestinal epithelium will not be absorbed and end up in the faeces, resulting in low AAC. The significantly low intestinal FPN1 expression related with the high liver HAMP possibly explains the very low AAC in M1 fed fish. Our results suggest that systemic Fe homeostasis in RT could be transcriptionally regulated by hepcidin and ferroportin, but further studies are required to better understand the mechanism.

In conclusion, the regulation of Fe absorption and metabolism in RT appears to depend on the dietary ingredient composition (fish- versus plant-ingredient based diets) and on the inclusion of mineral premix. It is suggested that the disturbances in Fe metabolism are secondary effects of hepato-biliary dysfunction in relation to cholesterol and bile metabolism when fed plant-ingredient based diets. Relevant molecular markers for revealing and studying such dietary interactions on the regulation of Fe homeostasis are ferroportin1 and hepcidin, as detected here in trout intestine and liver, respectively. Fig. 23 summarizes the differential changes observed with the different used methods.

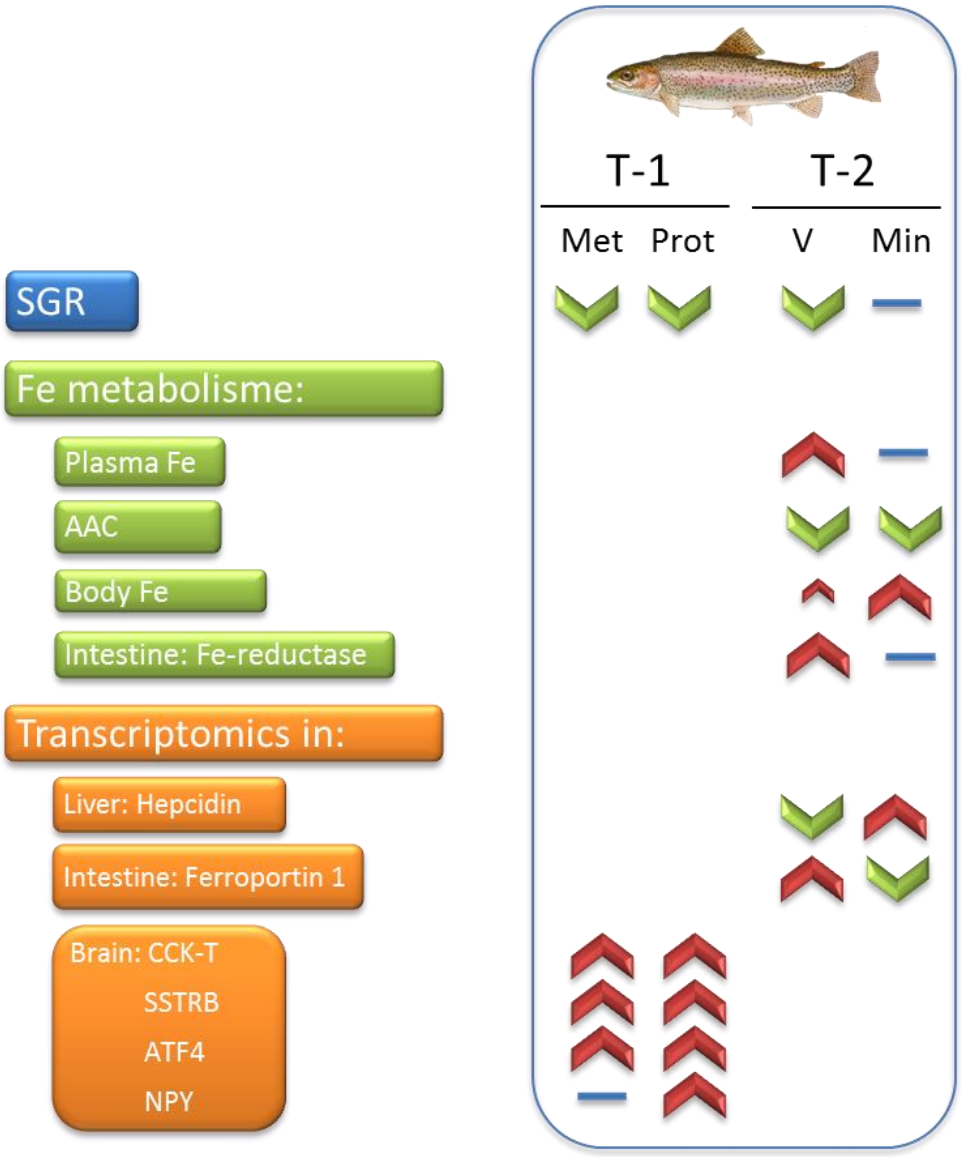

Figure 23. Corollary of the different growth, metabolic and molecular measurements done in trial 1 (T1) and 2 (T2) of RT. Significant changes are indicated by chevrons in red (up-regulation) and green (down-regulation). The size of the chevron indicates the intensity of the change. Blue dashes indicate no change.

5. Conclusions

- Stress response by confinement is a sensitive method for detecting differences in allostatic loads in GSB with a different nutritional history (fish oil *vs.* vegetable oils).
- Molecular profiling of mitochondrial biogenesis and OXPHOS is a robust tool for unravelling nutritional stress in GSB, with different signatures for changing diet composition and nutrient supply.
- The simultaneous measurement of the gene expression of mitochondria-related genes (> 150) highly contributes to refine the list of candidate genes for metabolic disturbances due to environmental (AQUAEXCEL Deliverable 7.3) or nutritional stressors (this report).
- The developed growth-chip with 89 selected markers of overall growth performance and muscle growth allows the establishment of different molecular signatures, which reflect the different tissue metabolic capabilities and the specific effect of a given essential nutrient on canonical pathways and biological processes in GSB.
- Skeletal muscle seems to be especially sensitive to deficiencies in vitamins, whereas liver is highly sensitive to deficiencies in FA and phosphorous in GSB. This differential response involve genes of GH/IGF system, muscle growth, oxidative stress and tissue repair, inflammatory/anti-inflammatory cytokines as well as mitochondria-related genes of oxidative phosphorylation and respiration uncoupling.
- Low protein and low methionine (at both protein levels) reduced feed intake and growth in RT.
- The brain gene expression of ATF4 (amino acid sensing) and CCK (anorectic feeding peptide), appear as relevant markers related to the amino acid-induced changes in RT feed intake.
- Iron metabolism in RT was affected by plant-based diet and mineral inclusion.
- Mineral premix inclusion decreased the AAC of Fe; increased the whole body Fe concentration; increased hepatic hepcidin and decreased intestinal ferroportin1 transcription in RT.
- The full vegetal diet decreased growth and AAC of Fe, increased whole body and plasma concentration of Fe; increased intestinal ferric reductase activity and decreased hepcidin transcripts, probably in relation with changes in cholesterol metabolism in RT.
- The gene expression of hepcidin (liver) and ferroportin 1 (intestine) appears as a relevant biomarkers to phenotype diet-induced changes in iron homeostasis in RT.
- In AS, a nutritional stress was produced by feeding SBM at 30 % of diet replacing fishmeal/other plant proteins
- Degraded performance in terms of reduced growth was induced in salmon fed 30 % SBM compared to fish fed 0 % SBM.
- The intestinal transcriptome response was dominated by specific response to SBM, whereas the liver response included gene expression responses that were likely more general.
- A set of 88 genes was differentially expressed only in liver and not intestine of AS, which included genes involved in digestion and energy metabolism that were up-regulated, but possibly more related to the specific nutritional stress. Genes in other pathways were generally anabolic genes and down-regulated.
- A set of 45 genes were regulated in both intestine and liver and most were similarly regulated as so possibly specific to SBM, but a few showed opposite regulation in the two tissues and may be less likely to be specific to SBM stress.

Multi-species conclusions:

- Meta-analyses of several different nutritional (or other) challenges or stresses still appears the better approach to identify potential biomarkers, although it is more likely to reveal “panels” of biomarker genes showing a pattern of response that can indicate particular physiological or metabolic states.
- The use of integrative tools combining conventional and “omic” approaches appears the most suitable way for performance phenotyping of farmed fish, although the extrapolation among species is difficult due to differences in nutrient requirements and life cycles.

6. References

Adzic, M., Djordjevic, A., Demonacos, C., Krstic-Demonacos, M., Radojcic, M.B. (2009). The role of phosphorylated glucocorticoid receptor in mitochondrial functions and apoptotic signalling in brain tissue of stressed Wistar rats. Int. J. Biochem. Cell Biol. 41: 2181-2188.

Alesci, S., Manoli, I., Michopoulos, V.J., Brouwers, F.M., Le, H., Gold, P.W., Blackman, M.R., Rennert, O.M., Su, Y.A., Chrousos, G.P. (2006). Development of a human mitochondria-focused cDNA microarray (hMitChip) and validation in skeletal muscle cells: implications for pharmaco- and mitogenomics. Pharmacogenomics J. 6: 333-342.

Altschul, S.F., Gish, W., Miller, W., Myers, E.W., Lipman, D.J. (1990). Basic local alignment search tool. J. Mol. Biol. 215: 403-410.

Aluru, N., Vijayan, M.M. (2009). Stress transcriptomics in fish: A role for genomic cortisol signaling. Gen. Comp. Endocrinol. 164: 142-150.

Alvarez, C.A., Santana, P.A., Guzman, F., Marshall, S., Mercado, L. (2013). Detection of the hepcidin prepropeptide and mature peptide in liver of rainbow trout. Dev. Comp. Immunol. 41: 77-81.

Andrews, N.C. (2000). Iron homeostasis: insights from genetics and animal models. Nat. Rev. Genet. 1: 208-217.

Anthony, T.G., Gietzen, D.W. (2013). Detection of amino acid deprivation in the central nervous system. Curr. Opin. Clin. Nutr. Metab. Care. 16: 96–101.

Antonicka, H., Mattman, A., Carlson, C.G., Glerum, D.M., Hoffbuhr, K.C., Leary, S.C., Kennaway, N.G., Shoubridge, E.A. (2003). Mutations in COX15 produce a defect in the mitochondrial heme biosynthetic pathway, causing early-onset fatal hypertrophic cardiomyopathy. Am. J. Hum. Genet. 72: 101-114.

Anttila, K., Jäntti, M., Mänttäri, S. (2010). Effects of training on lipid metabolism in swimming muscles of sea trout (*Salmo trutta*). J. Comp. Physiol. B. 180: 707-714.

Arumugam, T.V., Gleichmann, M., Tang, S.C., Mattson, M.P. (2006). Hormesis/preconditioning mechanisms, the nervous system and aging. Ageing Res. Rev. 5: 165-178.

Baeverfjord, G., Krogdahl, A. (1996). Development and regression of soybean meal induced enteritis in Atlantic salmon, *Salmo salar* L., distal intestine: a comparison with the intestines of fasted fish. J. Fish Dis. 19: 375-387.

Bakke-McKellep, A.M., Frøystad, M.K., Lilleeng, E., Dapra, F., Refstie, S., Krogdahl, Å, Landsverk, T. (2007). Response to soy: T-cell-like reactivity in the intestine of Atlantic salmon, *Salmo salar* L. J. Fish Dis. 30: 13-25.

Balasubramanian, M.N., Butterworth, E.A., Kilberg, M.S. (2013). Asparagine synthetase: regulation by cell stress and involvement in tumor biology. Am. J. Physiol. Endocrinol. Metab. 304: E789–E799.

Barbour, J.A., Turner, N. (2014). Mitochondrial stress signaling promotes cellular adaptations. Int. J. Biochem. Cell. Biol. 2014: 156020.

Bauer, M., Hamm, A.C., Bonaus, M., Jacob, A., Jaekel, J., Schorle, H., Pankratz, M.J., Katzenberger, J.D. (2004). Starvation response in mouse liver shows strong correlation with life-span-prolonging processes. Physiol. Genomics 17: 230-244.

Benedito-Palos, L., Ballester-Lozano, G., Pérez-Sánchez, J. (2014). Wide-gene expression analysis of lipid-relevant genes in nutritionally challenged gilthead sea bream (*Sparus aurata*). Gene 547: 34-42.

Benedito-Palos, L., Navarro, J.C., Kaushik, S., Pérez-Sánchez, J. (2010). Tissue-specific robustness of fatty acid signatures in cultured gilthead sea bream (*Sparus aurata* L.) fed practical diets with a combined high replacement of fish meal and fish oil. J. Anim. Sci. 88: 1759-1770.

Benedito-Palos, L., Saera-Vila, A., Calduch-Giner, J.A., Kaushik, S., Pérez-Sánchez, J. (2007). Combined replacement of fish meal and oil in practical diets for fast growing

juveniles of gilthead sea bream (*Sparus aurata* L.): Networking of systemic and local components of GH/IGF axis. Aquaculture 267: 199-212.

Bermejo-Nogales, A., Benedito-Palos, L., Calduch-Giner, J.A., Pérez-Sánchez, J. (2011). Feed restriction up-regulates uncoupling protein 3 (UCP3) gene expression in heart and red muscle tissues of gilthead sea bream (*Sparus aurata* L.): New insights in substrate oxidation and energy expenditure. Comp. Biochem. Physiol. A 159: 296-302.

Bermejo-Nogales, A., Benedito-Palos, L., Saera-Vila, A., Calduch-Giner, J.A., Sitjà-Bobadilla, A., Pérez-Sánchez, J. (2008). Confinement exposure induces glucose regulated protein 75 (GRP75/mortalin/mtHsp70/PBP74/HSPA9B) in the hepatic tissue of gilthead sea bream (*Sparus aurata* L.). Comp. Biochem. Physiol. B 149: 428-438.

Bermejo-Nogales, A., Calduch-Giner, J.A., Pérez-Sánchez, J. (2014). Tissue-specific gene expression and functional regulation of uncoupling protein 2 (UCP2) by hypoxia and nutrient availability in gilthead sea bream (*Sparus aurata*): implications on the physiological significance of UCP1-3 variants. Fish Physiol. Biochem. 40: 751-762.

Bermejo-Nogales, A., Nederlof, M., Benedito-Palos, L., Ballester-Lozano, G.F., Folkedal, O., Olsen, R.E., Sitjà-Bobadilla, A., Pérez-Sánchez, J. (2014). Metabolic and transcriptional responses of gilthead sea bream (*Sparus aurata* L.) to environmental stress: New insights in fish mitochondrial phenotyping. Gen. Comp. Endocrinol. 205: 305-315.

Bermejo-Nogales, A., Saera-Vila, A., Calduch-Giner, J.A., Navarro, J.C., Sitjà-Bobadilla, A., Pérez-Sánchez, J. (2007). Differential metabolic and gene expression profile of juvenile common dentex (*Dentex dentex* L.) and gilthead sea bream (*Sparus aurata* L.) in relation to redox homeostasis. Aquaculture 267: 213-224.

Bicskei, B., Bron, J., Glover, K., Taggart, J. (2014). A comparison of gene transcription profiles of domesticated and wild Atlantic salmon (*Salmo salar* L.) at early life stages, reared under controlled conditions. BMC Genomics 15: 884.

Calduch-Giner, J.A., Davey, G., Saera-Vila, A., Houeix, B., Talbot, A., Prunet, P., Cairns, M.T., Pérez-Sánchez, J. (2010). Use of microarray technology to asses the time course of liver stress response after confinement exposure in gilthead sea bream (*Sparus aurata* L.). BMC Genomics 11:193.

Calduch-Giner, J.A., Echasseriau, Y., Crespo, D., Baron, D., Planas, J.V., Prunet, P., Pérez-Sánchez, J. (2014). Transcriptional assessment by microarray analysis and large-scale meta-analysis of the metabolic capacity of cardiac and skeletal muscle tissues to cope with reduced nutrient availability in gilthead sea bream (*Sparus aurata* L.). Mar. Biotechnol. 16: 423-435.

Calduch-Giner, J.A., Mingarro, M., Vega-Rubín de Celis, S., Boujard, D., Pérez-Sánchez, J. (2003). Molecular cloning and characterization of gilthead sea bream (*Sparus aurata*) growth hormone receptor (GHR). Assessment of alternative splicing. Comp. Biochem. Physiol. B. 136: 1-13.

Carriquiriborde, P., Handy, R.D., Davies, S.J. (2004). Physiological modulation of iron metabolism in rainbow trout (*Oncorhynchus mykiss*) fed low and high iron diets. J. Exp. Biol. 207: 75-86.

Carroll, J., Fearnley, I.M., Skehel, J.M., Shannon, R.J., Hirst, J., Walker, J.E. (2006). Bovine complex I is a complex of 45 different subunits. J. Biol. Chem. 281: 32724-32727.

Chen, X., Easton, D., Oh, H.-J., Lee-Yoon, D.-S., Liu, X., Subjeck, J. (1996). The 170 kDa glucose regulated stress protein is a large HSP70- HSP110-like protein of the endoplasmic reticulum. FEBS Lett. 380: 68-72.

Chin, M.T. (2008). ATF-4 and vascular injury - Integration of growth factor signaling and the cellular stress response. Circ. Res. 103: 331-333.

Chomczynski, P., Mackey, K. (1995). Short technical reports. Modification of the TRI reagent procedure for isolation of RNA from polysaccharide- and proteoglycan-rich sources. BioTechniques 19: 942-945.

Chu, W. (2013). Tumor necrosis factor. Cancer Lett. 328: 222-225.

Collins, S.A., Øverland, M., Skrede, A., Drew, M.D. (2013). Effect of plant protein sources on

growth rate in salmonids: Meta-analysis of dietary inclusion of soybean, pea and canola/rapeseed meals and protein concentrates. Aquaculture 400-401: 85-100.

Collinson, I.R,, van Raaij, M.J., Runswick, M.J., Fearnley, I.M., Skehel, J.M., Orriss, G.L., Miroux, B., Walker, J.E. (1994). ATP synthase from bovine heart mitochondria: *In vitro* assembly of a stalk complex in the presence of F1-ATPase and in its absence. J. Mol. Biol. 242: 408-421.

Company, R., Sitjà-Bobadilla, A., Pujalte, M.J., Garay, E., Alvarez-Pellitero, P., Pérez-Sánchez, J. (1999). Bacterial and parasitic pathogens in cultured common dentex, *Dentex dentex* L. J. Fish Dis. 22: 299-309.

Cooper, C.A., Bury, N.R., Grosell, M. (2006). The effects of pH and the iron redox state on iron uptake in the intestine of a marine teleost fish, gulf toadfish (*Opsanus beta*). Comp. Biochem. Physiol. A 143: 292-298.

Coulibaly, I., Gahr, S.A., Palti, Y., Yao, J., Rexroad, C.E. (2006). Genomic structure and expression of uncoupling protein 2 genes in rainbow trout (*Oncorhynchus mykiss)*. BMC Genomics 7: 203.

Craig, E.A., Kramer, J., Shilling, J., Werner-Washburne, M., Holmes, S., Kosic-Smithers, J., Nicolet, C.M. (1989). Ssc1, an essential member of the yeast Hsp70 multigene family, encodes a mitochondrial protein. Mol. Cell. Biol. 9: 3000-3008.

Craven, S.E., French, D., Ye, W., de Sauvage, F., Rosenthal, A. (2005). Loss of Hspa9b in zebrafish recapitulates the ineffective hematopoiesis of the myelodysplastic syndrome. Blood 105: 3528-3534.

Da Costa, N., McGillivray, C., Bai, Q.F., Wood, J.D., Evans, G, Chang, K.C. (2004). Restriction of dietary energy and protein induces molecular changes in young porcine skeletal muscles. Journal of Nutrition 134: 2191-2199.

Dell'Agnello, C., Leo, S., Agostino, A., Szabadkai, G., Tiveron, C., Zulian, A., Prelle, A., Roubertoux, P., Rizzuto, R., Zeviani, M. (2007). Increased longevity and refractoriness to Ca^{2+}-dependent neurodegeneration in Surf1 knockout mice. Hum. Mol. Genet. 16: 431-444.

Désert, C., Duclos, M.J., Blavy, P., Lecerf, F., Moreews, F., Klopp C, Aubry, M., Herault, F., Le Roy, P., Berri, C., Douaire, M., Diot, C., Lagarrigue, S. (2008). Transcriptome profiling of the feeding-to-fasting transition in chicken liver. BMC Genomics 9: 611.

Donovan, A., Lima, C.A., Pinkus, J.L., Pinkus, G.S., Zon, L.I., Robine, S., Andrews, N.C. (2005). The iron exporter ferroportin/Slc40a1 is essential for iron homeostasis. Cell Metabolism 1: 191-200.

Drazen, D.L., Wortman, M.D., Seeley, R.J., Woods, S.C. (2005). Neuropeptide Y prepares rats for scheduled feeding. Am. J. Physiol. Regul. Integr. Comp. Physiol. 288: R1606-R1611.

Dutra, F.F., Bozza, M.T. (2014). Heme on innate immunity and inflammation. Front. Pharmacol. 5: 115.

Figueiredo-Silva, A.C., Saravanan, S., Schrama, J.W., Kaushik, S., Geurden, I. (2012). Macronutrient-induced differences in food intake relate with hepatic oxidative metabolism and hypothalamic regulatory neuropeptides in rainbow trout (*Oncorhynchus mykiss*). Physiol. Behav. 106: 499-505.

Fraenkel, P.G., Traver, D., Donovan, A., Zahrieh, D., Zon, L.I. (2005). Ferroportin1 is required for normal iron cycling in zebrafish. Journal of Clinical Investigation 115: 1532-1541.

Francis, G., Makkar, H.P.S., Becker, K. (2001). Antinutritional factors present in plant-derived alternate fish feed ingredients and their effects in fish. Aquaculture 199: 197-227.

Gabaldon, T., Rainey, D., Huynen, M.A. (2005). Tracing the evolution of a large protein complex in the eukaryotes, NADH : Ubiquinone oxidoreductase (Complex I). J. Mol. Biol. 348: 857-870.

Ganga, R., Montero, D., Bell, J.G., Atalah, E., Ganuza, E., Vega-Orellana, O., Tort, L., Acerete, L., Afonso, J.M., Benitez-Sanatana, T., Fernández Vaquero, A., Izquierdo, M. (2011). Stress response in sea bream (*Sparus aurata*) held under crowded conditions and fed diets containing linseed and/or soybean oil. Aquaculture 311: 215-

223.
Ganz, T., Nemeth, E. (2012). Hepcidin and iron homeostasis. BBA-Mol. Cell Res. 1823: 1434-1443.
Gatlin, D. M., Barrows, F. T., Brown, P., Dabrowski, K., Gaylord, T. G., Hardy, R. W., Herman, E., Hu, G., Krogdahl, Å, Nelson, R. Overturf, K., Rust, M., Sealey, W., Skonberg, D., Souza, E.J., Stone, D., Wilson, R., Wurtele, E. (2007). Expanding the utilization of sustainable plant products in aquafeeds: a review. Aquacult. Res. 38: 551-579.
Gentleman, R., Carey, V., Bates, D., Bolstad, B., Dettling, M., Dudoit, S., Ellis, B., Gautier, L., Ge, Y., Gentry, J., Hornik, K., Hothorn, T., Huber, W., Iacus, S., Irizarry, R., Leisch, F., Li, C., Maechler, M., Rossini, A.J., Sawitzki, G., Smith, C., Smyth, G., Tierney, L., Yang, J.Y., Zhang, J. (2004). Bioconductor: open software development for computational biology and bioinformatics. Genome Biol. 5: R80.
Ghezzi, D., Zeviani, M. (2012). Assembly factors of human mitochondrial respiratory chain complexes: physiology and pathophysiology. Adv. Exp. Med. Biol. 748: 65-106.
Gietzen, D.W., Hao, S., Anthony, T.G. (2007). Mechanisms of food intake repression in indispensable amino acid deficiency. Ann. Rev. Nutr. 27: 63–78.
Goto, S., Nagao, K., Bannai, M., Takahashi, M., Nakahara, K., Kangawa, K., Murakami, N. (2010). Anorexia in rats caused by a valine-deficient diet is not ameliorated by systemic ghrelin treatment. Neurosci. 166: 333–340.
Gu, M., Kortner, T.M., Penn, M., Hansen, A.K., Krogdahl, Å. (2014). Effects of dietary plant meal and soya-saponin supplementation on intestinal and hepatic lipid droplet accumulation and lipoprotein and sterol metabolism in Atlantic salmon (*Salmo salar*L.). Br. J. Nutr. 111: 432-444.
Habersetzer, J., Ziani, W., Larrieu, I., Stines-Chaumeil, C., Giraud, M.F., Brèthes, D., Dautant, A., Paumard, P. (2013). ATP synthase oligomerization: From the enzyme models to the mitochondrial morphology. Int. J. Biochem. Cell Biol. 45: 99-105.
Haiyan, D., Wensheng, L., Haoran, L. (2010) Comparative analyses of sequence structure, evolution, and expression of four somatostatin receptors in orange-spotted grouper (*Epinephelus coioides*). Mol. Cell. Endocrinol. 323: 125-136.
Hardy, R.W. (2001) Nutritional deficiencies in commercial aquaculture: likelihood, onset, and identification. In: Nutrition and Fish Health pp 131-147. Lim, C., Webster, C.D. (Eds), Haworth Press, Inc.
Hartl, M., Giri, A.P., Kaur, H., Baldwin, I.T. (2011). The multiple functions of plant serine protease inhibitors: Defense against herbivores and beyond. Plant Signaling & Behavior 6: 1009-1011.
Hirst, J., Carroll, J., Fearnley, I.M., Shannon, R.J., Walker, J.E. (2003). The nuclear encoded subunits of complex I from bovine heart mitochondria. BBA Bioenergetics 1604: 135-150.
Huttemann, M., Kadenbach, B., Grossman, L.I. (2001). Mammalian subunit IV isoforms of cytochrome c oxidase. Gene 267: 111-123.
Iwashita, Y., Suzuki, N., Matsunari, H., Sugita, T., Yamamoto, T. (2009) Influence of soya saponin, soya lectin, and cholyltaurine supplemented to a casein-based semipurified diet on intestinal morphology and biliary bile status in fingerling rainbow trout *Oncorhynchus mykiss*. Fisheries Science 75: 1307-1315.
Jain, U., Otley, A.R., Van Limbergen, J., Stadnyk, A.W. (2014). The complement system in inflammatory bowel disease. Inflammatory Bowel Disease 20: 1628-1637.
Jastroch, M., Wuertz, S., Kloas, W., Klingenspor, M. (2005). Uncoupling protein 1 in fish uncovers an ancient evolutionary history of mammalian nonshivering thermogenesis. Physiol. Genomics 22: 150-156.
Karpinski, B.A., Morle, G.D., Huggenvik, J., Uhler, M.D., Leiden, J.M. (1992). Molecular-cloning of human creb-2 - an atf/creb transcription factor that can negatively regulate transcription from the camp response element. Proc. Natl. Acad. Sci. USA. 89: 4820-4824.
Kaul, S.C., Deocaris, C.C., Wadhwa, R. (2007). Three faces of mortalin: A housekeeper,

guardian and killer. Exp. Gerontol. 42: 263-274.
Kaushik, S., Cravedi, J., Lalles, J., Sumpter, J., Fauconneau, B., Laroche. M. (1995). Partial or total replacement of fish meal by soybean protein on growth, protein utilization, potential estrogenic or antigenic effects, cholesterolemia and flesh quality in rainbow trout, *Oncorhynchus mykiss*. Aquaculture 133: 257-274.
Kilberg, M.S., Shan, J., Su, N. (2009). ATF4-dependent transcription mediates signaling of amino acid limitation. Trends Endocrinol. Metab. 20: 436-443.
Kortner, T.M., Gu, J., Krogdahl, Å, Bakke, A.M. (2013). Transcriptional regulation of cholesterol and bile acid metabolism after dietary soyabean meal treatment in Atlantic salmon (*Salmo salar* L.). Br. J. Nutr. 109: 593-604.
Kortner, T.M., Skugor, S., Penn, M.H., Mydland, L.T., Djordjevic, B., Hillestad, M., Krasnov, A., Krogdahl, A. (2012). Dietary soyasaponin supplementation to pea protein concentrate reveals nutrigenomic interactions underlying enteropathy in Atlantic salmon (*Salmo salar*). BMC Vet. Res. 8: 101.
Kortner, T.M., Valen, E.C., Kortner, H., Marjara, I.S., Krogdahl, Å, Bakke, A.M. (2011). Candidate reference genes for quantitative real-time PCR (qPCR) assays during development of a diet-related enteropathy in Atlantic salmon (*Salmo salar* L.) and the potential pitfalls of uncritical use of normalization software tools. Aquaculture 318: 355-363.
Krogdahl, Å, Penn, M., Thorsen, J., Refstie, S., Bakke, A.M. (2010). Important antinutrients in plant feedstuffs for aquaculture: an update on recent findings regarding responses in salmonids. Aquacult. Res. 41: 333-344.
Krossøy, C., Waagbø, R., Ørnsrud, R. (2011). Vitamin K in fish nutrition. Aquacult. Nutr. 17: 585–594.
Kumar, N., Prabhu, P.A.J., Pal, A.K., Remya, S., Aklakur, M., Rana, R.S., Gupta, S., Raman, R.P., Jadhao, S.B. (2011). Anti-oxidative and immuno-hematological status of tilapia (*Oreochromis mossambicus*) during acute toxicity test of endosulfan. Pestic. Biochem. Physiol. 99: 45-52.
Kwong, R.W., Hamilton, C.D., Niyogi, S. (2013). Effects of elevated dietary iron on the gastrointestinal expression of Nramp genes and iron homeostasis in rainbow trout (*Oncorhynchus mykiss*). Fish Physiol. Biochem. 39: 363-372.
Kwong, R.W.M., Niyogi, S. (2008). An *in vitro* examination of intestinal iron absorption in a freshwater teleost, rainbow trout (*Oncorhynchus mykiss*). J. Comp. Physiol. B 178: 963-975.
Kwong, R.W.M., Niyogi, S. (2009). The interactions of iron with other divalent metals in the intestinal tract of a freshwater teleost, rainbow trout (*Oncorhynchus mykiss*). Comp. Biochem. Physiol. C 150: 442-449.
Lall, S.P. (2002). The minerals. In: Fish Nutrition pp 259-308. Halver, J.E., Hardy, R.W. (Eds.), Academic Press.
Leary, S.C., Cobine, P.A., Kaufman, B.A., Guercin, G.H,, Mattman, A., Palatty, J., Lockitch, G., Winge, D.R., Rustin, P., Horvath, R., Shoubridge, E.A. (2007). The human cytochrome c oxidase assembly factors SCO1 and SCO2 have regulatory roles in the maintenance of cellular copper homeostasis. Cell Metab. 5: 9-20.
Lilley, B.N., Ploegh, H.L. (2004). A membrane protein required for dislocation of misfolded proteins from the ER. Nature 429: 834-840.
Linder, D., Freund, R., Kadenbach, B. (1995). Species-specific expression of cytochrome c oxidase isozymes. Comp. Biochem. Physiol. B 112: 461-469.
Little, A.G., Kocha, K.M., Lougheed, S.C., Moyes, C.D. (2010). Evolution of the nuclear-encoded cytochrome oxidase subunits in vertebrates. Physiol. Genomics 42: 76-84.
Livak, K.J., Schmittgen, T.D. (2001). Analysis of relative gene expression data using real-time quantitative PCR and the $2^{-\Delta\Delta C}_{T}$ method. Methods 25: 402-408.
Lkhagvadorj, S., Qu, L., Cai, W., Couture, O., Barb, C.R., Hausman, G.J., Nettleton, D., Anderson, L.L., Dekkers, J.C., Tuggle, CK. (2010). Gene expression profiling of the short-term adaptive response to acute caloric restriction in liver and adipose tissues of pigs differing in feed efficiency. Am. J. Physiol. Regul. Integr. Comp. Physiol. 298:

R494-507.
Ludwig, B., Bender, E., Arnold, S., Huttemann, M., Lee, I., Kadenbach, B. (2011). Cytochrome c oxidase and the regulation of oxidative phosphorylation. ChemBioChem. 2: 392-403.
Luo, W., Brouwer, C. (2013). Pathview: an R/Bioconductor package for pathway-based data integration and visualization. Bioinformatics 29: 1830-1831.
Luo, W., Friedman, M.S., Shedden, K., Hankenson, K.D., Woolf, P.J. (2009). GAGE: generally applicable gene set enrichment for pathway analysis. BMC Bioinformatics 10: 161.
Maloy, K.J., Powrie, F. (2011). Intestinal homeostasis and its breakdown in inflammatory bowel disease. Nature 474, 298-306.
Manoli, I., Alesci, S., Blackman, M.R., Su, Y.A., Rennert, O.M., Chrousos, G.P. (2007). Mitochondria as key components of the stress response. Trends Endocrinol. Metab. 18: 190-198.
Marshall, O.J. (2004). PerlPrimer: cross-platform, graphical primer design for standard, bisulphite and real-time PCR. Bioinformatics 20: 2471-2472.
Martinez-Rubio, L., Morais, S., Evensen, Ã, Wadsworth, S., Ruohonen, K., Vecino, J. L. G., Bell, J. G., Tocher, D. R. (2012). Functional feeds reduce heart inflammation and pathology in Atlantic salmon (*Salmo salar* L.) following experimental challenge with Atlantic salmon reovirus (ASRV). PLOS ONE 7: e40266.
Mattson, M.P., Kroemer, G. (2003). Mitochondria in cell death: novel targets for neuroprotection and cardioprotection. Trends Mol. Med. 9: 196-205.
Maurin, A.C., Jousse, C., Averous, J., Parry, L., Bruhat, A., Cherasse, Y., Zeng, H., Zhang, Y., Harding, H.P., Ron, D., Fafournoux, P. (2005). The GCN2 kinase biases feeding behavior to maintain amino acid homeostasis in omnivores. Cell Metabol. 1: 273–277.
McEwen, B.S. (2002). Sex, stress and the hippocampus: allostasis, allostatic load and the aging process. Neurobiol. Aging 23: 921-939.
Miller, K.M., Schulze, A.D., Ginther, N., Li, S., Patterson, D.A., Farrell, A.P., Hinch, S.G. (2009). Salmon spawning migration: Metabolic shifts and environmental triggers. Comp. Biochem. Physiol. D 4: 75-89.
Mommsen, T.P. (2004). Salmon spawning migration and muscle protein metabolism: the August Krogh principle at work. Comp. Biochem. Physiol. B 139: 383-400.
Morais, S., Silva, T., Cordeiro, O., Rodrigues, P., Guy, D.R., Bron, J.E., Taggart, J.B., Bell, J.G., Tocher, D.R. (2012a). Effects of genotype and dietary fish oil replacement with vegetable oil on the intestinal transcriptome and proteome of Atlantic salmon (*Salmo salar*). BMC Genomics 13: 448.
Morais, S., Taggart, J., Guy, D., Bell, J.G., Tocher, D. (2012b). Hepatic transcriptome analysis of inter-family variability in flesh n-3 long-chain polyunsaturated fatty acid content in Atlantic salmon. BMC Genomics 13: 410.
Moriya, Y., Itoh, M., Okuda, S., Yoshizawa, A.C., Kanehisa, M. (2007). KAAS: an automatic genome annotation and pathway reconstruction server. Nucleic Acids Res. 35: W182-W185.
Muller, M., Kersten, S. (2003). Nutrigenomics: goals and strategies. Nat. Rev. Genet. 4: 315-322.
Murray, H.M., Lall, S.P., Rajaselvam, R., Boutilier, L.A., Blanchard, B., Flight, R.M., Colombo, S., Mohindra, V., Douglas, S.E. (2010). A nutrigenomic analysis of intestinal response to partial soybean meal replacement in diets for juvenile Atlantic halibut, *Hippoglossus hippoglossus*, L. Aquaculture 298: 282-293.
Nakahara, K., Takata, S., Ishii, A., Nagao, K., Bannai, M., Takahashi, M., Murakami, N. (2012). Somatostatin is involved in anorexia in mice fed a valine-deficient diet. Amino Acids 42: 1397–1404.
National Research Council (NRC). (2011). Nutrient Requirements of Fish and Shrimp, National Academies Press.
Nelson, L.E., Sheridan, M.A. (2005). Regulation of somatostatins and their receptors in fish. Gen. Comp. Endocrinol. 142: 117–133.

Ogilvie, I., Kennaway, N.G., Shoubridge, E.A. (2005). A molecular chaperone for mitochondrial complex I assembly is mutated in a progressive encephalopathy. J. Clin. Invest. 115: 2784-2792.

Oliva-Teles, A. (2012) Nutrition and health of aquaculture fish. J. Fish. Dis. 35: 83-108.

Park, J., Easton, D.P., Chen, X., MacDonald, I.J., Wang, X.-Y., Subjeck, J.R. (2003). The chaperoning properties of mouse Grp170, a member of the third family of Hsp70 related proteins. Biochemistry 42: 14893-14902.

Parsons, W.J., Williams, R.S., Shelton, J.M., Luo, Y.A., Kessler, D.J., Richardson, J.A. (1996). Developmental regulation of cytochrome oxidase subunit VIa isoforms in cardiac and skeletal muscle. Am. J. Physiol. Heart Circ. Physiol. 270: H567-H574.

Pereira Maduenho, L., Martinez, C.B.R. (2008). Acute effects of diflubenzuron on the freshwater fish *Prochilodus lineatus*. Comp. Biochem. Physiol. C 148: 265-272.

Pérez-Sánchez, J., Bermejo-Nogales, A., Calduch-Giner, J.A., Kaushik, S., Sitjà-Bobadilla, A. (2011). Molecular characterization and expression analysis of six peroxiredoxin paralogous genes in gilthead sea bream (*Sparus aurata*): Insights from fish exposed to dietary, pathogen and confinement stressors. Fish Shellfish Immunol. 31: 294-302.

Pérez-Sánchez, J., Borrel, M., Bermejo-Nogales, A., Benedito-Palos, L., Saera-Vila, A., Calduch-Giner, J.A., Kaushik, S. (2013). Dietary oils mediate cortisol kinetics and the hepatic mRNA expression profile of stress-responsive genes in gilthead sea bream (*Sparus aurata*) exposed to crowding stress. Implications on energy homeostasis and stress susceptibility. Comp. Biochem. Physiol. D 8: 123-130.

Pfaffl, M.W. (2001). A new mathematical model for relative quantification in real-time RT-PCR. Nucleic Acids Res. 29: e45.

Pierron, D., Wildman, D.E., Huttemann, M., Markondapatnaikuni, G.C., Aras, S., Grossman, L.I. (2012). Cytochrome c oxidase: Evolution of control via nuclear subunit addition. BBA Bioenergetics 1817: 590-597.

Poss K.D., Tonegawa S. (1997). Heme oxygenase 1 is required for mammalian iron reutilization. Proc. Natl. Acad. Sci. USA. 94: 10919-10924.

Pujalte, M.J., Sitjà-Bobadilla, A., Macian, M.C., Belloch, C., Álvarez-Pellitero, P., Pérez-Sánchez, J., Uruburu, F., Garay, E. (2003). Virulence and molecular typing of *Vibrio harveyi* strains isolated from cultured dentex, gilthead sea bream and European sea bass. Syst. Appl. Microbiol. 26: 284-292.

Pujolar, J.M., Marino, I.A.M., Milan, M., Coppe, A., Maes, G.E., Capoccioni, F., Ciccotti, E., Bervoets, L., Covaci, A., Belpaire, C., Cramb, G., Patarnello, T., Bargelloni, L., Bortoluzzi, S., Zane, L. (2012). Surviving in a toxic world: transcriptomics and gene expression profiling in response to environmental pollution in the critically endangered European eel. BMC Genomics 13: 507.

Pujolar, J.M., Milan, M., Marino, I.A.M., Capoccioni, F., Ciccotti, E., Belpaire, C., Covaci, A., Malarvannan, G., Patarnello, T., Bargelloni, L., Zane, L., Maes, G.E. (2013). Detecting genome-wide gene transcription profiles associated with high pollution burden in the critically endangered European eel. Aquatic Toxicol. 132: 157-164.

R Core Team (2013). R: A language and environment for statistical computing. R Foundation for Statistical Computing, Vienna, Austria.

Ritchie, M.E., Silver, J., Oshlack, A., Holmes, M., Diyagama, D., Holloway, A., Smyth, G.K. (2007). A comparison of background correction methods for two-colour microarrays. Bioinformatics 23: 2700-2707.

Roberts, R.J. (2002). Nutritional pathology. In: Fish Nutrition pp 453-504. Halver, J.E., Hardy, R.W. (Eds), Academic Press.

Rui, L.Y. (2014). Energy metabolism in the liver. Compr. Physiol. 4: 177-197.

Russell, S., Meadows, L.A., Russell, R.R. (2009). Microarray Technology in Practice. Elsevier.

Saera-Vila, A., Benedito-Palos, L., Sitjà-Bobadilla, A., Nácher-Mestre, J., Serrano, R., Kaushik, S., Pérez-Sánchez, J. (2009a). Assessment of the health and antioxidant trade-off in gilthead sea bream (*Sparus aurata* L.) fed alternative diets with low levels of contaminants. Aquaculture 296: 87-95.

Saera-Vila, A., Calduch-Giner, J.A., Prunet, P., Pérez-Sánchez, J. (2009b). Dynamics of liver GH/IGF axis and selected stress markers in juvenile gilthead sea bream (*Sparus aurata*) exposed to acute confinement. Differential stress response of growth hormone receptors. Comp. Biochem. Physiol. A 154: 197-203.

Sahlmann, C., Sutherland, B.J.G., Kortner, T.M., Koop, B.F., Krogdahl, Å, Bakke, A.M. (2013). Early response of gene expression in the distal intestine of Atlantic salmon (*Salmo salar* L.) during the development of soybean meal induced enteritis. Fish Shellfish Immunol. 34: 599-609.

Santigosa, E., García-Meilán, I., Valentin, J. M., Pérez-Sánchez, J., Médale, F., Kaushik, S., Gallardo, M.A. (2011). Modifications of intestinal nutrient absorption in response to dietary fish meal replacement by plant protein sources in sea bream (*Sparus aurata*) and rainbow trout (*Onchorynchus mykiss*). Aquaculture 317: 146-154.

Sargent, J.R., Tocher, D.R., Bell, J.G. (2002). The lipids. In: Fish Nutrition pp 181-257. Halver, J.E., Hardy, R.W. (Eds), Academic Press.

Sarwar Gilani, G., Wu Xiao, C., Cockell, K.A. (2012). Impact of antinutritional factors in food proteins on the digestibility of protein and the bioavailability of amino acids and on protein quality. Br. J. Nutr. 108: S315-S332.

Schaaf, M.J.M., Chatzopoulou, A., Spaink, H.P. (2009). The zebrafish as a model system for glucocorticoid receptor research. Comp. Biochem. Physiol. A 153: 75-82.

Schaefer, A.M., Walker, M., Turnbull, D.M., Taylor, R.W. (2013). Endocrine disorders in mitochondrial disease. Mol. Cell. Endocrinol. 379: 2-11.

Silver, J.D., Ritchie, M.E., Smyth, G.K. (2009). Microarray background correction: maximum likelihood estimation for the normal-exponential convolution. Biostatistics 10: 352-363.

Sitjà-Bobadilla, A., Pujalte, M.J., Bermejo, A., Garay, E., Alvarez-Pellitero, P., Pérez-Sánchez, J. (2007). Bacteria associated with winter mortalities in laboratory-reared common dentex (*Dentex dentex* L.). Aquacult. Res. 38: 733-739.

Skugor, S., Grisdale-Helland, B., Refstie, S., Afanasyev, S., Vielma, J., Krasnov, A. (2011). Gene expression responses to restricted feeding and extracted soybean meal in Atlantic salmon (*Salmo salar* L.). Aquacult. Nutr. 17: 505-517.

Smyth, G.K. (2004). Linear models and empirical bayes methods for assessing differential expression in microarray experiments. Stat. Appl. Genet. Mol. Biol. 3: Article3.

Smyth, G.K., Speed, T. (2003). Normalization of cDNA microarray data. Methods 31: 265-273.

Soto, I.C. (2012). Biogenesis and assembly of eukaryotic cytochrome c oxidase catalytic core. Biochim. Biophys. Acta 1817: 883-897.

Standal, H., Dehli, A., Rorvik, K.A., Andersen, O. (1999). Iron status and dietary levels of iron affect the bioavailability of haem and nonhaem iron in Atlantic salmon *Salmo salar*. Aquacult. Nutr. 5: 193-198.

Sterling, P., Eyer, J. (1998). Allostasis: a new paradigm to explain arousal pathology, In: Handbook of life stress, cognition and health pp 629-649. Fisher, S., Reason, J. (Eds), Wiley.

Sun, F., Huo, X., Zhai, Y.J., Wang. A.J., Xu, J.X., Su, D., Bartlam, M., Rao, Z. (2005). Crystal structure of mitochondrial respiratory membrane protein complex II. Cell 121: 1043-1057.

Suzuki, J., Shen, W.J., Nelson, B.D., Selwood, S.P., Murphy, G.M., Kanehara, H., Takahashi, S., Oida, K., Miyamori, I., Kraemer, F.B. (2002). Cardiac gene expression profile and lipid accumulation in response to starvation. Am. J. Physiol. Endocrinol. Metab. 283: E94-E102.

Suzuki, R. and Shimodaira, H. (2011). pvclust: Hierarchical clustering with P-values via multiscale bootstrap resampling. http://CRAN.R-project.org/package=pvclust

Tacchi, L., Bron, J.E., Taggart, J.B., Secombes, C.J., Bickerdike, R., Adler, M.A., Takle, H., Martin, S.A.M. (2011). Multiple tissue transcriptomic responses to *Piscirickettsia salmonis* in Atlantic salmon (*Salmo salar*). Physiol. Genomics 43: 1241-1254.

Tekin, D., Dursun, A.D., Xi, L. (2010). Hypoxia inducible factor 1 (HIF-1) and cardioprotection. Acta Pharmacol. Sin. 31: 1085-1094.

Urán, P.A., Schrama, J.W., Rombout, J.H.W.M., Taverne-Thiele, J.J., Obach, A., Koppe, W., Verreth, J.A.J. (2009). Time-related changes of the intestinal morphology of Atlantic salmon, *Salmo salar* L., at two different soybean meal inclusion levels. J. Fish Dis. 32: 733-744.

Urán, P.A., Schrama, J.W., Rombout, J.H.W.M., Obach, A., Jensen, L., Kopper, W., Verreth, J.A.J. (2008). Soybean meal-induced enteritis in Atlantic salmon (*Salmo salar* L.) at different temperatures. Aquacult. Nutr. 14: 324-330.

Waagbø, R. (2008). Reducing production related diseases in farmed fish In: Improving farmed fish quality and safety chapeter 15. Lie, Ø. (Ed), Woodhead Publishing Limited.

Wadhwa, R. (2002). An Hsp70 family chaperone, mortalin/mthsp70/PBP74/Grp75: what, when, and where? Cell Stress Chaperones 7: 309-316.

Wadhwa, R., Taira, K., Kaul, S.C. (2002). Mortalin: a potential candidate for biotechnology and biomedicine. Histol. Histopathol. 17: 1173-1177.

Welle, S., Brooks, A.I., Delehanty, J.M., Needler, N., Thornton, C.A. (2003). Gene expression profile of aging in human muscle. Physiol. Genomics 14: 149-159.

Wickham, H. (2009). ggplot2: elegant graphics for data analysis. Springer.

Wisløff, U., Najjar, S.M., Ellingsen, Ø., Haram, P.M., Swoap, S., Al-Share, Q., Fernström, M., Rezaei, K., Lee, S.J., Koch, L.G., Britton, S.L. (2005). Cardiovascular risk factors emerge after artificial selection for low aerobic capacity. Science 307: 418-420.

World Bank (2013). Fish to 2030 : prospects for fisheries and aquaculture. Agriculture and environmental services discussion paper ; no. 3. Washington DC ; World Bank Group. http://documents.worldbank.org/curated/en/2013/12/18882045/fish-2030-prospects-fisheries-aquaculture

Yamamoto, T., Suzuki, N., Furuita, H., Sugita, T., Tanaka, N., Goto, T. (2007) Supplemental effect of bile salts to soybean meal-based diet on growth and feed utilization of rainbow trout *Oncorhynchus mykiss*. Fisheries Science 73: 123-131.

Yeh, K.Y., Yeh, M., Glass, J. (2004). Hepcidin regulation of ferroportin 1 expression in the liver and intestine of the rat. American Journal of Physiology-Gastrointestinal and Liver Physiology 286: G385-G394.

Zara, V., Conte, L., Trumpower, B.L. (2009). Biogenesis of the yeast cytochrome bc1 complex. BBA-Mol. Cell Res. 1793: 89-96.

Zhan, J.M., Sonu, R., Vogel, H., Crane, E., Mazan-Mamczarz, K., Rabkin, R., Davis, R.W., Becker, K.G., Owen, A.B., Kim, S.K. (2006). Transcriptional profiling of aging in human muscle reveals a common aging signature. PLoS Genetics 2: e115.

Zhang, J., Guo, L., Feng, L., Jiang, W., Kuang, S., Liu, Y., Hu, K., Jiang, J., Li, S., Tang, L., Zhou, X.Q. (2013). Soybean ß-conglycinin induces inflammation and oxidation and causes dysfunction of intestinal digestion and absorption in fish. *PLOS ONE* 8: e58115.

Annex 1 - Gilthead sea bream

Supplementary Figure 1. Schematic representation of annotated genes of the OXPHOS pathway in GSB, used in the transcriptomic study of trial 2. Mitochondrial-encoded genes are highlighted in bold. Assembly factors are indicated in italics.

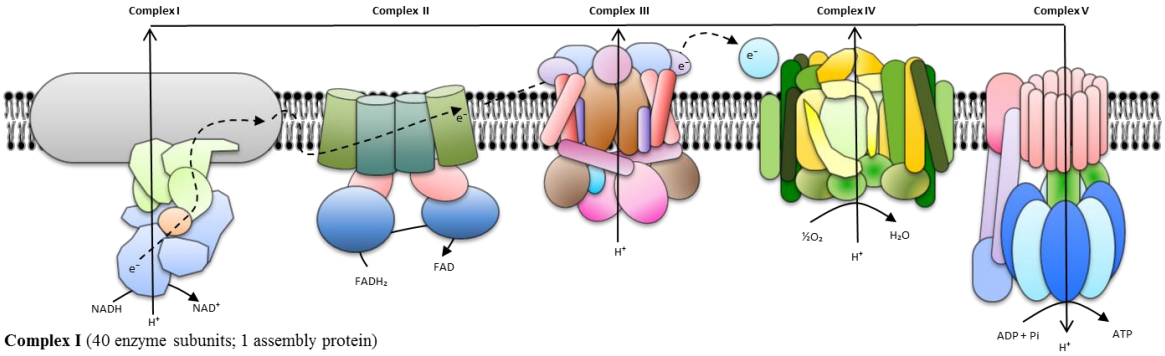

Complex I (40 enzyme subunits; 1 assembly protein)

ND1	**ND2**	**ND5**	**ND6**											
NDUFA1	NDUFA2	NDUFA3	NDUFA4	NDUFA4-L2	NDUFA5	NDUFA6	NDUFA7	NDUFA8	NDUFA9	NDUFA10	NDUFA11	NDUFA12	NDUFA13	
NDUFB1	NDUFB2	NDUFB3	NDUFB4	NDUFB5	NDUFB6	NDUFB7	NDUFB8	NDUFB9	NDUFB10	NDUFB11	NDUFC1	NDUFC2		
NDUFS2	NDUFS3	NDUFS4	NDUFS5	NDUFS6	NDUFS7	NDUFV1	NDUFV2	NDUFV3						
NDUFAF2														

Complex II (4 enzyme subunits; 2 assembly proteins)

SDHA	SDHB	SDHC	SDHD	
SDHAF1	*SDHAF2*			

Complex III (12 enzyme subunits; 1 assembly protein)

CYB									
CYC1	UQCRFS1	UQCRC1	UQCRC2	UQCRH	UQCRB	UQCRQ	UQCR10	UQCR11-A	UQCR11-B
CYC									
UQCC									

Complex IV (20 enzyme subunits; 3 assembly proteins)

COXI	**COXII**	COXIII										
COX4a	COX4b	COX5a1	COX5a2	COX5b1	COX5b2	COX6a1	COX6a2	COX6b1a	COX6b1b	COX6c	COX7a1	COX7a2
COX7b	COX7c	COX8a	COX8b									
COX15	*SURF1*	*SCO1*										

Complex V (15 enzyme subunits; 1 assembly protein)

ATP6	**ATP8**											
ATP5A1	ATP5B	ATP5C1	ATP5D	ATP5E	ATP5F1	ATP5G1	ATP5H	ATP5I	ATP5J2	ATP5L	ATP5O	OSCP1
ATPAF2												

Supplemental Table 1. Classification of identified genes according to BLAST searches used in trial 1 of gilthead sea bream.

Contig	F[1]	size (nt)	Annotation[2]	Best match[3]	E[4]	CDS[5]
C2_997	458	3067	CAT	AAU44617	0	82-1671
C2_270	526	787	Cox4a	Q9I8U0	2E-106	71-580
C2_4920	97	2907	CPT1A	ADH04490	0	<1-921
C2_3305	135	1979	CREB-2	XP_003443277	4E-133	271-1554
C2_17301	15	789	DER-1	XP_003443742	8E-136	132->788
C2_3722	235	1553	ECH	XP_003441229	3E-180	107-982
C2_2999	265	2342	ERdj3	XP_003456324	0	117-1199
C2_49696	7	414	GRP-170	ADX97080	3E-36	<1->414
C2_1490	399	2920	GRP-94	XP_003443932	0	240-2663
C2_5598	299	1287	GST3	BAE06150	5E-143	365-1033
C2_465	947	1219	HADH	ACO09265	5E-170	98-1033
C2_168	330	943	H-FABP	ABY90513	2E-75	125-526
C2_4447	222	3462	HIF-1α	ABD32158	0	273-2528
C2_3027	222	3940	LAL	ABY90514	0	65-1273
C2_368	901	919	Cu-Zn-SOD	AAO15363	3E-100	89-553
C2_1642	276	1021	Mn-SOD	AAW29024	7E-162	92-769

[1]Number of reads composing the assembled sequences.
[2]Gene identity determined through BLAST searches. CAT, catalase; Cox4a, cytochrome C oxidase subunit IV isoform 1; CPT1A, carnitine palmitoyltransferase 1A; CREB-2, cyclic AMP response element-binding protein 2; DER-1, derlin 1; ECH, enoyl-CoA hydratase; ERdj3, ER-associated Hsp40 co-chaperone; GRP-170, glucose-regulated protein, 170 kDa; GRP-94, glucose-regulated protein 94 kDa; GST3, glutathione S-transferase 3; HADH, hydroxyacyl-CoA dehydrogenase; H-FABP, heart-fatty acid binding protein; HIF-1α, hypoxia inducible factor-1 alpha; LAL, lysosomal acid lipase; Mn-SOD, superoxide dismutase [Mn]; Cu-Zn-SOD, superoxide dismutase [Cu-Zn].
[3]Best BLAST-X protein sequence match (lowest E value).
[4]Expectation value.
[5]Codifying domain sequence.

Supplemental Table 2. Forward and reverse primers for real-time PCR in GSB trial 1.

Gene name	Symbol	Accession number		Primer sequence
β-actin	ACTB	X89920	F	TCC TGC GGA ATC CAT GAG A
			R	GAC GTC GCA CTT CAT GAT GCT
Aryl hydrocarbon receptor 1	AHR1	EU254480	F	CCT GGG ACT GAA CGC CGA AG
			R	GCT AAG TGT TGG GAT GTG GTT GG
Carnitine palmitoyltransferase 1A	CPT1A	JQ308822[1]	F	GTG CCT TCG TTC GTT CCA TGA TC
			R	TGA TGC TTA TCT GCT GCC TGT TTG
Catalase	CAT	JQ308823[1]	F	TGG TCG AGA ACT TGA AGG CTG TC
			R	AGG ACG CAG AAA TGG CAG AGG
Cyclic AMP response element-binding protein 2	CREB-2	JQ308824[1]	F	TTC ATA TAA AGC CAG TCC ACC CTC TC
			R	CTT CTC CAG CAG CAC CTC GTA G
Cytochrome C oxidase subunit IV isoform 1	Cox4a	JQ308835[1]	F	ACC CTG AGT CCA GAG CAG AAG TCC
			R	AGC CAG TGA AGC CGA TGA GAA AGA AC
Cytochrome P450 1A1	CYP1A1	AF011223	F	GCA TCA ACG ACC GCT TCA ACG C
			R	CCT ACA ACC TTC TCA TCC GAC ATC TGG
Derlin-1	DER-1	JQ308825[1]	F	ACT GCC TCG GTT GCC TTT CC
			R	TGG CTG TCA CAA GTC TCC AGA TAT G
Enoyl-CoA hydratase	ECH	JQ308826[1]	F	GCC CAA GAA GCC AAG CAA TCA G
			R	CTT TAG CCA TAG CAG AGA CCA GTT TG
ER-associated Hsp40 co-chaperone	ERdj3	JQ308827[1]	F	AAC CGA CAG CAG CAG GAC AG
			R	ACT TCT TCA AGC GTG ACC TCC AG
Estrogen receptor alpha	ER-α	AF136979	F	TCT AAG GGT CTG GAG CAC
			R	TCG GTA TAG GGT CGG TTC
Fatty acid binding protein, heart	H-FABP	JQ308834[1]	F	CTG GGT GTG GGC TTC GCT AC
			R	CTC TGT GTT CTT GAT GGT GCT CTG
Glucocorticoid receptor	GCR	DQ486890	F	CCA GGA CAG GTG CCG AAC G
			R	TGG AGG AAC TGC TGC TGA ACC
Glucose-regulated protein, 170 kDa	GRP-170	JQ308821[1]	F	CAG AGG AGG CAG ACA GCA AGA C
			R	TTC TCA GAC TCA GCA TTT CCA GAT TTC
Glucose-regulated protein, 94 kDa	GRP-94	JQ308820[1]	F	AAG GCA CAG GCT TAC CAG ACA G
			R	CTT CAG CAT CAT CGC CGA CTT TC
Glucose-regulated protein, 75 kDa	GRP-75	DQ524993	F	TCC GGT GTG GAT CTG ACC AAA GAC
			R	TGT TTA GGC CCA GAA GCA TCC ATG
Glutathione peroxidase 1	GPX1	DQ524992	F	GAA GGT GGA TGT GAA TGG AAA AGA TG
			R	CTG ACG GGA CTC CAA ATG ATG G
Glutathione peroxidase 4	GPX4	AM977818	F	TGC GTC TGA TAG GGT CCA CTG TC
			R	GTC TGC CAG TCC TCT GTC GG
Glutathione reductase	GR	AJ937873	F	TGT TCA GCC ACC CAC CCA TCG G
			R	GCG TGA TAC ATC GGA GTG AAT GAA GTC TTG
Glutathione S-transferase 3	GST3	JQ308828[1]	F	CCA GAT GAT CAG TAC GTG AAG ACC GTC
			R	CTG CTG ATG TGA GGA ATG TAC CGT AAC
Hepatic lipase	HL	EU254479	F	TTG TAG AAG GTG AGG AAA ACT G
			R	GCT CTC CAT CAG ACC ATC C
Hepcidin	HEPC	AM749960	F	ACT CCT GGA AGA TGC CGT ATG C
			R	AAC TTA CAC CTC CTG CGT CCA C
Hormone-sensitive lipase	HSL	EU254478	F	GCT TTG CTT CAG TTT ACC ACC ATT TC
			R	GAT GTA GCG ACC CTT CTG GAT GAT GTG

Suppl. Table 2 continued

Gene name	Symbol	Accession number		Primer sequence
Hydroxyacyl-CoA dehydrogenase	HADH	JQ308829[1]	F	GAA CCT CAG CAA CAA GCC AAG AG
			R	CTA AGA GGC GGT TGA CAA TGA ATC C
Hypoxia inducible factor-1 alpha	HIF-1α	JQ308830[1]	F	CAG ATG AGC CTC TAA CTT GTG GAC
			R	TTA GCA AGA ATG GTG GCA AGA TGA G
Lipoprotein lipase	LPL	AY495672	F	CGT TGC CAA GTT TGT GAC CTG
			R	AGG GTG TTC TGG TTG TCT GC
Lysosomal acid lipase	LAL	JQ308831[1]	F	TAC TAC ATC GGA CAC TCT CAA GGA AC
			R	GTG GAG AAC GCT ATG AAT GCT ATC G
Peroxiredoxin 3	PRDX3	GQ252681	F	ATC AAC ACC CCA CGC AAG ACT G
			R	ACC GTT TGG ATC AAT GAG GAA CAG ACC
Peroxiredoxin 5	PRDX5	GQ252683	F	GAG CAC GGA ACA GAT GGC AAG G
			R	TCC ACA TTG ATC TTC TTC ACG ACT CC
Superoxide dismutase [Cu-Zn]	Cu-Zn-SOD	JQ308832[1]	F	TCA CGG ACA AGA TGC TCA CTC TC
			R	GGT TCT GCC AAT GAT GGA CAA GG
Superoxide dismutase [Mn]	Mn-SOD	JQ308833[1]	F	CCT GAC CTG ACC TAC GAC TAT GG
			R	AGT GCC TCC TGA TAT TTC TCC TCT G
Uncoupling protein 1	UCP1	FJ710211	F	GCA CAC TAC CCA ACA TCA CAA G
			R	CGC CGA ACG CAG AAA CAA AG

[1]New GSB sequences uploaded to GenBank

Supplemental Table 3. PCR-array layout (88 genes) with extra-wells for housekeeping genes (ACTB) and general controls of PCR performance used in GSB trial 2. The GenBank accession number for each gene in the OXPHOS-array is reported. Mitochondrial-encoded catalytic subunits are in bold and red. Nuclear-encoded catalytic subunits are in red. Nuclear-encoded regulatory subunits are in black. Nuclear-encoded assembly factors are in blue and italics.

	1	2	3	4	5	6	7	8	9	10	11	12
A	**ND2**	NDUFA6	NDUFB4	NDUFC2	NDUFV3	**CYB**	UQCRQ	Cox4a	COX6b1b	*SCO1*	ATP5F1	PPC1
B	**ND5**	NDUFA7	NDUFB5	NDUFS2	*NDUFAF2*	CYCS	UQCR10	COX4b	COX6c1	*SURF1*	ATP5G1	PPC2
C	NDUFA1	NDUFA8	NDUFB6	NDUFS4	SDHA	CYC1	UQCR11-A	COX5a1	COX7a1	*COX15*	ATP5I	PPC3
D	NDUFA2	NDUFA9	NDUFB8	NDUFS5	SDHB	UQCRFS1	UQCR11-B	COX5a2	COX7a2	ATP5A1	ATP5J2	PPC4
E	NDUFA3	NDUFA12	NDUFB9	NDUFS6	SDHC	UQCRC1	*UQCC*	COX5b2	COX7b	ATP5B	ATP5L	NPC
F	NDUFA4	NDUFB1	NDUFB10	NDUFS7	SDHD	UQCRC2	**COXI**	COX6a1	COX7c	ATP5C1	ATP5O	ACTB
G	NDUFA4-like2	NDUFB2	NDUFB11	NDUFV1	*SDHAF1*	UQCRH	**COXII**	COX6a2	COX8a	ATP5D	OSCP	ACTB
H	NDUFA5	NDUFB3	NDUFC1	NDUFV2	*SDHAF2*	UQCRB	**COXIII**	COX6b1a	COX8b	ATP5E	*ATPAF2*	ACTB

Position	Symbol	Description	Accession No.
A1	**ND2**	NADH-ubiquinone oxidoreductase chain 2	KC217558
B1	**ND5**	NADH-ubiquinone oxidoreductase chain 5	KC217559
C1	NDUFA1	NADH dehydrogenase [ubiquinone] 1 alpha subcomplex subunit 1	KC217562
D1	NDUFA2	NADH dehydrogenase [ubiquinone] 1 alpha subcomplex subunit 2	KC217563
E1	NDUFA3	NADH dehydrogenase [ubiquinone] 1 alpha subcomplex subunit 3	KC217564
F1	NDUFA4	NADH dehydrogenase [ubiquinone] 1 alpha subcomplex subunit 4	KC217565
G1	NDUFA4-like2	NADH dehydrogenase [ubiquinone] 1 alpha subcomplex subunit 4-like 2	KC217566
H1	NDUFA5	NADH dehydrogenase [ubiquinone] 1 alpha subcomplex subunit 5	KC217567
A2	NDUFA6	NADH dehydrogenase [ubiquinone] 1 alpha subcomplex subunit 6	KC217568
B2	NDUFA7	NADH dehydrogenase [ubiquinone] 1 alpha subcomplex subunit 7	KC217569
C2	NDUFA8	NADH dehydrogenase [ubiquinone] 1 alpha subcomplex subunit 8	KC217570
D2	NDUFA9	NADH dehydrogenase [ubiquinone] 1 alpha subcomplex subunit 9	KC217571
E2	NDUFA12	NADH dehydrogenase [ubiquinone] 1 alpha subcomplex subunit 12	KC217574
F2	NDUFB1	NADH dehydrogenase [ubiquinone] 1 beta subcomplex subunit 1	KC217576
G2	NDUFB2	NADH dehydrogenase [ubiquinone] 1 beta subcomplex subunit 2	KC217577
H2	NDUFB3	NADH dehydrogenase [ubiquinone] 1 beta subcomplex subunit 3	KC217578
A3	NDUFB4	NADH dehydrogenase [ubiquinone] 1 beta subcomplex subunit 4	KC217579
B3	NDUFB5	NADH dehydrogenase [ubiquinone] 1 beta subcomplex subunit 5	KC217580
C3	NDUFB6	NADH dehydrogenase [ubiquinone] 1 beta subcomplex subunit 6	KC217581
D3	NDUFB8	NADH dehydrogenase [ubiquinone] 1 beta subcomplex subunit 8	KC217583
E3	NDUFB9	NADH dehydrogenase [ubiquinone] 1 beta subcomplex subunit 9	KC217584
F3	NDUFB10	NADH dehydrogenase [ubiquinone] 1 beta subcomplex subunit 10	KC217585
G3	NDUFB11	NADH dehydrogenase [ubiquinone] 1 beta subcomplex subunit 11	KC217586
H3	NDUFC1	NADH dehydrogenase 1 subunit C1	KC217587
A4	NDUFC2	NADH dehydrogenase 1 subunit C2	KC217588
B4	NDUFS2	NADH dehydrogenase iron-sulfur protein 2	KC217589
C4	NDUFS4	NADH dehydrogenase iron-sulfur protein 4	KC217591
D4	NDUFS5	NADH dehydrogenase iron-sulfur protein 5	KC217592
E4	NDUFS6	NADH dehydrogenase iron-sulfur protein 6	KC217593
F4	NDUFS7	NADH dehydrogenase iron-sulfur protein 7	KC217594
G4	NDUFV1	NADH dehydrogenase [ubiquinone] flavoprotein 1	KC217595
A5	NDUFV3	NADH dehydrogenase [ubiquinone] flavoprotein 3	KC217597
A5	NDUFV3	NADH dehydrogenase [ubiquinone] flavoprotein 3	KC217597
B5	*NDUFAF2*	NADH dehydrogenase (ubiquinone) 1 alpha subcomplex, assembly factor 2	KC217598
C5	SDHA	Succinate dehydrogenase [ubiquinone] flavoprotein subunit	KC217615
D5	SDHB	Succinate dehydrogenase [ubiquinone] iron-sulfur subunit	KC217616
E5	SDHC	Succinate dehydrogenase cytochrome b560 subunit	KC217617
F5	SDHD	Succinate dehydrogenase [ubiquinone] cytochrome b small subunit B	KC217618

Supplemental Table 3. Continued.

Position	Symbol	Description	Accession No.
G5	*SDHAF1*	Succinate dehydrogenase assembly factor 1	KC217619
H5	*SDHAF2*	Succinate dehydrogenase assembly factor 2	KC217620
A6	**CYB**	Cytochrome b	DQ198005
B6	CYCS	Cytochrome c	KC217632
C6	CYC1	Cytochrome c1, heme protein	KC217621
D6	UQCRFS1	Cytochrome b-c1 complex subunit Rieske	KC217622
E6	UQCRC1	Cytochrome b-c1 complex subunit 1	KC217623
F6	UQCRC2	Cytochrome b-c1 complex subunit 2	KC217624
G6	UQCRH	Cytochrome b-c1 complex subunit 6	KC217625
H6	UQCRB	Cytochrome b-c1 complex subunit 7	KC217626
A7	UQCRQ	Cytochrome b-c1 complex subunit 8	KC217627
B7	UQCR10	Cytochrome b-c1 complex subunit 9	KC217628
C7	UQCR11-A	Cytochrome b-c1 complex subunit 10 isoform A	KC217629
D7	UQCR11-B	Cytochrome b-c1 complex subunit 10 isoform B	KC217630
E7	*UQCC*	Ubiquinol-cytochrome c reductase complex chaperone CBP3 homolog	KC217631
F7	**COXI**	Cytochrome c oxidase subunit I	KC217652
G7	**COXII**	Cytochrome c oxidase subunit II	KC217653
H7	**COXIII**	Cytochrome c oxidase subunit II	KC217654
A8	Cox4a	Cytochrome c oxidase subunit 4 isoform 1	JQ308835
B8	COX4b	Cytochrome c oxidase subunit 4 isoform 2	KC217633
C8	COX5a1	Cytochrome c oxidase subunit 5A, mitochondrial-like isoform 1	KC217634
D8	COX5a2	Cytochrome c oxidase subunit 5A, mitochondrial-like isoform 2	KC217635
E8	COX5b2	Cytochrome c oxidase subunit 5B isoform 2	KC217637
F8	COX6a1	Cytochrome c oxidase subunit 6A isoform 1	KC217638
G8	COX6a2	Cytochrome c oxidase subunit 6A isoform 2	KC217639
H8	COX6b1a	Cytochrome c oxidase subunit VIb isoform 1a	KC217640
A9	COX6b1b	Cytochrome c oxidase subunit VIb isoform 1b	KC217641
B9	COX6c1	Cytochrome c oxidase subunit 6C-1	KC217642
C9	COX7a1	Cytochrome c oxidase subunit 7A1	KC217643
D9	COX7a2	Cytochrome c oxidase subunit 7A2	KC217644
E9	COX7b	Cytochrome c oxidase subunit 7B	KC217645
F9	COX7c	Cytochrome c oxidase subunit 7C	KC217646
G9	COX8a	Cytochrome c oxidase subunit 8A	KC217647
H9	COX8b	Cytochrome c oxidase subunit 8B	KC217648
A10	*SCO1*	SCO1 protein homolog, mitochondrial	KC217649
B10	*SURF1*	Surfeit locus protein 1	KC217650
C10	*COX15*	Cytochrome c oxidase assembly protein COX15 homolog	KC217651
D10	ATP5A1	ATP synthase subunit alpha	KC217601
E10	ATP5B	ATP synthase subunit beta	KC217602
F10	ATP5C1	ATP synthase subunit gamma	KC217603
G10	ATP5D	ATP synthase subunit delta	KC217604
H10	ATP5E	ATP synthase subunit epsilon	KC217605
A11	ATP5F1	ATP synthase subunit b	KC217606
B11	ATP5G1	ATP synthase lipid-binding protein	KC217607
C11	ATP5I	ATP synthase subunit e	KC217609
D11	ATP5J2	ATP synthase subunit f	KC217610
E11	ATP5L	ATP synthase subunit g	KC217611
F11	ATP5O	ATP synthase subunit O	KC217612
G11	OSCP	Protein OSCP1	KC217613
H11	*ATPAF2*	Mitochondrial F1 complex assembly factor 2	KC217614
A12-D12	PPC	Positive PCR control (serial dilutions of standard gene)	AY590304
G12	NPC	Negative PCR control	
F12-H12	ACTB	ß-Actin	X89920

Supplemental Table 4. Characteristics of the new GSB assembled sequences of Complex I used in GSB trial 2. Mitochondrial-encoded catalytic subunits are in bold and red. Nuclear-encoded catalytic subunits are in red. Nuclear-encoded regulatory subunits are in black. Nuclear-encoded assembly factors are in blue and italics.

Contigs	F[a]	Size (nt)	Annotation[b]	Best match[c]	E[d]	CDS[e]	Accession No[f]
C2_1453	555	1036	**ND1**	YP_001256939	0	9-983	KC217558
C2_994	706	1086	**ND2**	YP_001974735	5e-135	7-1062	KC217559
C2_87	2349	2499	**ND5**	YP_001256949	0	73-1914	KC217560
C2_2144	142	812	**ND6**	YP_001256950	2e-80	73-594	KC217561
C2_8082	80	587	NDUFA1	ACQ58283	6e-38	123-335	KC217562
C2_1985	179	468	NDUFA2	CAF92313	6e-55	46-348	KC217563
C2_4897	71	431	NDUFA3	XP_00340957	1e-43	72-314	KC217564
C2_3631	147	696	NDUFA4	AEM37711	2e-47	128-376	KC217565
C2_1577	173	1230	NDUFA4-like2	XP_003444820	2e-46	120-368	KC217566
C2_22864	63	590	NDUFA5	XP_003455688	2e-64	47-397	KC217567
C2_9313	102	607	NDUFA6	CAG01654	2e-64	47-433	KC217568
C2_2419	111	580	NDUFA7	XP_003449062	2e-61	52-378	KC217569
C2_1373	277	1027	NDUFA8	XP_003444379	2e-116	161-679	KC217570
C2_332	905	1301	NDUFA9	ACQ58220	0	48-1193	KC217571
C2_1225	484	1334	NDUFA10	XP_003457387	0	87-1154	KC217572
C2_4493	81	523	NDUFA11	XP_003448809	1e-83	41-448	KC217573
C2_110117	42	549	NDUFA12	XP_003448116	2e-68	27-470	KC217574
C2_121074	116	596	NDUFA13	XP_003438233	2e-93	50-484	KC217575
C2_9246	57	401	NDUFB1	CAG03553	1e-31	73-249	KC217576
C2_15870	122	553	NDUFB2	ACI68020	7e-58	126-434	KC217577
C2_15466	38	448	NDUFB3	XP_003457472	2e-55	81-362	KC217578
C2_3428	100	505	NDUFB4	XP_003443537	3e-50	38-421	KC217579
C2_467	696	702	NDUFB5	ACQ58904	7e-97	45-602	KC217580
C2_3928	73	588	NDUFB6	XP_003452285	1e-80	106-489	KC217581
C2_1170	317	614	NDUFB7	XP_003450021	6e-65	162-530	KC217582
C2_1305	310	685	NDUFB8	XP_003441843	5e-89	48-623	KC217583
C2_3902	244	958	NDUFB9	XP_003458631	6e-117	55-582	KC217584
C2_497	427	925	NDUFB10	XP_003456422	3e-105	236-751	KC217585
C2_6703	101	572	NDUFB11	XP_003454298	4e-77	61-498	KC217586
C2_5740	92	518	NDUFC1	ACQ58409	4e-30	191-400	KC217587
C2_4941	159	617	NDUFC2	ACO09452	8e-49	143-475	KC217588
C2_961	352	1581	NDUFS2	ACQ58471	0	26-1426	KC217589
C2_1740	354	919	NDUFS3	XP_003456935	6e-161	37-819	KC217590
C2_1717	308	648	NDUFS4	XP_003451066	3e-96	46-555	KC217591
C2_9639	39	515	NDUFS5	XP_003454647	1e-48	83-403	KC217592
C2_10276	92	486	NDUFS6	XP_003443820	2e-76	23-412	KC217593
C2_1860	262	1160	NDUFS7	XP_003449069	1e-133	46-705	KC217594
C2_675	598	1690	NDUFV1	XP_003452502	0	95-1507	KC217595
C2_3103	204	905	NDUFV2	ACQ58245	0	84-818	KC217596
C2_4224	86	552	NDUFV3	XP_003456249	9e-15	38-361	KC217597
C2_1316	682	1007	*NDUFAF2*	XP_003446117	2e-88	119-607	KC217598

[a]Number of reads composing the assembled sequences.

[b]Gene identity determined through BLAST searches: ND1, NADH-ubiquinone oxidoreductase chain 1; ND2, NADH-ubiquinone oxidoreductase chain 2; ND5, NADH-ubiquinone oxidoreductase chain 5; ND6, NADH dehydrogenase subunit 6. NDUFA1, NADH dehydrogenase [ubiquinone] 1 alpha subcomplex subunit 1; NDUFA2, NADH dehydrogenase [ubiquinone] 1 alpha subcomplex subunit 2; NDUFA3, NADH dehydrogenase [ubiquinone] 1 alpha subcomplex subunit 3; NDUFA4, NADH dehydrogenase [ubiquinone] 1 alpha subcomplex subunit 4; NDUFA4-like2, NADH dehydrogenase [ubiquinone] 1 alpha subcomplex subunit 4-like 2; NDUFA5, NADH dehydrogenase [ubiquinone] 1 alpha subcomplex subunit 5; NDUFA6, NADH dehydrogenase [ubiquinone] 1 alpha subcomplex subunit 6; NDUFA7, NADH dehydrogenase [ubiquinone] 1 alpha subcomplex subunit 7; NDUFA8, NADH dehydrogenase [ubiquinone] 1 alpha subcomplex subunit 8; NDUFA9, NADH dehydrogenase [ubiquinone] 1 alpha subcomplex subunit

9; NDUFA10, NADH dehydrogenase [ubiquinone] 1 alpha subcomplex subunit 10; NDUFA11, NADH dehydrogenase [ubiquinone] 1 alpha subcomplex subunit 11; NDUFA12, NADH dehydrogenase [ubiquinone] 1 alpha subcomplex subunit 12; NDUFA13, NADH dehydrogenase [ubiquinone] 1 alpha subcomplex subunit 13; NDUFB1, NADH dehydrogenase [ubiquinone] 1 beta subcomplex subunit 1; NDUFB2, NADH dehydrogenase [ubiquinone] 1 beta subcomplex subunit 2; NDUFB3, NADH dehydrogenase [ubiquinone] 1 beta subcomplex subunit 3; NDUFB4, NADH dehydrogenase [ubiquinone] 1 beta subcomplex subunit 4; NDUFB5, NADH dehydrogenase [ubiquinone] 1 beta subcomplex subunit 5; NDUFB6, NADH dehydrogenase [ubiquinone] 1 beta subcomplex subunit 6; NDUFB7, NADH dehydrogenase [ubiquinone] 1 beta subcomplex subunit 7; NDUFB8, NADH dehydrogenase [ubiquinone] 1 beta subcomplex subunit 8; NDUFB9, NADH dehydrogenase [ubiquinone] 1 beta subcomplex subunit 9; NDUFB10, NADH dehydrogenase [ubiquinone] 1 beta subcomplex subunit 10; NDUFB11, NADH dehydrogenase [ubiquinone] 1 beta subcomplex subunit 11; NDUFC1, NADH dehydrogenase 1 subunit C1; NDUFC2, NADH dehydrogenase 1 subunit C2; NDUFS2, NADH dehydrogenase iron-sulfur protein 2; NDUFS3, NADH dehydrogenase iron-sulfur protein 3; NDUFS4, NADH dehydrogenase iron-sulfur protein 4; NDUFS5, NADH dehydrogenase iron-sulfur protein 5; NDUFS6, NADH dehydrogenase iron-sulfur protein 6; NDUFS7, NADH dehydrogenase iron-sulfur protein 7; NDUFV1, NADH dehydrogenase [ubiquinone] flavoprotein 1; NDUFV2, NADH dehydrogenase [ubiquinone] flavoprotein 2; NDUFV3, NADH dehydrogenase [ubiquinone] flavoprotein 3; NDUFAF2, NADH dehydrogenase (ubiquinone) 1 alpha subcomplex, assembly factor 2.

[c]Best BLAST-X protein sequence match (lowest E value).

[d]Expectation value.

[e]Codifying sequence.

[f]GenBank accession number.

Supplemental Table 5. Characteristics of the new GSB assembled sequences of Complex II used in GSB trial 2. Nuclear-encoded catalytic subunits are in red. Nuclear-encoded regulatory subunits are in black. Nuclear-encoded assembly factors are in blue and italics.

Contigs	F[a]	Size (nt)	Annotation[b]	Best match[c]	E[d]	CDS[e]	Accession No[f]
C2_1571	314	3316	SDHA	XP_003443735	0	23-2014	KC217615
C2_791	529	1381	SDHB	ACQ58642	0	47-898	KC217616
C2_4148	125	711	SDHC	XP_003447506	8e-99	34-546	KC217617
C2_628	560	1275	SDHD	XP_003457657	6e-94	46-522	KC217618
C2_4511	107	1187	*SDHAF1*	XP_003455545	1e-41	697-945	KC217619
C2_1531	318	1211	*SDHAF2*	XP_003442349	5e-95	159-650	KC217620

[a]Number of reads composing the assembled sequences.

[b]Gene identity determined through BLAST searches: SDHA, Succinate dehydrogenase [ubiquinone] flavoprotein subunit; SDHB, Succinate dehydrogenase [ubiquinone] iron-sulfur subunit ; SDHC, Succinate dehydrogenase cytochrome b560 subunit; SDHD, Succinate dehydrogenase [ubiquinone] cytochrome b small subunit B; SDHAF1, Succinate dehydrogenase assembly factor 1; SDHAF2, Succinate dehydrogenase assembly factor 2.

[c]Best BLAST-X protein sequence match (lowest E value).

[d]Expectation value.

[e]Codifying sequence.

[f]GenBank accession number.

Supplemental Table 6. Characteristics of the new GSB assembled sequences of Complex III used in GSB trial 2. Nuclear-encoded catalytic subunits are in red. Nuclear-encoded regulatory subunits are in black. Nuclear-encoded assembly factors are in blue and italics.

Contigs	F[a]	Size (nt)	Annotation[b]	Best match[c]	E[d]	CDS[e]	Accession No[f]
C2_785	309	1600	Cyc1	XP_003448417	0	98-1021	KC217621
C2_507	523	1386	UQCRFS1	XP_003460177	3e-160	74-895	KC217622
C2_1152	599	1960	UQCRC1	CBN81058	0	43-1479	KC217623
C2_633	410	1745	UQCRC2	CBN81230	0	73-1452	KC217624
C2_2118	238	841	UQCRH	ACM9291	2e-35	140-466	KC217625
C2_516	324	513	UQCRB	CAF99385	7e-52	42-374	KC217626
C2_12420	124	526	UQCRQ	ACQ58134	1e-51	98-346	KC217627
C2_1166	168	564	UQCR10	ACQ58386	7e-33	71-262	KC217628
C2_2080	113	523	UQCR11-A	ACQ582208	1e-27	88-267	KC217629
C2_2411	201	677	UQCR11-B	CAG07741	7e-27	113-283	KC217630
C2_2189	191	1662	CYCS	ACQ58095	1e-62	125-439	KC217632
C2_1918	180	1862	*UQCC*	XP_003456273	4e-174	138-995	KC217631

[a]Number of reads composing the assembled sequences.
[b]Gene identity determined through BLAST searches: Cyc1, Cytochrome c1, heme protein; UQCRFS1, Cytochrome b-c1 complex subunit Rieske; UQCRC1, Cytochrome b-c1 complex subunit 1; UQCRC2, Cytochrome b-c1 complex subunit 2; UQCRH, Cytochrome b-c1 complex subunit 6; UQCRB, Cytochrome b-c1 complex subunit 7; UQCRQ, Cytochrome b-c1 complex subunit 8; UQCR10, Cytochrome b-c1 complex subunit 9; UQCR11-A, Cytochrome b-c1 complex subunit 10 isoform A; UQCR11-B, Cytochrome b-c1 complex subunit 10 isoform B; UQCC, Ubiquinol-cytochrome c reductase complex chaperone CBP3 homolog; CYCS, Cytochrome c.
[c]Best BLAST-X protein sequence match (lowest E value).
[d]Expectation value.
[e]Codifying sequence.
[f]GenBank accession number.

Supplemental Table 7. Characteristics of the new GSB assembled sequences of Complex IV used in GSB trial 2. Mitochondrial-encoded catalytic subunits are in bold and red. Nuclear-encoded regulatory subunits are in black. Nuclear-encoded assembly factors are in blue and italics.

Contigs	F[a]	Size (nt)	Annotation[b]	Best match[c]	E[d]	CDS[e]	Accession No[f]
C2_5	408	1809	**COXI**	YP_001256941	0	1-1566	KC217652
C2_80	1718	722	**COXII**	YP_001256942	1e-124	36-722	KC217653
C2_5715	799	783	**COXIII**	YP_001256945	3e-151	1-783	KC217654
C2_462	742	935	COX4b	P80971	7e-90	131-661	KC217633
C2_238	553	1195	COX5a1	XP_003443919	2e-88	114-539	KC217634
C2_745	287	655	COX5a2	XP_003437607	2e-92	80-505	KC217635
C2_498	458	635	COX5b1	XP_003437607	6e-68	105-491	KC217636
C2_7644	41	845	COX5b2	XP_003441102	1e-68	30-410	KC217637
C2_16418	28	586	COX6a1	XP_003445626	7e-48	22-357	KC217638
C2_132	590	607	COX6a2	AF051370	2e-52	177-476	KC217639
C2_737	427	603	COX6b1a	ACQ58800	1e-53	88-348	KC217640
C2_1197	147	532	COX6b1b	CBN81268	1e-59	78-338	KC217641
C2_2923	122	501	COX6c1	P80977	2e-27	117-347	KC217642
C2_5899	107	508	COX7a1	XP_003448990	1e-39	99-344	KC217643
C2_1148	223	517	COX7a2	CAG01459	5e-42	72-323	KC217644
C2_3512	123	489	COX7b	ACO09254	2e-38	84-326	KC217645
C2_24926	24	389	COX7c	ADG29167	1e-35	64-255	KC217646
C2_3031	80	518	COX8a	XP_003458202	2e-25	67-279	KC217647
C2_203	548	1045	COX8b	AER42691	2e-24	254-457	KC217648
C2_6516	101	1371	*SCO1*	ACQ59007	2e-155	88-1008	KC217649
C2_5469	93	1150	*SURF1*	NP_001135069	8e-163	100-1017	KC217650
C2_2595	220	2114	*COX15*	XP_003441034	0	139-1362	KC217651

[a]Number of reads composing the assembled sequences.
[b]Gene identity determined through BLAST searches: COXI, Cytochrome c oxidase subunit 1; COXII, Cytochrome c oxidase subunit 2; COXIII, Cytochrome c oxidase subunit 3; COX4b, Cytochrome c oxidase subunit 4 isoform 2; COX5a1, Cytochrome c oxidase subunit 5A isoform 1; COX5a2, Cytochrome c oxidase subunit 5A isoform 2; COX5b1, Cytochrome c oxidase subunit 5B isoform 1; COX5b2, Cytochrome c oxidase subunit 5B isoform 2; COX6a1, Cytochrome c oxidase subunit 6A isoform 1; COX6a2, Cytochrome c oxidase subunit 6A isoform 2; COX6b1a, Cytochrome c oxidase subunit VIb isoform 1a; COX6b1b, Cytochrome c oxidase subunit VIb isoform 1b ; COX6c1, Cytochrome c oxidase subunit 6C-1; COX7a1, Cytochrome c oxidase subunit 7A1; COX7a2, Cytochrome c oxidase subunit 7A2; COX7b, Cytochrome c oxidase subunit 7B; COX7c, Cytochrome c oxidase subunit 7C; COX8a, Cytochrome c oxidase subunit 8A; COX8b, Cytochrome c oxidase subunit 8B; COX15, Cytochrome c oxidase assembly protein COX15 homolog; SCO1, SCO1 protein homolog; SURF1, Surfeit locus protein 1.
[c]Best BLAST-X protein sequence match (lowest E value).
[d]Expectation value.
[e]Codifying sequence.
[f]GenBank accession number.

Supplemental Table 8. Characteristics of the new GSB assembled sequences of Complex V used in GSB trial 2. Mitochondrial-encoded catalytic subunits are in bold and red. Nuclear-encoded catalytic subunits are in red. Nuclear-encoded regulatory subunits are in black. Nuclear-encoded assembly factors are in blue and italics.

Contigs	F[a]	Size (nt)	Annotation[b]	Best match[c]	E[d]	CDS[e]	Accession No[f]
C3_39963	134	671	**ATP6**	YP_001256944	9e-45	273->671	KC217599
C3_114147	10	214	**ATP8**	YP_001256943	3e-22	1-165	KC217600
C2_1751	446	1891	ATP5A1	CAF96443	0	88-1743	KC217601
C2_1973	282	1782	ATP5B	XP_003447376	0	68-1624	KC217602
C2_18579	502	1302	ATP5C1	XP_003448120	0	50-931	KC217603
C2_6419	109	709	ATP5D	CAF92415	2e-94	55-549	KC217604
C2_24277	85	409	ATP5E	XP_003444817	3e-20	61-219	KC217605
C2_176	883	1091	ATP5F1	ACQ58228	1e-146	150-902	KC217606
C2_107	762	1116	ATP5G1	ADG29151	6e-69	233-652	KC217607
C2_6236	132	586	ATP5H	XP_003450004	2e-94	51-536	KC217608
C2_7051	97	901	ATP5I	CAG12583	6e-17	85-300	KC217609
C2_1188	233	546	ATP5J2	CAF95291	7e-51	47-316	KC217610
C2_1627	245	506	ATP5L	CAF94261	6e-58	91-402	KC217611
C2_123	968	969	ATPO	CAF99056	1e-122	187-816	KC217612
C2_19166	23	1381	OSCP1	XP_003450561	0	<1-1030	KC217613
C2_2673	262	1925	*ATPAF2*	CBN81217	5e-177	289-1146	KC217614

[a] Number of reads composing the assembled sequences.
[b] Gene identity determined through BLAST searches: ATP6, ATP synthase subunit a; ATP8, ATP synthase protein 8; ATP5A1, ATP synthase subunit alpha; ATP5B, ATP synthase subunit beta; ATP5C1, ATP synthase subunit gamma; ATP5D, ATP synthase subunit delta; ATP5E, ATP synthase subunit epsilon; ATP5F1, ATP synthase subunit b; ATP5G1, ATP synthase lipid-binding protein; ATP5H, ATP synthase subunit d; ATP5I, ATP synthase subunit e; ATP5J2, ATP synthase subunit f; ATP5L, ATP synthase subunit g; ATP5O, ATP synthase subunit O; OSCP1, Protein OSCP1; ATPAF2, ATP synthase mitochondrial F1 complex assembly factor 2.
[c] Best BLAST-X protein sequence match (lowest E value).
[d] Expectation value.
[e] Codifying domain sequence.
[f] GenBank accession number.

Supplemental Table 9. Forward and reverse primers for real-time PCR of Complex I used in GSB trial 2. Mitochondrial-encoded catalytic subunits are in bold and red. Nuclear-encoded catalytic subunits are in red. Nuclear-encoded regulatory subunits are in black. Nuclear-encoded assembly factors are in blue and italics.

Gene name	Symbol		Primer sequence
NADH-ubiquinone oxidoreductase chain 2	**ND2**	F	TAG GTT GAA TGA CCA TCG TA
		R	GGC TAA GGA GTT GAG GTT
NADH-ubiquinone oxidoreductase chain 5	**ND5**	F	CCT AAA CGC CTG AGC CCT GG
		R	GCT GTA AAC GAG GTG GCT AGA AGG
NADH dehydrogenase [ubiquinone] 1 alpha subcomplex subunit 1	NDUFA1	F	CGG GTT CCG TGG CAG TGG TA
		R	TCC TGT TCC TGA TAC TCG CTT GTC TCT
NADH dehydrogenase [ubiquinone] 1 alpha subcomplex subunit 2	NDUFA2	F	CCA CCT CTG CCA GAC CTC
		R	ACT CAC ATA GTG CTG CTC CA
NADH dehydrogenase [ubiquinone] 1 alpha subcomplex subunit 3	NDUFA3	F	TCG GAG CGT TCC TGA AGA ATG C
		R	GAA GAG CCA TAC CTA TCA GTC CAA TAC CA
NADH dehydrogenase [ubiquinone] 1 alpha subcomplex subunit 4	NDUFA4	F	GCT CGT CTG GGC TTG AGA AAC C
		R	GCT CTG GGT TGT TCT TGC GAT CC
NADH dehydrogenase [ubiquinone] 1 alpha subcomplex subunit 4-like 2	NDUFA4-like2	F	TCG GAC AGC AGT AGA GCA T
		R	CGC CCA TTC CCA AAC AGA T
NADH dehydrogenase [ubiquinone] 1 alpha subcomplex subunit 5	NDUFA5	F	ATG GCT GGC TTG CTG AAA
		R	AGA CGC TCA TGT GGA TTG TT
NADH dehydrogenase [ubiquinone] 1 alpha subcomplex subunit 6	NDUFA6	F	TCA GGG AAG GGA CAA AGT GAG GGA GAT G
		R	CGT GGG TCG GTG ACA TGC TTG TTC TT
NADH dehydrogenase [ubiquinone] 1 alpha subcomplex subunit 7	NDUFA7	F	CCG AGC CAC AAG TAT GCC AGC AAC TA
		R	AGC CTC CCT GCG TCC ATC TCT G
NADH dehydrogenase [ubiquinone] 1 alpha subcomplex subunit 8	NDUFA8	F	GCT CCC AGT GTG ACA AAC CCA ACA AAG A
		R	CCT TCT CCT CCC AGC GGC AGA G
NADH dehydrogenase [ubiquinone] 1 alpha subcomplex subunit 9	NDUFA9	F	GGC TGC TCT CCT GCT GTG TT
		R	CCT CTG CTG GAC TGT GGT GAC
NADH dehydrogenase [ubiquinone] 1 alpha subcomplex subunit 12	NDUFA12	F	TGG CGG AGT ATG CGA ACC T
		R	CTC GGA CTC CAC CAT GAC CT
NADH dehydrogenase [ubiquinone] 1 beta subcomplex subunit 1	NDUFB1	F	CCG TGA GCA TTG GGT GAA CAT CTT
		R	TTC TGG TCC TGC TGT TTG TCA AGG T
NADH dehydrogenase [ubiquinone] 1 beta subcomplex subunit 2	NDUFB2	F	CAG AGG ATA ACG ACC AGA AAG GC
		R	CCC TGT ACT GTG GCT CAA TGT G
NADH dehydrogenase [ubiquinone] 1 beta subcomplex subunit 3	NDUFB3	F	GGA ACG AGG CAT GGA GAT AC
		R	CTA CAG CCA GAG CAA CAG TAA

Supp. Table 9. Continued.

Gene name	Symbol		Primer sequence
NADH dehydrogenase [ubiquinone] 1 beta subcomplex subunit 4	NDUFB4	F	TCG TGG GTC TGC TGT TTG GAG TTG TG
		R	ATC TGT GCC TCC TTC CTA TCC CTG TCT GT
NADH dehydrogenase [ubiquinone] 1 beta subcomplex subunit 5	NDUFB5	F	TGC GTC GGC AGA TGA GGA T
		R	CTT GTT GAG GGT GTT CAC CTG GAA
NADH dehydrogenase [ubiquinone] 1 beta subcomplex subunit 6	NDUFB6	F	GAG CCC AAG AGC CTG TGG AGA CT
		R	CAG GTA GCA GGA GGC GTG TTA ATG TGA A
NADH dehydrogenase [ubiquinone] 1 beta subcomplex subunit 8	NDUFB8	F	AAG GGA AGG GCT CTG GCA TTT
		R	GGC GGT CCA AGT ACA GTA TCC T
NADH dehydrogenase [ubiquinone] 1 beta subcomplex subunit 9	NDUFB9	F	CAA AGA CCG AAG CCC TCC
		R	TGA CAT ACT GCC ACC ACA A
NADH dehydrogenase [ubiquinone] 1 beta subcomplex subunit 10	NDUFB10	F	ACT GTG CCC ACG AAC TGA A
		R	ATG CTC CCA GGT CTC CAT AG
NADH dehydrogenase [ubiquinone] 1 beta subcomplex subunit 11	NDUFB11	F	GTG ACC CTG TGG TGG ATG AGT GGA A
		R	ACT GAG ATG CCG AAG AAG AAG CCA ACC T
NADH dehydrogenase 1 subunit C1	NDUFC1	F	GCA CTC GTC AGC AGA GTT GGA T
		R	GTT GGC AGT GTC AGG CTT GGA
NADH dehydrogenase 1 subunit C2	NDUFC2	F	CTT CAG AAT GCC ATC AAC CAC AG
		R	CCG AGG AAC CAG CCA ACT
NADH dehydrogenase iron-sulfur protein 2	NDUFS2	F	GTA TCA GAC GGC TCC AGC AGA C
		R	AGA CCA GCC AAG TGA GCG AAT
NADH dehydrogenase iron-sulfur protein 4	NDUFS4	F	AGC CAA CAC CAA GAA GTG GAA GA
		R	AAG CCC AGC CCA TCA GAG G
NADH dehydrogenase iron-sulfur protein 5	NDUFS5	F	CAG CAG CGT GAC AAG ATG GTG AA
		R	CAG GGC GGT GGC GTG TAG
NADH dehydrogenase iron-sulfur protein 6	NDUFS6	F	GCC GTA CCT GTT CAT CGT TA
		R	TTC GCA TCG TAG ACC TGT C
NADH dehydrogenase iron-sulfur protein 7	NDUFS7	F	AAC GGA GGA GGC TAC TAC CAC TAC T
		R	CGG TAC GAT TCG GTC ACA ACC TCT AAC
NADH dehydrogenase [ubiquinone] flavoprotein 1	NDUFV1	F	CGT GCT CCA GTT GCT GTC AG
		R	TGT GTG CTG TTG AAT CGG GTG ATA
NADH dehydrogenase [ubiquinone] flavoprotein 2	NDUFV2	F	CAG GCA GGT CAG GAA TCT
		R	CAG CAT TGT TGT CAG GAG TAT
NADH dehydrogenase [ubiquinone] flavoprotein 3	NDUFV3	F	ACT GCG AGC ACC ACA CCT ACA AC
		R	CAC GTC CAG GTC GGC GAA TGT
NADH dehydrogenase (ubiquinone) 1 alpha subcomplex, assembly factor 2	*NDUFAF2*	F	AGG CAG CAT ACC GAT AGA G
		R	ACT CAT TCT TCA GCA ACT CCT

Supplemental Table 10. Forward and reverse primers for real-time PCR of Complex II used in GSB trial 2. Nuclear-encoded catalytic subunits are in red. Nuclear-encoded regulatory subunits are in black. Nuclear-encoded assembly factors are in blue and italics.

Gene name	Symbol		Primer sequence
Succinate dehydrogenase [ubiquinone] flavoprotein subunit	SDHA	F	CAA TCT CTG GAT GAG CAG GAC TGT
		R	GTA GGA GCG GAT GGC AGG AG
Succinate dehydrogenase [ubiquinone] iron-sulfur subunit	SDHB	F	TGG TGG CGG TGC GGT ATG
		R	ATT CTG GGT TGT GCT GCT GGA G
Succinate dehydrogenase cytochrome b560 subunit	SDHC	F	AGT GAC ACA CAG AGG AAC TGG AGT
		R	CAG GGC AAA GGC GGA GAT AGC
Succinate dehydrogenase [ubiquinone] cytochrome b small subunit B	SDHD	F	CAT CAG GAG CAG CCG TAC A
		R	CCA GAG GCA GCG TAC AGA G
Succinate dehydrogenase assembly factor 1	*SDHAF1*	F	CCA GGA CAA ACC AGG CTT CAT C
		R	GTC TTC TTG ATG CGA GCG TTC T
Succinate dehydrogenase assembly factor 2	*SDHAF2*	F	CCA GCG AGT CCA TTG ACA TCA
		R	CCC TCT TTC GGC TCT CAT ACA G

Supplemental Table 11. Forward and reverse primers for real-time PCR of Complex III used in GSB trial 2. Mitochondrial-encoded catalytic subunits are in bold and red. Nuclear-encoded catalytic subunits are in red. Nuclear-encoded regulatory subunits are in black. Nuclear-encoded assembly factors are in blue and italics.

Gene name	Symbol		Primer sequence
Cytochrome b	**CYB**	F	TGA CAG GGC TAT TCC TCG CTA TGC
		R	AGA TGT GGG CTA CGG AAG AGA AGG
Cytochrome c	CYCS	F	CAT ACA CTG ACG CCA ACA AGA GTA AAG GT
		R	GGG TTC TCC AGG TAC TCC ATC AAG GT
Cytochrome c1, heme protein, mitochondrial	Cyc1	F	GCT GAG GAG GTG GAG GTT GT
		R	CCT GGA CGG GTG AAC ATC TCT
Cytochrome b-c1 complex subunit Rieske, mitochondrial	UQCRFS1	F	GCG ACT TCG GTG GTT ACT ACT G
		R	GCG ACC TGA GGC GTC ATA ATG
Cytochrome b-c1 complex subunit 1, mitochondrial	UQCRC1	F	TGT CCT GCT GTG GTT GCT GTT
		R	CGC ACT CTG TTG TAG TCG GGT AG
Cytochrome b-c1 complex subunit 2	UQCRC2	F	GAG CAA TTC CTC AAC ATT CG
		R	TCT CAC CTC CAC GAT ACT G
Cytochrome b-c1 complex subunit 6	UQCRH	F	AAG TGT GAG CAG ACT GAA C
		R	TCA GTG TGG GAT CTG GAG
Cytochrome b-c1 complex subunit 7	UQCRB	F	CGA CAG GAC CTT CAG GAT G
		R	CTC TCA CGG ACC ACC TCA T
Cytochrome b-c1 complex subunit 8	UQCRQ	F	GTC AGA CAT ATT ATC ACC TA
		R	GAT TCC CTT TGA GAA GTA
Cytochrome b-c1 complex subunit 9	UQCR10	F	GCT GGC GAA GTC CGT CTA CAA
		R	AGA GAA CCG CTC CAA CCA TGA TG
Cytochrome b-c1 complex subunit 10 isoform A	UQCR11-A	F	CTA TTC TGA GGG CGT GGG
		R	TCT GTG AAG TAG ACG AGC G
Cytochrome b-c1 complex subunit 10 isoform B	UQCR11-B	F	GGG CTC AGT GGG AGG TGT A
		R	ACA ATC GCC AGT CTG TGA AGT G
Ubiquinol-cytochrome c reductase complex chaperone CBP3 homolog	*UQCC*	F	CAG TCC TTC GTC AGA ACC GCT TT
		R	GCA GGC TTC TTG ATC TAA CAC CTT TCC

Supplemental Table 12. Forward and reverse primers for real-time PCR of Complex IV used in GSB trial 2. Mitochondrial-encoded catalytic subunits are in bold and red. Nuclear-encoded regulatory subunits in black. Nuclear-encoded assembly factors in blue and italics.

Gene name	Symbol		Primer sequence
Cytochrome c oxidase subunit 1	**COXI**	F	GTC CTA CTT CTT CTG TCC CTT CCT GTT CT
		R	AGG TTT CGG TCT GTA AGG AGC ATT GTA ATC
Cytochrome c oxidase subunit 2	**COXII**	F	ACT GCC TAC ACA GGA CCT TGC C
		R	GTC TGC TTC CAG GAG ACG GAA TTG T
Cytochrome c oxidase subunit 3	**COXIII**	F	CCA AGC ACA CGC ATA CCA CAT A
		R	GCG GCA ACT GCA CCT GTA
Cytochrome c oxidase subunit 4 isoform 2, mitochondrial	COX4b	F	TCG TGT GGT GGC AGA GCA TCT AC
		R	CGA AGG TCC TGG GGC GTT CA
Cytochrome c oxidase subunit 5A, mitochondrial-like isoform 1	COX5a1	F	CAC GCA ACC ACG GTG CCA AG
		R	TGT CTC CTG CTT GCC ATG TGA GTA AC
Cytochrome c oxidase subunit 5A, mitochondrial-like isoform 2	COX5a2	F	CGC CAT CCG CAT CCT TGA
		R	GGC TTC AAC TCT TGG ATC AGG TAGG
Cytochrome c oxidase subunit 5B isoform 1, mitochondrial	COX5b1	F	GCC AGA CCG TTA CAC CGT GCT AT
		R	CCT GTT CCT CAT CTG TTG GTA TTC CTC TCA
Cytochrome c oxidase subunit 5B isoform 2, mitochondrial	COX5b2	F	GAT GAA GCC GAA GGA GTA CG
		R	GAT GGA GGG AAC GAG GTG
Cytochrome c oxidase subunit 6A isoform 1, mitochondrial	COX6a1	F	GAG CAG AGT CAC AGC CAC GAG
		R	TTG CTG CGA ATG CGA AGA TGG
Cytochrome c oxidase subunit 6A isoform 2, mitochondrial	COX6a2	F	TGT TGG CTG CTG CGT CAC ATT C
		R	CAG AAT CTT CCA GGT CCT CGC TCC
Cytochrome c oxidase subunit VIb isoform 1a	COX6b1a	F	TCA GCC AGA GAC CAG GAC AC
		R	GGG CAG AGG CTC TTG TAA ACC
Cytochrome c oxidase subunit VIb isoform 1b	COX6b1b	F	CCA ACC AGA ACC AGA CCA GGA ACT
		R	GGC AGC GGT GAT AGT CCA GGT AG
Cytochrome c oxidase subunit 6C-1	COX6c1	F	TCT CTC TGT CAC TCC TGG CTG CGA TAG
		R	CCT GGG CTC TGT CAC TGC GTA CTT G
Cytochrome c oxidase subunit 7A1	COX7a1	F	GGC GAC CAT GAC GTT AAC CAT CAC AGG AA
		R	GGT GAG CAG CCA GTA GCA GGA GTA ACA
Cytochrome c oxidase subunit 7A2	COX7a2	F	AAG GAG GCA GCA GCG ATG
		R	TCC AGC ACC GAG GAC AGT
Cytochrome c oxidase subunit 7B	COX7b	F	TCT TCT GTG TGG CTG TGT GGT CAT ACG
		R	TTC CCA ACA GGT GAC AAA TTC CAG GTG AT
Cytochrome c oxidase subunit 7C	COX7c	F	GGT GGT GTT CTT TGG CAG TGG CTT T
		R	CAG GAT CTG ATG TCT GAC GAC GAT GAA GG
Cytochrome c oxidase subunit 8A	COX8a	F	GCA GAC CGC CCA AAG ACG
		R	CAT GCC AAT TCC GAC GAC AGT T
Cytochrome c oxidase subunit 8B, mitochondrial	COX8b	F	TCC GCT GGT CCC TGT GGC TAA
		R	CCT CCA CTG ATA TTG TGT TTG GCA GGT TTG
SCO1 protein homolog, mitochondrial	*SCO1*	F	ACA ACA ACA AGC CCA CCA AGA
		R	GAC AGT GAG TGA ACC CGA AGT AGA T
Surfeit locus protein 1	*SURF1*	F	AGA TGG AAG GTG AAG TGG AGG TGG TC
		R	GCG TTG CTC TGT CTG CCG AAC T
Cytochrome c oxidase assembly protein COX15 homolog	*COX15*	F	CAT ACT AGG TCG CTG GTT AG
		R	GAT TCC GTG AGC CTT GTG

Supplemental Table 13. Forward and reverse primers for real-time PCR of Complex V used in GSB trial 2. Nuclear-encoded catalytic subunits are in red. Nuclear-encoded regulatory subunits are in black. Nuclear-encoded assembly factors are in blue and italics.

Gene name	Symbol		Primer sequence
ATP synthase subunit alpha, mitochondrial	ATP5A1	F	CGT CAT CTC CAT CAC AGA CGG ACA GA
		R	CGA ATA CCC TTG TAG AAC AGC TCA GTC TCC
ATP synthase subunit beta, mitochondrial	ATP5B	F	GTA GCA CTG GTG TAT GGT CAG ATG AAC GA
		R	TCT GGC ACG GGC ACC TGG
ATP synthase subunit gamma	ATP5C1	F	GAG GAG AAG GTC GCC AAG CAT
		R	GCC ACA GAG ACC ACG ATC AGA G
ATP synthase subunit delta	ATP5D	F	TGC CCA TGT ACC CAC CCT
		R	ACA GCG GAA CCG TCA TCA TT
ATP synthase subunit epsilon	ATP5E	F	TGG TCG CAT ACT GGA GAC AAG CA
		R	GCA GAT AGA GGA GAA GCG GAT GTA GC
ATP synthase subunit b	ATP5F1	F	CCG CAG GAT GGA GCA GGA G
		R	TGC CGA CGA CGC TCT TCT C
ATP synthase lipid-binding protein	ATP5G1	F	GGA GTC GCT GGA TCT GGA GCT GG TAT T
		R	ATA GCC AAT GAT GAG ACT GCC GAA CAC TGT
ATP synthase subunit e	ATP5I	F	CTC CAG TTG CAG TGT CGC CTC TGA TTA
		R	TCT CCT TTT GCC GTA GAT GAT CCC AGC
ATP synthase subunit f	ATP5J2	F	GTT GCC ATT GTT GAG AAG CGT CTG A
		R	CCT CCA AGC CAG GTT CCA AGC
ATP synthase subunit g	ATP5L	F	ACC TTC ACC TGC CGA GAT
		R	CAG CCT GGA AGC TCT TGA TG
ATP synthase subunit O	ATP5O	F	GCT ATG CCA CCG CTC TGT TCT C
		R	CTG CTC CAC TTG GTC CAG TTT CTT C
Protein OSCP1	OSCP1	F	CAG CGG TCC TGT GCC TTA TGG
		R	GCC TGG TCG TCT CTT CAC CTG TA
ATP synthase mitochondrial F1 complex assembly factor 2	*ATPAF2*	F	CGT TCT GGC GAT GGC GAT GAT TGA CA
		R	TGG AGA GCA GCA CAG CCT GTT CTA CG

Supplemental Table 14. Relative gene expression of OXPHOS genes in liver, white skeletal muscle (WSM) and heart of control and fasted GSB in trial 2. Values are the mean ± SEM (n = 5-7). β-Actin was used as housekeeping gene. NDUFC2, NDUFA5 and NDUFB2 were used as reference genes (arbitrary values of 1) in liver, WM and heart, respectively. Within each tissue, means with asterisk are significantly different from control fish (P<0.05; Student's t test). Mitochondrial-encoded catalytic subunits are in bold and red. Nuclear-encoded catalytic subunits are in red. Nuclear-encoded regulatory subunits are in black. Nuclear-encoded assembly factors are in blue and italics.

Gene name+	Liver		WSM		Heart	
	CTRL	Fasted	CTRL	Fasted	CTRL	Fasted
ND2	27.13 ± 3.43	10 ± 1.41*	11.43 ± 1.26	11.71 ± 1.56	24.06 ± 4.21	22.5 ± 1.36
ND5	9.6 ± 0.36	2.94 ± 0.35*	4.97 ± 0.61	3.99 ± 0.57	9.49 ± 0.89	11.28 ± 0.57
NDUFA1	0.91 ± 0.06	0.47 ± 0.04*	0.83 ± 0.06	1.13 ± 0.1*	0.94 ± 0.09	1.21 ± 0.13
NDUFA2	0.6 ± 0.08	0.34 ± 0.04*	0.87 ± 0.11	0.73 ± 0.1	1.47 ± 0.14	1.26 ± 0.16
NDUFA3	0.81 ± 0.08	0.36 ± 0.03*	0.52 ± 0.06	0.63 ± 0.07	1.15 ± 0.07	1.15 ± 0.12
NDUFA4	6.41 ± 0.24	3.91 ± 0.46*	4.65 ± 0.42	5.96 ± 0.55*	3.71 ± 0.12	6.55 ± 0.43*
NDUFA4-like2	0.29 ± 0.01	0.14 ± 0.02*	0.13 ± 0.05	0.06 ± 0.04	0.003 ± 0.00	0.002 ± 0.00
NDUFA5	1.02 ± 0.08	0.48 ± 0.04*	1.04 ± 0.16	1.03 ± 0.08	1.53 ± 0.13	1.45 ± 0.12
NDUFA6	0.4 ± 0.05	0.29 ± 0.01*	0.49 ± 0.05	0.71 ± 0.05*	0.98 ± 0.12	0.92 ± 0.08
NDUFA7	0.25 ± 0.02	0.17 ± 0.02*	0.24 ± 0.03	0.42 ± 0.04*	0.51 ± 0.03	0.61 ± 0.04
NDUFA8	0.11 ± 0.01	0.07 ± 0.01*	0.14 ± 0.01	0.18 ± 0.02*	0.3 ± 0.04	0.31 ± 0.03
NDUFA9	0.5 ± 0.08	0.22 ± 0.02*	0.38 ± 0.04	0.5 ± 0.06	0.68 ± 0.03	0.59 ± 0.04
NDUFA12	0.52 ± 0.06	0.27 ± 0.02*	0.43 ± 0.08	0.43 ± 0.04	0.89 ± 0.04	0.92 ± 0.08
NDUFB1	0.58 ± 0.13	0.31 ± 0.02	0.57 ± 0.06	0.44 ± 0.04	1.19 ± 0.11	1.08 ± 0.13
NDUFB2	0.48 ± 0.05	0.24 ± 0.01*	0.56 ± 0.05	0.67 ± 0.07	0.94 ± 0.05	0.94 ± 0.05
NDUFB3	2.08 ± 0.28	1.46 ± 0.13*	1.34 ± 0.24	1.43 ± 0.22	1.97 ± 0.28	2.04 ± 0.26
NDUFB4	0.31 ± 0.07	0.14 ± 0.02*	0.51 ± 0.04	0.58 ± 0.08	1.27 ± 0.07	0.98 ± 0.07
NDUFB5	0.58 ± 0.1	0.33 ± 0.02*	0.73 ± 0.06	1.22 ± 0.17*	1.22 ± 0.15	1.2 ± 0.1
NDUFB6	0.25 ± 0.06	0.14 ± 0.01*	0.34 ± 0.03	0.34 ± 0.06	0.92 ± 0.1	0.73 ± 0.08
NDUFB8	1.2 ± 0.21	0.78 ± 0.09	1.03 ± 0.11	1.29 ± 0.2	1.62 ± 0.22	1.6 ± 0.15
NDUFB9	0.005 ± 0.00	0.003 ± 0.00*	0.006 ± 0.00	0.009 ± 0.00*	0.006 ± 0.00	0.005 ± 0.00
NDUFB10	1.07 ± 0.11	0.55 ± 0.06*	1.01 ± 0.1	1.46 ± 0.11*	1.47 ± 0.12	1.22 ± 0.1
NDUFB11	0.3 ± 0.04	0.15 ± 0.01*	0.35 ± 0.04	0.47 ± 0.06	0.53 ± 0.04	0.57 ± 0.03
NDUFC1	0.59 ± 0.05	0.38 ± 0.03*	0.62 ± 0.07	0.78 ± 0.07	0.98 ± 0.08	1.05 ± 0.07
NDUFC2	1.02 ± 0.09	1.04 ± 0.11	1.22 ± 0.13	1.88 ± 0.24*	1.9 ± 0.17	2.12 ± 0.21
NDUFS2	0.73 ± 0.1	0.26 ± 0.02*	0.69 ± 0.07	0.84 ± 0.08	1.04 ± 0.08	0.82 ± 0.07
NDUFS4	0.43 ± 0.06	0.21 ± 0.01*	0.57 ± 0.05	0.82 ± 0.08*	0.97 ± 0.09	1.14 ± 0.07
NDUFS5	0.3 ± 0.04	0.17 ± 0.01*	0.34 ± 0.04	0.34 ± 0.03	0.66 ± 0.06	0.7 ± 0.07
NDUFS6	0.18 ± 0.07	0.18 ± 0.07	0.15 ± 0.08	0.29 ± 0.12	0.43 ± 0.2	0.61 ± 0.23
NDUFS7	0.78 ± 0.08	0.38 ± 0.03*	0.66 ± 0.08	1.06 ± 0.13*	1.31 ± 0.14	1.29 ± 0.12
NDUFV1	0.74 ± 0.08	0.36 ± 0.04*	0.68 ± 0.07	0.89 ± 0.08	1.27 ± 0.1	1.26 ± 0.07
NDUFV2	0.55 ± 0.07	0.28 ± 0.03*	0.6 ± 0.09	0.55 ± 0.06	1.27 ± 0.08	1.05 ± 0.06
NDUFV3	0.37 ± 0.04	0.2 ± 0.01*	0.3 ± 0.03	0.3 ± 0.05	0.59 ± 0.05	0.54 ± 0.03
NDUFAF2	0.15 ± 0.01	0.07 ± 0.01*	0.08 ± 0.01	0.18 ± 0.01*	0.12 ± 0.01	0.17 ± 0.01*

Supplemental Table 14. Continued I.

Gene name+	Liver		WSM		Heart	
	CTRL	Fasted	CTRL	Fasted	CTRL	Fasted
SDHA	0.46 ± 0.04	0.22 ± 0.02*	0.38 ± 0.04	0.41 ± 0.03	0.72 ± 0.05	0.82 ± 0.06
SDHB	0.2 ± 0.04	0.13 ± 0.01	0.18 ± 0.02	0.28 ± 0.04*	0.31 ± 0.03	0.4 ± 0.03
SDHC	0.77 ± 0.04	0.35 ± 0.03*	0.37 ± 0.04	0.56 ± 0.05*	0.88 ± 0.09	1.03 ± 0.11
SDHD	1.01 ± 0.18	0.42 ± 0.05*	0.31 ± 0.05	0.45 ± 0.04*	0.74 ± 0.05	0.74 ± 0.06
SDHAF1	0.05 ± 0.00	0.04 ± 0.00	0.02 ± 0.00	0.03 ± 0.01	0.04 ± 0.00	0.05 ± 0.00*
SDHAF2	0.27 ± 0.01	0.11 ± 0.01*	0.08 ± 0.01	0.08 ± 0.01	0.11 ± 0.01	0.14 ± 0.01*
CYB	43.23 ± 4.41	22.76 ± 2.64*	23.59 ± 2.93	30.08 ± 3.21	35.21 ± 4.3	56.55 ± 2.22*
CYC	0.08 ± 0.02	0.09 ± 0.02	1.74 ± 0.20	1.91 ± 0.31	4.32 ± 0.47	4.19 ± 0.21
CYC1	1.33 ± 0.20	0.95 ± 0.08	1.69 ± 0.20	2.07 ± 0.18	4.3 ± 0.44	4.48 ± 0.42
UQCRFS1	0.31 ± 0.05	0.18 ± 0.02*	0.45 ± 0.04	0.63 ± 0.04*	0.48 ± 0.04	0.48 ± 0.04
UQCRC1	1.19 ± 0.16	0.76 ± 0.05*	0.74 ± 0.11	1.46 ± 0.28*	2.41 ± 0.20	2.7 ± 0.22
UQCRC2	1.28 ± 0.17	0.65 ± 0.04*	1.15 ± 0.10	2.25 ± 0.15*	2.25 ± 0.14	2.17 ± 0.17
UQCRH	0.67 ± 0.08	0.44 ± 0.04*	0.06 ± 0.01	0.09 ± 0.01*	0.35 ± 0.03	0.4 ± 0.03
UQCRB	2.5 ± 0.35	1.41 ± 0.11*	3.44 ± 0.4	4.16 ± 0.61	5.57 ± 0.44	5.42 ± 0.5
UQCRQ	3.16 ± 0.42	1.59 ± 0.1*	2.84 ± 0.21	4.16 ± 0.41*	4.20 ± 0.27	3.63 ± 0.31
UQCR10	0.92 ± 0.06	0.36 ± 0.03*	0.86 ± 0.09	1.45 ± 0.18*	2.74 ± 0.31	2.27 ± 0.26
UQCR11-A	2.46 ± 0.09	1.7 ± 0.19*	0.86 ± 0.11	1.57 ± 0.18	3.27 ± 0.41	4.95 ± 0.41
UQCR11-B	0.4 ± 0.03	0.25 ± 0.03*	0.26 ± 0.03	0.25 ± 0.03	0.58 ± 0.04	0.57 ± 0.04
UQCC	0.14 ± 0.01	0.12 ± 0.01	0.29 ± 0.02	0.58 ± 0.04*	0.34 ± 0.04	0.37 ± 0.03
COXI	29.86 ± 2.32	14.95 ± 1.83*	16.91 ± 2.36	26.72 ± 4.83	36.79 ± 4.54	65.58 ± 3.76*
COXII	15.99 ± 1.06	6.12 ± 0.88*	6.96 ± 0.74	9.72 ± 1.4	13.77 ± 1.55	23.55 ± 1.46*
COXIII	20.38 ± 1.74	8.09 ± 0.9*	9.3 ± 1.1	9.9 ± 1.16	18.04 ± 1.99	32.43 ± 1.78*
COX4a	3.23 ± 0.19	2.23 ± 0.21*	0.71 ± 0.07	0.91 ± 0.13	4.62 ± 0.41	3.46 ± 0.32
COX4b	2.20 ± 0.1	1.04 ± 0.13*	1.54 ± 0.15	1.37 ± 0.25	3.96 ± 0.47	4.82 ± 0.32
COX5a1	0.10 ± 0.01	0.08 ± 0.01	0.14 ± 0.02	0.27 ± 0.04*	0.27 ± 0.03	0.27 ± 0.01
COX5a2	1.85 ± 0.17	0.82 ± 0.06*	0.91 ± 0.13	1.73 ± 0.21*	4.29 ± 0.56	3.85 ± 0.31
COX5b2	0.28 ± 0.08	0.12 ± 0.01*	0.09 ± 0.01	0.07 ± 0.01	0.32 ± 0.04	0.27 ± 0.03
COX6a1	0.26 ± 0.05	0.17 ± 0.02	0.11 ± 0.01	0.09 ± 0.01	1.11 ± 0.10	0.97 ± 0.10
COX6a2	2.68 ± 0.19	0.9 ± 0.05*	2.24 ± 0.25	2.56 ± 0.37	3.76 ± 0.27	3.48 ± 0.22
COX6b1a	2.39 ± 0.26	1.33 ± 0.13*	2.09 ± 0.15	2.6 ± 0.27	1.96 ± 0.21	2.75 ± 0.16*
COX6b1b	3.19 ± 0.21	1.84 ± 0.16*	0.31 ± 0.11	0.43 ± 0.09	3.67 ± 0.49	4.42 ± 0.30
COX6c1	3.98 ± 0.38	1.53 ± 0.16*	3.09 ± 0.30	4.32 ± 0.52	6.42 ± 0.73	5.78 ± 0.47
COX7a1	1.27 ± 0.14	0.58 ± 0.06*	1.27 ± 0.14	1.47 ± 0.16	2.66 ± 0.13	2.51 ± 0.17
COX7a2	1.07 ± 0.23	0.46 ± 0.04*	0.11 ± 0.02	0.13 ± 0.01	0.66 ± 0.08	0.56 ± 0.05
COX7b	8.97 ± 0.82	1.74 ± 0.11*	2.43 ± 0.28	2.66 ± 0.34	5.64 ± 0.63	4.52 ± 0.52
COX7c	1.79 ± 0.23	0.69 ± 0.04*	1.81 ± 0.2	2.29 ± 0.19	4.45 ± 0.45	4.06 ± 0.45
COX8a	0.19 ± 0.02	0.14 ± 0.01	0.11 ± 0.02	0.07 ± 0.01*	0.78 ± 0.06	0.73 ± 0.03
COX8b	3.99 ± 0.33	1.4 ± 0.10*	2.47 ± 0.23	3.56 ± 0.46*	9.69 ± 1.17	9.96 ± 1.03
SCO1	0.05 ± 0.01	0.04 ± 0.00	0.02 ± 0.00	0.04 ± 0.01*	0.04 ± 0.00	0.04 ± 0.00
SURF1	0.17 ± 0.01	0.11 ± 0.01*	0.09 ± 0.01	0.17 ± 0.01*	0.12 ± 0.01	0.16 ± 0.00*
COX15	0.07 ± 0.01	0.05 ± 0.01	0.07 ± 0.01	0.10 ± 0.02	0.13 ± 0.02	0.20 ± 0.03

Supplemental Table 14. Continued II.

Gene name[+]	Liver		WSM		Heart	
	CTRL	Fasted	CTRL	Fasted	CTRL	Fasted
ATP5A1	3.29 ± 0.48	1.58 ± 0.11*	1.90 ± 0.25	2.94 ± 0.3*	4.95 ± 0.5	3.69 ± 0.19
ATP5B	5.52 ± 0.77	1.73 ± 0.16*	4.87 ± 0.61	5.79 ± 0.85	7.35 ± 0.82	5.34 ± 0.66
ATP5C1	2.99 ± 0.32	1.10 ± 0.09*	2.41 ± 0.19	3.20 ± 0.35	3.67 ± 0.38	3.97 ± 0.25
ATP5D	1.96 ± 0.21	1.09 ± 0.11*	1.29 ± 0.11	1.72 ± 0.2	2.15 ± 0.21	2.07 ± 0.13
ATP5E	2.23 ± 0.16	0.89 ± 0.08*	2.21 ± 0.29	2.71 ± 0.3	3.21 ± 0.26	3.53 ± 0.29
ATP5F1	3.23 ± 0.36	1.63 ± 0.16*	2.57 ± 0.22	3.11 ± 0.22	4.47 ± 0.39	5.22 ± 0.32
ATP5G1	8.00 ± 1.18	3.04 ± 0.34*	5.80 ± 0.53	5.49 ± 0.55	10.08 ± 0.81	9.21 ± 0.86
ATP5I	0.19 ± 0.01	0.10 ± 0.01*	0.57 ± 0.06	0.63 ± 0.12	0.88 ± 0.08	0.76 ± 0.07
ATP5J2	3.20 ± 0.38	1.21 ± 0.11*	1.84 ± 0.21	1.84 ± 0.22	4.91 ± 0.52	4.16 ± 0.35
ATP5L	4.07 ± 0.23	2.56 ± 0.23*	1.15 ± 0.17	1.54 ± 0.18	1.59 ± 0.14	1.96 ± 0.11
ATP5O	3.80 ± 0.35	1.33 ± 0.12*	2.05 ± 0.41	3.19 ± 0.37*	4.59 ± 0.45	4.66 ± 0.51
OSCP	0.004 ± 0.00	0.003 ± 0.00	0.003 ± 0.00	0.002 ± 0.00	0.006 ± 0.00	0.008 ± 0.00
ATPAF2	0.02 ± 0.00	0.02 ± 0.00	0.01 ± 0.00	0.02 ± 0.00	0.04 ± 0.00	0.04 ± 0.00

[+] Gene identity determined through BLAST searches: Complex I: ND2, NADH-ubiquinone oxidoreductase chain 2; ND5, NADH-ubiquinone oxidoreductase chain 5; NDUFA1, NADH dehydrogenase [ubiquinone] 1 alpha subcomplex subunit 1; NDUFA2, NADH dehydrogenase [ubiquinone] 1 alpha subcomplex subunit 2; NDUFA3, NADH dehydrogenase [ubiquinone] 1 alpha subcomplex subunit 3; NDUFA4, NADH dehydrogenase [ubiquinone] 1 alpha subcomplex subunit 4; NDUFA4-like2, NADH dehydrogenase [ubiquinone] 1 alpha subcomplex subunit 4-like 2; NDUFA5, NADH dehydrogenase [ubiquinone] 1 alpha subcomplex subunit 5; NDUFA6, NADH dehydrogenase [ubiquinone] 1 alpha subcomplex subunit 6; NDUFA7, NADH dehydrogenase [ubiquinone] 1 alpha subcomplex subunit 7; NDUFA8, NADH dehydrogenase [ubiquinone] 1 alpha subcomplex subunit 8; NDUFA9, NADH dehydrogenase [ubiquinone] 1 alpha subcomplex subunit 9; NDUFA12, NADH dehydrogenase [ubiquinone] 1 alpha subcomplex subunit 12; NDUFB1, NADH dehydrogenase [ubiquinone] 1 beta subcomplex subunit 1; NDUFB2, NADH dehydrogenase [ubiquinone] 1 beta subcomplex subunit 2; NDUFB3, NADH dehydrogenase [ubiquinone] 1 beta subcomplex subunit 3; NDUFB4, NADH dehydrogenase [ubiquinone] 1 beta subcomplex subunit 4; NDUFB5, NADH dehydrogenase [ubiquinone] 1 beta subcomplex subunit 5; NDUFB6, NADH dehydrogenase [ubiquinone] 1 beta subcomplex subunit 6; NDUFB8, NADH dehydrogenase [ubiquinone] 1 beta subcomplex subunit 8; NDUFB9, NADH dehydrogenase [ubiquinone] 1 beta subcomplex subunit 9; NDUFB10, NADH dehydrogenase [ubiquinone] 1 beta subcomplex subunit 10; NDUFB11, NADH dehydrogenase [ubiquinone] 1 beta subcomplex subunit 11; NDUFC1, NADH dehydrogenase 1 subunit C1; NDUFC2, NADH dehydrogenase 1 subunit C2; NDUFS2, NADH dehydrogenase iron-sulfur protein 2; NDUFS4, NADH dehydrogenase iron-sulfur protein 4; NDUFS5, NADH dehydrogenase iron-sulfur protein 5; NDUFS6, NADH dehydrogenase iron-sulfur protein 6; NDUFS7, NADH dehydrogenase iron-sulfur protein 7; NDUFV1, NADH dehydrogenase [ubiquinone] flavoprotein 1; NDUFV2, NADH dehydrogenase [ubiquinone] flavoprotein 2; NDUFV3, NADH dehydrogenase [ubiquinone] flavoprotein 3; NDUFAF2, NADH dehydrogenase (ubiquinone) 1 alpha subcomplex, assembly factor 2; Complex II: SDHA, Succinate dehydrogenase [ubiquinone] flavoprotein subunit; SDHB, Succinate dehydrogenase [ubiquinone] iron-sulfur subunit; SDHC, Succinate dehydrogenase cytochrome b560 subunit; SDHD, Succinate dehydrogenase [ubiquinone] cytochrome b small subunit B; SDHAF1, Succinate dehydrogenase assembly factor 1; SDHAF2, Succinate dehydrogenase assembly factor 2; Complex III: Cytb, Cytochrome b; CYCS, Cytochrome c; Cyc1, Cytochrome c1, heme protein; UQCRFS1, Cytochrome b-c1 complex subunit Rieske; UQCRC1, Cytochrome b-c1 complex subunit 1; UQCRC2, Cytochrome b-c1 complex subunit 2; UQCRH, Cytochrome b-c1 complex subunit 6; UQCRB, Cytochrome b-c1 complex subunit 7; UQCRQ, Cytochrome b-c1 complex subunit 8; UQCR10, Cytochrome b-c1 complex subunit 9; UQCR11-A, Cytochrome b-c1 complex subunit 10 isoform A; UQCR11-B, Cytochrome b-c1 complex subunit 10 isoform B; UQCC, Ubiquinol-cytochrome c reductase complex chaperone CBP3 homolog; COXI, Cytochrome c oxidase subunit I; Complex IV : COXII, Cytochrome c oxidase subunit II; COXIII, Cytochrome c oxidase subunit III; COX4a, Cytochrome c oxidase subunit 4 isoform 1; COX4b, Cytochrome c oxidase subunit 4 isoform 2; COX5a1, Cytochrome c oxidase subunit 5A, mitochondrial-like isoform 1; COX5a2, Cytochrome c oxidase subunit 5A, mitochondrial-like isoform 2; COX5b2, Cytochrome c oxidase subunit 5B isoform 2; COX6a1, Cytochrome c oxidase subunit 6A isoform 1; COX6a2, Cytochrome c oxidase subunit 6A isoform 2; COX6b1a, Cytochrome c oxidase subunit VIb isoform 1a; COX6b1b, Cytochrome c oxidase subunit VIb isoform 1b; COX6c1, Cytochrome c oxidase subunit 6C-1; COX7a1, Cytochrome c oxidase subunit 7A1; COX7a2, Cytochrome c oxidase subunit 7A2; COX7b, Cytochrome c oxidase subunit 7B; COX7c, Cytochrome c oxidase subunit 7C; COX8a, Cytochrome c oxidase subunit 8A; COX8b, Cytochrome c oxidase subunit 8B; SCO1, SCO1 protein homolog; SURF1, Surfeit

locus protein 1; COX15, Cytochrome c oxidase assembly protein COX15 homolog; Complex V : ATP5A1, ATP synthase subunit alpha; ATP5B, ATP synthase subunit beta; ATP5C1, ATP synthase subunit gamma; ATP5D, ATP synthase subunit delta; ATP5E, ATP synthase subunit épsilon; ATP5F1, ATP synthase subunit b; ATP5G1, ATP synthase lipid-binding protein; ATP5I, ATP synthase subunit e; ATP5J2, ATP synthase subunit f; ATP5L, ATP synthase subunit g; ATP5O, ATP synthase subunit O; OSCP, Protein OSCP1; ATPAF2, Mitochondrial F1 complex assembly factor 2.

Supplemental Table 15. Ingredients and chemical composition of experimental diets in GSB trial 3.

	Diet						
	CTRL	SAA	n-3 LC-PUFA	PL	P	Min	Vit
Ingredient (%)							
Casein	20	20	20	20	20	20	20
Casein hydrolisate	5	5	5	5	5	5	5
Gelatin	5.78	5.78	5.78	5.78	5.78	5.78	5.78
Soy protein concentrate (Soycomil PC)	34.5	34.5	34.5	34.5	34.5	34.5	34.5
DL-Methionine	0.4	0	0.4	0.4	0.4	0.4	0.4
L-Threonine	0.02	0.02	0.02	0.02	0.02	0.02	0.02
Dextrine	11.2	11.2	11.2	11.2	11.2	11.2	11.2
Soy lecithin	2	2	2	0	2	2	2
Fish oil	13.9	13.9	0	13.9	13.9	13.9	13.9
Vegetable oil	0	0	13.9	0	0	0	0
Cellulose	0	0.4	0	0	2.2	1.5	1.5
CaHPO4.2H2O (18%P)	2.2	2.2	2.2	2.2	0	2.2	2.2
Mineral premix-INRA[1]	2	2	2	2	2	0.5	2
Vitamin premix-INRA[2]	2	2	2	2	2	2	0.5
Taurine	0.3	0.3	0.3	0.3	0.3	0.3	0.3
Betaine	0.3	0.3	0.3	0.3	0.3	0.3	0.3
Glucosamine	0.4	0.4	0.4	0.4	0.4	0.4	0.4
Ethoxyquin (75%)	0.1	0.1	0.1	0.1	0.1	0.1	0.1
Proximate composition							
Dry matter (DM, %)	92.4	92.5	95.4	93.3	95.5	92.2	92.8
Crude protein (% DM)	51.8	51.5	50.8	51.1	50.8	52.0	52.5
Crude fat (% DM)	15.0	15.1	15.5	15.6	14.4	14.7	14.7
EPA+DHA (% DM)	2.68	2.68	0.03	2.83	2.60	2.64	2.37

[1]Supplied the following (g/kg mix): calcium hydrogen phosphate 500, calcium carbonate (40% Ca) 215, sodium chloride 40, ferrous sulphate (21% Fe) 20, manganese sulphate 3, zinc sulphate 4, copper sulphate 3, cobalt (II) chloride (25% Co) 0.02, potassium iodine 0.04, sodium selenite 0.03, sodium fluoride 1, magnesium hydroxide (60% Mg) 124, potassium chloride 90.
[2]Supplied the following (g/kg mix, except as noted): retinyl acetate 1, DL-cholecalciferol 2.5, DL-α tocopheryl acetate 5, menadione sodium bisulphite 1, ascorbic acid 20, thiamin 0.1, riboflavin 0.4, pyridoxine 0.3, vitamin B12 10 mg, nicotinic acid 1, pantothenic acid 2, folic acid 0.1, biotin 10 mg, choline chloride 200, inositol 30.

SupplementalTable 16. Fatty acid composition of experimental diets (% total FAME) in GSB trial 3.

	Diet						
Fatty acid	CTRL	SAA	n-3 LC-PUFA	PL	P	Min	Vit
14:0	6.81	7.06	0.51	7.38	7.03	7.06	7.50
15:0	0.61	0.74	0.24	0.79	0.76	0.68	1.01
16:0	17.56	18.11	15.48	18.53	18.58	18.47	19.13
16:1n-7	7.36	7.44	0.24	7.60	7.29	7.31	7.46
16:2	0.91	0.92	0.12	1.06	1.02	1.23	1.13
16:3	1.25	1.25	0.06	1.29	1.20	1.26	1.21
16:4	1.37	1.37	0.08	1.41	1.31	1.36	1.30
17:0	0.48	0.49	tr	0.52	0.51	0.51	0.53
18:0	3.36	3.47	4.68	3.48	3.62	3.56	3.69
18:1n-9	10.87	10.79	30.57	10.68	10.84	10.76	10.95
18:1n-7	2.49	2.52	0.98	2.57	2.52	2.52	2.57
18:2n-6	3.98	3.87	16.46	2.09	3.81	3.81	3.66
18:3n-3	1.10	1.07	27.44	1.10	1.13	1.09	1.01
18:3n-6	0.30	0.30	0.09	0.31	0.29	0.30	0.29
18:4n-3	2.21	2.22	tr	2.26	2.14	2.23	2.07
20:0	0.29	0.28	0.32	0.29	0.30	0.29	0.33
20:1n-9	2.32	0.81	0.38	2.51	2.46	2.43	2.48
20:1n-7	0.21	0.21	tr	0.22	0.21	0.21	0.22
20:2n-6	0.15	0.15	0.07	0.15	0.15	0.15	0.15
20:3n-3	0.07	0.07	tr	0.07	0.07	0.07	0.06
20:3n-6	0.07	0.05	tr	0.05	0.05	0.05	0.06
20:4n-6	0.90	0.91	tr	0.92	0.88	0.91	0.85
20:4n-3	0.61	0.61	tr	0.62	0.60	0.61	0.58
20:5n-3 (EPA)	12.98	13.01	0.18	13.17	12.56	13.06	11.88
21:0	0.08	0.10	tr	0.08	0.09	0.09	0.08
21:5n-3	0.48	0.49	tr	0.49	0.47	0.49	0.44
22:0	0.12	0.13	0.19	0.11	0.13	0.13	0.14
22:1n-11	3.34	3.58	tr	3.66	3.69	3.61	3.61
22:1n-9	0.20	0.11	0.05	0.11	0.08	0.11	0.10
22:4n-6	0.08	0.08	tr	0.08	0.08	0.09	0.08
22:5n-3	1.39	1.40	0.10	1.41	1.36	1.40	1.27
22:6n-3 (DHA)	9.94	9.95	0.07	10.05	9.60	9.98	8.96
Total	94.14	93.81	98.37	95.28	95.10	95.00	96.08
Saturates	29.31	30.38	21.44	31.19	31.03	30.79	32.40
Monoenes	26.79	25.48	32.26	27.34	27.09	26.96	27.39
n-6 LC-PUFA [1]	0.98	0.99	tr	1.00	0.95	0.99	0.93
n-3 LC-PUFA[1]	25.41	25.45	0.38	25.73	24.59	25.55	23.13

Values are means of two determinations; tr = trace value < 0.05.
[1] Fatty acids with at least 20 carbon atoms and more than 3 double bonds.

Supplemental Table 17. PCR-array layout of 89 genes with extra-wells for housekeeping genes and general controls of PCR performance, for the GSB analysis of samples from trial 3.

	1	2	3	4	5	6	7	8	9	10	11	12
A	GHR-I	IGFALS	MSTN	PCNA	CTSB	UCHL3	mtHsp10	DER-1	IL-8	SIRT2	NDUFAF2	PPARγ
B	GHR-II	INSR	MEF2A	PAX7	CTSD	UBE2A	Hsp30	ERdj3	IL-8RA	SIRT3	COXI	PPC1
C	IGF-I	IGFR1	MEF2C	SOX3	CTSL	UBE2D2	mtHsp60	IL-1β	IL-10	SIRT4	SCO1	PPC2
D	IGF-II	IGFR2	FST	MET	CTSS	UBE2L3	mtHsp70	IL-1R1	IL-10RA	SIRT5	UCP1	PPC3
E	IGFBP1	MyoD1	CAV3	CAPN1	PSMD4	UBE2N	Hsp90α	IL-1R2	IL-10RB	PGC1α	UCP2	PPC4
F	IGFBP2	MyoD2	DES	CAPN2	PSD12	CUL2	Hsp90β	IL-6	TNF-α	CPT1A	UCP3	NPC
G	IGFBP4	Myf5	VIM	CAPN3	PSMA5	CUL3	GRP-170	IL-6RA	TRADD	CS	LXRα	ACTB
H	IGFBP7	Myf6	CDH15	CAST	PSMB1	CUL5	GRP-94	IL-6RB	SIRT1	ND2	PPARα	ACTB

Position	Symbol	Description	Accession No.
A1	GHR-I	Growth hormone receptor I	AF438176
B1	GHR-II	Growth hormone receptor II	AY573601
C1	IGF-I	Insulin-like growth factor-I	EF563837
D1	IGF-II	Insulin-like growth factor-II	EF563836
E1	IGFBP1	Insulin-like growth factor binding protein 1	KM522771
F1	IGFBP2	Insulin-like growth factor binding protein 2	AF377998
G1	IGFBP4	Insulin-like growth factor binding protein 4	KM658998
H1	IGFBP7	Insulin-like growth factor binding protein 7	KM522772
A2	IGFALS	Insulin-like growth factor-binding protein complex acid labile subunit	KM522773
B2	INSR	Insulin receptor	KM522774
C2	IGFR1	Insulin-like growth factor receptor I	KM522775
D2	IGFR2	Insulin-like growth factor receptor II	KM522776
E2	MyoD1	Myoblast determination protein 1	AF478568
F2	MyoD2	Myoblast determination protein 2	AF478569
G2	Myf5	Myogenic factor 5	JN034420
H2	Myf6	Myogenic factor 6	JN034421
A3	MSTN	Growth/ differentiation factor 8	AF258448
B3	MEF2A	Myocyte-specific enhancer factor 2A	KM522777
C3	MEF2C	Myocyte-specific enhancer factor 2C	KM522778
D3	FST	Follistatin	AY544167
E3	CAV3	Caveolin 3	KM522779
F3	DES	Desmin	KM522780
G3	VIM	Vimentin	KF857332
H3	CDH15	Cadherin 15	KM522781
A4	PCNA	Proliferating cell nuclear antigen	KF857335
B4	PAX7	Paired box 7	KM522782
C4	SOX3	Transcription factor SOX3	KM522783
D4	MET	c-met/hepatocyte growth factor receptor	KM522784
E4	CAPN1	Calpain 1	KF444899
F4	CAPN2	Calpain 2	KF444900
G4	CAPN3	Calpain 3	KM522785
H4	CAST	Calpastatin	KM522786
A5	CTSB	Cathepsin B	KJ524457

Suppl. Table 17. Continued I.

Position	Symbol	Description	Accession No.
B5	CTSD	Cathepsin D	AF03619
C5	CTSL	Cathepsin L	KM522787
D5	CTSS	Cathepsin S	KM522788
E5	PSMD4	26S proteasome non-ATPase regulatory subunit 4	KM522789
F5	PSD12	26S proteasome non-ATPase regulatory subunit 12	KM522790
G5	PSMA5	Proteasome subunit alpha type-5	KM522791
H5	PSMB1	Proteasome subunit beta type-1	KM522792
A6	UCHL3	Ubiquitin carboxyl-terminal hydrolase isozyme L3	KM522793
B6	UBE2A	Ubiquitin-conjugating enzyme E2 A	KM522794
C6	UBE2D2	Ubiquitin-conjugating enzyme E2 D2	KM522795
D6	UBE2L3	Ubiquitin-conjugating enzyme E2 L3	KM522796
E6	UBE2N	Ubiquitin-conjugating enzyme E2N	KM522797
F6	CUL2	Cullin 2	KM522798
G6	CUL3	Cullin 3	KM522799
H6	CUL5	Cullin 5	KM522800
A7	mtHsp10	10 kDa heat shock protein, mitochondrial	JX975224
B7	Hsp30	30 kDa heat shock protein	KM522801
C7	mtHsp60	60 kDa heat shock protein, mitochondrial	JX975227
D7	mtHsp70	70 kDa heat shock protein, mitochondrial	DQ524993
E7	Hsp90α	90 kDa heat shock protein alpha 1	KM522802
F7	Hsp90β	90 kDa heat shock protein beta	KM522803
G7	GRP-170	Glucose-regulated protein, 170 kDa	JQ308821
H7	GRP-94	Glucose-regulated protein, 94 kDa	JQ308820
A8	DER-1	Derlin-1	JQ308825
B8	ERdj3	ER-associated Hsp40 co-chaperone	JQ308827
C8	IL-1β	Interleukin-1 beta	AJ419178
D8	IL-1R1	Interleukin-1 beta receptor 1	JX976615
E8	IL-1R2	Interleukin-1 beta receptor 2	AM296027
F8	IL-6	Interleukin-6	EU244588
G8	IL-6RA	Interleukin-6 receptor A	JX976616
H8	IL-6RB	Interleukin-6 receptor B	JX976617
A9	IL-8	Interleukin-8	JX976619
B9	IL-8RA	Interleukin-8 receptor A	JX976620
C9	IL-10	Interleukin-10	JX976621
D9	IL-10RA	Interleukin-10 receptor A	JX976622
E9	IL-10RB	Interleukin-10 receptor B	JX976623
F9	TNF-α	Tumor necrosis factor-alpha	AJ413189
G9	TRADD	Tumor necrosis factor receptor type 1-associated DEATH domain protein	KM522804
H9	SIRT1	Sirtuin1	KF018666
A10	SIRT2	Sirtuin 2	KF018667
B10	SIRT3	Sirtuin3	KF018668
C10	SIRT4	Sirtuin4	KF018669
D10	SIRT5	Sirtuin5	KF018670
E10	PGC1α	Proliferator-activated receptor gamma coactivator 1 alpha	JX975264

Suppl. Table 17. Continued II.

Position	Symbol	Description	Accession No.
F10	CPT1A	Carnitine palmitoyltransferase 1A	JQ308822
G10	CS	Citrate synthase	JX975229
H10	ND2	NADH-ubiquinone oxidoreductase chain 2	KC217558
A11	NDUFAF 2	NADH dehydrogenase (ubiquinone) 1 alpha subcomplex, assembly factor 2	KC217598
B11	COXI	Cytochrome c oxidase subunit I	KC217652
C11	SCO1	SCO1 protein homolog, mitochondrial	KC217649
D11	UCP1	Uncoupling protein 1	FJ710211
E11	UCP2	Uncoupling protein 2	JQ859959
F11	UCP3	Uncoupling protein 3	EU555336
G11	LXRα	Liver X receptor α	FJ502320
H11	PPARα	Peroxisome proliferator-activated receptor α	AY590299
A12	PPARγ	Peroxisome proliferator-activated receptor γ	AY590304
B12-E12	PPC	Positive PCR control (serial dilutions of standard gene)	AY590304
F12	NPC	Negative PCR control	
G12-H12	ACTB	B-actin	X89920

GH/IGF system: GHR-I, GHR-II, IGF-I, IGF-II, IGFBP1, IGFBP2, IGFBP4, IGFBP7, IGFALS, INSR, IGFR1, IGFR2
Muscle growth and differentiation: MyoD1, MyoD2, Myf5, Myf6, MSTN, MEF2A, MEF2C, FST, CAV3, DES, VIM, CDH15, PCNA, PAX7, SOX3, MET
Protein breakdown: CAPN1, CAPN2, CAPN3, CAST, CTSB, CTSD, CTSL, CTSS, PSMD4, PSD12, PSMA5, PSMB1, UCHL3, UBE2A, UBE2D2, UBE2L3, UBE2N, CUL2, CUL3, CUL5
Protein folding and assembly: mtHsp10, Hsp30, mtHsp60, mtHsp70, Hsp90α, Hsp90β, GRP-170, GRP-94, DER-1, ERdj3
Inflammatory/anti-inflammatory response : IL-1β, IL-1R1, IL-1R2, IL-6, IL-6RA,IL-6RB, IL-8, IL-8RA, IL-10, IL-10RA, IL-10RB, TNF-α, TRADD
Energy sensors: SIRT1, SIRT2, SIRT3, SIRT4, SIRT5
Oxidative phosphorylation: PGC1α, CPT1A, CS, ND2, NDUFAF2, COXI, SCO1
Mitochondrial respiration uncoupling: UCP1, UCP2, UCP3
Transcription-related factors of lipid metabolism: LXRα, PPARα, PPARγ

Supplemental Table 18. GSB forward and reverse primers for real-time PCR used in trial 3.

Gene name	Symbol		Primer sequence
Growth hormone receptor I	GHR-I	F	ACC TGT CAG CCA CCA CAT GA
		R	TCG TGC AGA TCT GGG TCG TA
Growth hormone receptor II	GHR-II	F	GAG TGA ACC CGG CCT GAC AG
		R	GCG GTG GTA TCT GAT TCA TGG T
Insulin-like growth factor-I	IGF-I	F	TGT CTA GCG CTC TTT CCT TTC A
		R	AGA GGG TG TGG CTA CAG GAG ATA C
Insulin-like growth factor-II	IGF-II	F	TGG GAT CGT AGA GGA GTG TTG T
		R	CTG TAG AGA GGT GGC CGA CA
Insulin-like growth factor binding protein 1	IGFBP1	F	ACA AAC CAA AAC AGT GCG AGT CCT C
		R	CCG TTC CAA GAG TTC ACA CAC CAG
Insulin-like growth factor binding protein 2	IGFBP2	F	AGC GAT GTG TCC TGA GAT AGT GAG
		R	GCA CCG TGG CGT GTA GAC C
Insulin-like growth factor binding protein 4	IGFBP4	F	GGC ATC AAA CAC CCG CAC AC
		R	ATC CAC GCA CCA GCA CTT CC
Insulin-like growth factor binding protein 7	IGFBP7	F	GCC ACA GCT CCG ATC ATC GTC ACT
		R	AGC CAC TCA CAT TGT AGA CCT CAC CTG
Insulin-like growth factor binding protein complex acid labile subunit	IGFALS	F	GCT CGG AAC TTC ACT CAA GTC CCA TC
		R	AGT TGC CAT CCA GCC AGA TAG AAT GA
Insulin receptor	INSR	F	ACG GAC AGC AAG AAG GCA GAG AAT C
		R	GGC TTC AAC GGT CGG ATC AGG T
Insulin-like growth factor 1 receptor	IGF1R	F	TCA ACG ACA AGT ACG ACT ACC GCT GCT
		R	CAC ACT TTC TGG CAC TGG TTG GAG GTC
Cation-indipendent mannose-6-phosphate receptor	IGF2R	F	ACA TTC GGG CAG CAC TCC TAA GAT
		R	CCA GTT CAC CTC GTA GCG ACA GTT
Myoblast determination protein 1	MyoD1	F	ATG GAG CTG TCG GAT ATC TCT TTC
		R	GAA GCA GGG GTC ATC GTA GAA ATC
Myoblast determination protein 2	MyoD2	F	CCA ACT GCT CTG ATG GCA TGA TGG ATT TC
		R	GAC CGT TTG CTT CTC CTG GAC TCG TAT G
Myogenic factor 5	Myf5	F	GCA TGG TTG ACA GCA ACA GTC CAG TGT
		R	TGT CTT ATC GCC CAA AGT GTC GTT CTT CAT
Myogenic factor 6	Myf6/MRF4/herculin	F	GCA GCA ATG ACA AAC CAG AGA GAC GGA ACA
		R	GAG GCT GGA GGA CGC CGA AGA TTC A
Growth/ differentiation factor 8	MSTN/GDF-8	F	AAG AGC AGA TCA TCT ACG GCA AGA TCC
		R	TCA AGA GCA TCC ACA ACG GTC TAC CA
Myocyte-specific enhancer factor 2A	MEF2A	F	ATG GAC GAG AGG AAC AGG CAG GTT A
		R	GGC TAT CTC ACA GTC ACA TAG TAC GCT CAG
Myocyte-specific enhancer factor 2C	MEF2C	F	TAG CAA CTC CCA CTC TAC CAG GAC AAG
		R	GGA ATA CTC GGC ACC ATA AGA AGT CG

Supplemental Table 18. Continued I

Gene name	Symbol		Primer sequence
Follistatin	FST	F	GGA CCA GAC AAA CAA CGC ATA TTG
		R	CAT AGA TGA TCC CGT CGT TTC CAC
Caveolin 3	CAV3	F	CAC CAC CTT CAC TGT GTC CAA
		R	CGA CGG GGA TGC CAA AGA C
Desmin	DES	F	ATT CAC CAG AAG GAG GAG GCT GAG AAC AAC
		R	GAG TGG CAT TGT CAA CAT CGG CTC TGA
Vimentin	VIM	F	GCT TCA GAC AGG ATG TGG ACA AC
		R	AGT GAT TCT ACC TTC CGC TCC AG
Cadherin-15	CDH15	F	AAC GCT TAT CTG AGC TAC TCT ATC ATT GG
		R	CTG GTT GTT GAT ACC GAA CAT TGT
Proliferating cell nuclear antigen	PCNA	F	CGT ATC TGC CGT GAC CTG T
		R	AGA ACT TGA CTC CGT CCT TGG
Paired box protein 7	PAX7	F	GAA CGT GAG CTT GTC CAC CCA GAG G
		R	GCC GAG TGG TCT CCC AGT TTC ATC C
Trascription factor SOX3	SOX3	F	ACA TGA AGG AGC ACC CGG ATT ATA AAT ACC
		R	GGG CAA AGA ATA CTT GTC TTT CTT GAG CAA
Hepatocyte growth factor receptor	MET	F	GCC ACA GGA AAC AAG ATT ACT AAA GTC CCT
		R	AGC AAA CAG GAA GTA CAG GTG GTA AGC
Calpain 1	CAPN1	F	CAG AAC CAC AAC GCC GTG AAG TTT
		R	AGG CAC TGG GCT TTA AGA CTC TCG
Calpain 2	CAPN2	F	CAT CTA TAA GAA GAA CGA CTC GGA CAA CTC
		R	TGT TGA GGC TGA AAC CTG CGT CTT TA
Calpain 3	CAPN3	F	TAC GAA GAG GAT GAC GAC CCA GAG
		R	GCA TCA GAG CCA CAA CGA GAG T
Calpastatin	CAST	F	CCC AAA CCC GAG CCC ACC AT
		R	GAC AAG AAG TCC AGA GCG TCT CCA GTA
Cathepsin B	CTSB	F	TGA TTC CCA TGT CGG TTG TC
		R	GGG TCT ACT GCC ATT CAC AT
Cathepsin D	CTSD	F	CAC ACT GGG AGA CCT GCA CTA TGT CAA TG
		R	ATT GCC AAC TTG AAG TCC GTC CAT ACC
Cathepsin L	CTSL	F	GGG AAC GGA TGA CCA GCC TTG T
		R	CGG TGT CAT TGG CAG AGT TGT AGT TG
Cathepsin S	CTSS	F	CCA CAT GGG AGA CCT GAC ACC AGA GGA GAT
		R	TCA GTG GGA GGA ATG AAT GTG GCG AAA GAC
26S proteasome non-ATPase regulatory subunit 4	PSMD4	F	CAT CCA CAC CTG CTC TAC CAG ACT TCA
		R	CGT AGG CGA TCT GTT CAT CCT CTG TCA T

Supplemental Table 18. Continued II

Gene name	Symbol		Primer sequence
26S proteasome non-ATPase regulatory subunit 12	PSMD12	F	CCT GCC ACA GAT GTC TTC TCT TAT TCA
		R	GCC ATT ATT CTG ATG TTA TGC TCC ACC A
Proteasome subunit alpha type-5	PSMA5	F	TGA CAA GAT CGG AGT ATG ACA GAG GTG TGA
		R	CCT CGA TGG CAT ATT CAA CCT GGA ACA ATC
Proteasome subunit beta type-1	PSMB1	F	TGG ATG AAG AGG GCA AAG GAG CAG TGT A
		R	TTG TAT GTG TCT CTC TGG TAG GAG CCC ACT
Ubiquitin carboxyl-terminal hydrolase isozyme L3	UCHL3	F	CAG TGA CAG AGA AGT ATG AGA CAT TCA A
		R	CGT TTC CAA TAG TTT GCT TAA TGA AGT AGA
Ubiquitin-conjugating enzyme E2 A	UBE2A	F	CAT CAT GGT GTG GAA TGC AGT CAT ATT TGG
		R	GGG TTT GTT GGG GTA TTC TTC TGT GAA CT
Ubiquitin-conjugating enzyme E2 D2	UBE2D2	F	TCT GCT GTG CGA CCC AAA CC
		R	GAT GCG GGC GAT CTC GGG TA
Ubiquitin-conjugating enzyme E2 L3	UBE2L3	F	CCT CAT TGC ATT GGT GAA CG
		R	TTG AGT ATT CTT CTG CTA GGT CAG
Ubiquitin-conjugating enzyme E2 N	UBE2N	F	TTG CCT CGT AGG ATT ATT AAG GAG AC
		R	CCT GAA ATG ACC ACA TGG AAG TAA CG
Cullin 2	CUL2	F	GGC ATC CGA GGC ACC AGT AAC C
		R	TGA ACC TCC AGC ACT GAC TCC ACA A
Cullin 3	CUL3	F	AAA GGA GGA TGG TTC AGA AGT TGG
		R	CAG TAT GTG CTT ACG GGT GTT AGA G
Cullin 5	CUL 5	F	CAA ACT CAA GAG GCA GGT GTT GTC GTA
		R	GTA GAA TAG TGT TCC CTC TGC GAA GTC T
10 kDa heat shock protein, mitochondria	mtHsp10	F	CAT GCT GCC AGA GAA GTC TCA AGG
		R	AGG TCC CAC TGC CAC TAC TGT
30kDa heat shock protein	Hsp30	F	ATC TCT CAA CAA GAC CAC ACA ACA CT
		R	TAC AGG CCA GTA CAA GTC CAT GAA TG
60 kDa heat shock protein, mitochondrial	mtHsp60	F	TGT GGC TGA GGA TGT GGA TGG AGA G
		R	GCC TGT TGA GAA CCA AGG TGC TGA G
70 kDa heat shock protein, mitochondrial	mtHsp70/ GRP-75	F	TCC GGT GTG GAT CTG ACC AAA GAC
		R	TGT TTA GGC CCA GAA GCA TCC ATG
90kDa heat shock protein alpha 1	Hsp90a	F	CTC ACA GTT CAT CGG CTA CCC TAT CA
		R	AAC TTC CTC TTC CTT CTC TCC CTC ATC AAG
90kDa heat shock protein beta	Hsp90b	F	AGA ATA ACA TCA AGC TGT ACG TCA GGA GAG
		R	CAC CAC ACC ACG GAC AAA GTT CAG ATA CTC
Glucose-regulated protein, 170 kDa	GRP-170	F	CAG AGG AGG CAG ACA GCA AGA C
		R	TTC TCA GAC TCA GCA TTT CCA GAT TTC
Glucose-regulated protein, 94 kDa	GRP-94	F	AAG GCA CAG GCT TAC CAG ACA G
		R	CTT CAG CAT CAT CGC CGA CTT TC

Supplemental Table 18. Continued III

Gene name	Symbol		Primer sequence
Derlin-1	DER-1	F	ACT GCC TCG GTT GCC TTT CC
		R	TGG CTG TCA CAA GTC TCC AGA TAT G
ER-associated Hsp40 co-chaperone	ERdj-3	F	AAC CGA CAG CAG CAG GAC AG
		R	ACT TCT TCA AGC GTG ACC TCC AG
Interleukin-1 beta	IL-1β	F	GCG ACC TAC CTG CCA CCT ACA CC
		R	TCG TCC ACC GCC TCC AGA TGC
Interleukin-1 beta receptor 1	IL-1R1	F	GAA GCT GTA CGA CGC CTA C
		R	CTC CAC TGC CTT ACT GTA TCC
Interleukin-1 beta receptor 2	IL-1R2	F	CCT GAC CTC TCC GTG ACC TCT AA
		R	TGG CTG CTG CTG CTG ATG A
Interleukin-6	IL-6	F	TCT TGA AGG TGG TGC TGG AAG TG
		R	TCT TGA AGG TGG TGC TGG AAG TG
Interleukin-6 receptor A	IL-6RA	F	GCA GTG CTC GTA CTC TTC
		R	CTC CGC TCT TCC TCA TTG
Interleukin-6 receptor B	IL-6RB	F	CAG TGT CGG AGT ATG TGG TTG AGT
		R	CCC TCT GCC AGT CTG TCC AA
Interleukin-8	IL-8	F	CAG CAG AGT CTT CAT CGT CAC TAT TG
		R	AGG CTC GCT TCA CTG ATG G
Interleukin-8 receptor A	IL-8RA	F	CTT GTT TCA TCT GAC GAT AG
		R	AAG AGG ATG CTT GTG TAG
Interleukin-10	IL-10	F	AAC ATC CTG GGC TTC TAT CTG
		R	GTG TCC TCC GTC TCA TCT G
Interleukin-10 receptor A	IL-10RA	F	GAG GAC AAT GAA GAG GAA GAC AGG AG
		R	TGT TCG TAG CGG AGT TGG ACT
Interleukin-10 receptor B	IL-10RB	F	AGA CCC ACA GGC TTC AGA T
		R	GCA GCG TCA CCA GGT TAG
Tumor necrosis factor -alpha	TNF-α	F	CAG GCG TCG TTC AGA GTC TC
		R	CTG TGG CTG AGA GCT GTG AG
Tumor necrosis factor receptor type 1-associated DEATH domain protein	TRADD	F	GAG GGA AAG TTC ATC GTG TTC AAA GTC ATC
		R	AAC GGA TCA GCA TCA TGG ACC TTA AGT A
Sirtuin1	SIRT1	F	GGT TCC TAC AGT TTC ATC CAG CAG CAC ATC
		R	CCT CAG AAT GGT CCT CGG ATC GGT CTC
Sirtuin2	SIRT2	F	GAA CAA TCC GAC GAC AGC AGT GAA G
		R	AGG TTA CGC AGG AAG TCC ATC TCT
Sirtuin3	SIRT3	F	CTG CCA AGT CCT CAT CCC
		R	CTT CAC CAG ACG AGC CAC
Sirtuin4	SIRT4	F	GGC TGG CGG AGT CGG ATG
		R	TCC TGA ATA CAC CTG TGA CGA AGA C

Supplemental Table 18. Continued IV.

Gene name	Symbol		Primer sequence
Sirtuin5	SIRT5	F	CAG ACA TCC TAA CCC GAG CAG AG
		R	CCA CGA GGC AGA GGT CAC A
Proliferator-activated receptor gamma coactivator 1 alpha	PGC1α	F	CGT GGG ACA GGT GTA ACC AGG ACT C
		R	ACC AAC CAA GGC AGC ACA CTC TAA TTC T
Carnitine palmitoyltransferase 1A	CPT1A	F	GTG CCT TCG TTC GTT CCA TGA TC
		R	TGA TGC TTA TCT GCT GCC TGT TTG
Cytrate synthase	CS	F	TCC AGG AGG TGA CGA GCC
		R	GTG ACC AGC AGC CAG AAG AG
NADH-ubiquinone oxidoreductase chain 2	ND2	F	TAG GTT GAA TGA CCA TCG TA
		R	GGC TAA GGA GTT GAG GTT
NADH dehydrogenase (ubiquinone) 1 alpha subcomplex, assembly factor 2	NDUFAF2	F	AGG CAG CAT ACC GAT AGA G
		R	ACT CAT TCT TCA GCA ACT CCT
Cytochrome c oxidase subunit I	COXI	F	GTC CTA CTT CTT CTG TCC CTT CCT GTT CT
		R	AGG TTT CGG TCT GTA AGG AGC ATT GTA ATC
SCO1 protein homolog, mitochondrial	SCO1	F	ACA ACA ACA AGC CCA CCA AGA
		R	GAC AGT GAG TGA ACC CGA AGT AGA T
Uncoupling protein 1	UCP1	F	GCA CAC TAC CCA ACA TCA CAA G
		R	CGC CGA ACG CAG AAA CAA AG
Uncoupling protein 2	UCP2	F	CGG CGG CGT CCT CAG TTG
		R	AAG CAA GTG GTC CCT CTT TGG TCA T
Uncoupling protein 3	UCP3	F	AGG TGC GAC TGG CTG ACG
		R	TTC GGC ATA CAA CCT CTC CAA AG
Liver X receptor α	LXRα	F	GCA CTT CGC CTC CAG GAC AAG
		R	CAG TCT TCA CAC AGC CAC ATC AGG
Peroxisome proliferator-activated receptor α	PPARα	F	TCT CTT CAG CCC ACC ATC CC
		R	ATC CCA GCG TGT CGT CTC C
Peroxisomeproliferator-activated receptor γ	PPARγ	F	CGC CGT GGA CCT GTC AGA GC
		R	GGA ATG GAT GGA GGA GGA GGA GAT GG

Table 19. Effect of nutrient deficiencies on the relative mRNA expression of growth-related genes in liver of GSB in trial 3. Data are the mean (SEM) of 6 fish. Different superscript letters in each row indicate significant differences among dietary treatments (SNK test, *P*<0.05).

	CTRL	SAA	n-3 LC-PUFA	PL	P	Min	Vit	P-value[1]
GHR-I	22.04±2.56^{a}	18.45±2.46^{a}	9.93±0.98^{b}	22.98±3.1^{a}	9.04±0.98^{b}	19.44±2.67^{a}	17.63±2.32^{a}	<0.001
GHR-II	12.53±2.21	12.4±1.97	8.45±1.23	10.76±2.19	12.07±1.83	16.02±1.44	16.94±2.35	0.068
IGF-I	78.57±5.77^{a}	66.99±8.31^{a}	30.75±2.29^{b}	65.31±5.62^{a}	26.21±4.65^{b}	70.1±4.88^{a}	60.97±7.82^{a}	<0.001
IGF-II	28.94±2.98^{ab}	23.83±4.08^{ab}	18.3±2.81^{b}	23.43±5.32^{ab}	7.56±1.89^{c}	25.28±4.63^{ab}	38.22±3.59^{a}	<0.001
IGFBP1	0.14±0.01	0.12±0.02	0.11±0.01	0.18±0.05	0.15±0.02	0.17±0.03	0.21±0.02	0.070
IGFBP2	17.41±1.54^{ab}	17.07±2.35^{ab}	12.21±0.34^{b}	16.05±0.9^{ab}	16.46±1.44^{ab}	19.4±1.86^{a}	16.67±1.88^{ab}	0.149
IGFBP4	7.56±0.69^{a}	6.25±0.87^{ab}	4.72±0.18^{b}	6.85±0.49^{ab}	2.48±0.27^{c}	5.65±0.75^{ab}	6.64±0.87^{ab}	<0.001
IGFBP7	4.57±0.34	3.78±0.47	4.32±0.26	10.88±3.2	3.8±0.39	8.89±2.38	7.8±1.98	0.028
IGFALS	159.5±22.08^{a}	141.3±23.15^{ab}	99.55±3.27^{b}	138.6±15.67^{ab}	47.61±5.38^{c}	176.35±17.58^{a}	173.6±12.36^{a}	<0.001
INSR	4.18±0.56	3.51±0.45	3.12±0.38	3.94±0.29	3.37±0.27	3.93±0.27	4.28±0.37	0.283
IGFR1	0.24±0.02	0.22±0.02	0.23±0.03	0.23±0.02	0.24±0.03	0.22±0.02	0.25±0.02	0.963
IGFR2	1.01±0.06	0.98±0.07	1.11±0.06	1.15±0.06	1.11±0.11	1.04±0.11	1.1±0.09	0.820
MEF2A	2.88±0.31	2.83±0.2	2.78±0.27	3.27±0.27	3.3±0.25	3.07±0.33	3.05±0.28	0.750
MEF2C	0.2±0.02	0.18±0.02	0.17±0.01	0.16±0.03	0.21±0.02	0.18±0.02	0.16±0.01	0.579
VIM	0.37±0.05^{ab}	0.41±0.05^{ab}	0.23±0.03^{a}	0.38±0.05^{ab}	0.35±0.05^{ab}	0.46±0.07^{b}	0.40±0.04^{ab}	0.156
PCNA	5.49±0.53^{ab}	4.89±0.76^{ab}	3.03±0.47^{a}	6.15±1.23^{ab}	4.43±0.95^{ab}	4.61±0.94^{ab}	7.61±0.77^{b}	0.020
MET	4.7±0.38^{ab}	3.89±0.4^{a}	5.03±0.61^{ab}	5.53±0.64^{ab}	4.9±0.53^{ab}	6.81±0.76^{b}	6.95±0.59^{b}	0.004
CAPN1	4.06±0.51^{a}	4.06±0.29^{a}	2.37±0.3^{b}	4.13±0.66^{a}	2.15±0.28^{b}	2.99±0.24^{ab}	3.29±0.37^{ab}	0.002
CAPN2	1.04±0.07	1.04±0.11	1.22±0.17	1.22±0.14	1.59±0.27	0.99±0.14	1.17±0.22	0.275
CAPN3	0.08±0.01	0.14±0.02	0.12±0.02	0.12±0.01	0.08±0.01	0.1±0.02	0.11±0.01	0.063
CAST	4.24±0.37	3.29±0.46	4.59±0.39	4.35±0.36	3.47±0.35	3.69±0.35	4.74±0.22	0.035
CTSB	23.47±1.08	23.51±5.76	26.7±2.78	26.35±2.91	27.41±4.44	26.18±4.03	26.35±3.64	0.988
CTSD	3.15±0.29^{a}	1.86±0.28^{ab}	1.41±0.17^{b}	2.04±0.44^{ab}	3.02±0.43^{a}	1.81±0.33^{ab}	1.80±0.29^{ab}	0.006
CTSL	58.37±8.65^{abc}	42.55±7.96^{ab}	68.88±6.24^{bc}	75.85±10.13^{c}	30.42±3.73^{a}	48.40±5.88^{abc}	58.57±6.99^{abc}	0.001
CTSS	1.67±0.25	2.44±0.27	2.27±0.2	2.01±0.08	1.98±0.39	2.17±0.24	2.46±0.27	0.443
PSMD4	1.81±0.12	1.92±0.29	1.46±0.04	2.25±0.41	1.94±0.23	1.61±0.17	1.84±0.11	0.323
PSD12	2.5±0.18	2.44±0.39	2.44±0.16	4.03±0.83	3.09±0.34	2.51±0.35	2.84±0.12	0.068

Suppl. Table 19. Continued I.

	CTRL	SAA	n-3 LC-PUFA	PL	P	Min	Vit	*P*-value1
PSMA5	2.13±0.27	2.1±0.56	1.72±0.08	3.28±1.1	2.55±0.43	1.6±0.31	1.91±0.14	0.262
PSMB1A	6.12±0.82	5.13±0.85	5.07±0.23	8.98±3.69	6.24±0.86	5.12±0.87	5.48±0.14	0.533
UCHL3	1.64±0.09	1.29±0.26	1.55±0.15	1.83±0.44	2.45±0.65	1.36±0.2	1.43±0.16	0.302
UBE2A	1.91±0.17	1.45±0.17	1.72±0.05	1.98±0.28	2.35±0.29	1.91±0.21	1.95±0.17	0.143
UBE2D2	5.68±0.26	5.32±0.48	5.1±0.22	5.75±0.42	6.22±0.46	6.21±0.7	5.92±0.28	0.464
UBE2L3	10.55±0.61	9.43±1.13	8.68±0.31	11.56±1.43	11.6±1.35	9.77±0.96	10.67±0.52	0.356
UBE2N	3.12±0.4	2.66±0.39	2.87±0.18	2.92±0.65	3.24±0.45	2.69±0.41	3.03±0.24	0.941
CUL2	0.94±0.06	0.92±0.11	0.9±0.05	1.07±0.15	1.16±0.23	0.93±0.11	0.9±0.04	0.715
CUL3	0.96±0.08	0.82±0.1	0.8±0.06	0.99±0.1	0.98±0.09	0.83±0.1	0.85±0.06	0.501
CUL5	0.41±0.03	0.45±0.06	0.41±0.04	0.5±0.07	0.44±0.04	0.44±0.05	0.48±0.02	0.812
mtHsp10	6.9±0.61	7.29±0.97	5.42±0.26	5.43±0.75	6.99±0.92	7.32±1.03	5.22±0.77	0.245
mtHsp30	0.06±0.01	0.06±0	0.07±0.01	0.06±0.01	0.06±0.01	0.06±0.02	0.06±0.01	0.994
mtHsp60	2.3±0.26	2.49±0.35	1.86±0.11	2.04±0.25	2.57±0.22	3.08±0.4	2.56±0.45	0.212
mtHsp70	3.13±0.34	3.27±0.5	2.71±0.32	3.31±0.47	5.37±1.19	4.09±0.37	3.86±0.56	0.127
Hsp90β	192.44±14.25	164.35±13.5	181.49±7.07	201.97±24.52	218.17±34.41	199.52±14.75	169.95±11.31	0.528
GRP-170	8.33±0.83^{ab}	9.30±1.65^{ab}	4.88±0.49^{a}	10.86±2.78^{ab}	11.45±1.26^{ab}	12.1±1.81^{b}	9.86±0.74^{ab}	0.066
GRP-94	25.95±2.53^{ab}	20.56±4.77^{a}	19.68±1.4^{a}	30.07±5.8^{ab}	18.12±1.74^{a}	38.34±5.82^{b}	27.09±4.11^{ab}	0.013
DER-1	9.67±0.87^{ab}	8.14±1.20^{ab}	5.84±0.17^{a}	10.83±2.08^{b}	7.47±0.61^{ab}	10.38±1.42^{ab}	10.29±0.63^{ab}	0.025
IL-1β	0.01±0.01	0.03±0.01	0.02±0.01	0.05±0.04	0.01±0.01	0.01±0.01	0.01±0.01	0.627
IL-1R1	3.32±0.62^{ab}	2.6±0.24^{ab}	2.65±0.18^{ab}	4.58±0.60^{b}	1.75±0.18^{a}	3.44±0.52^{ab}	4.75±1.00^{b}	0.005
IL-1R2	0.01±0	0.03±0.02	0.05±0.02	0.04±0.03	0.01±0	0.02±0	0.02±0.01	0.146
IL-6	0.01±0	0.01±0	0.01±0	0.01±0	0.01±0	0.01±0	0.01±0	0.615
IL-6RA	9.39±0.93	7.06±0.45	10.8±0.79	11.51±2.12	8.03±0.74	11.71±2.04	10.56±0.73	0.087
IL-6RB	8.25±0.67^{ab}	6.86±0.74^{abc}	5.41±0.37^{c}	8.88±1.01^{a}	5.81±0.42^{bc}	8.21±0.80^{ab}	9.41±0.66^{a}	0.001
IL-8	0.01±0	0.03±0.01	0.03±0	0.03±0.02	0.02±0.01	0.01±0	0.02±0.01	0.692
IL-8RA	0.11±0.02	0.21±0.07	0.11±0.04	0.17±0.04	0.08±0.02	0.19±0.06	0.17±0.02	0.208
IL-10	0.04±0.01	0.05±0.01	0.03±0.01	0.03±0.01	0.03±0.01	0.04±0.01	0.03±0	0.505
IL-10RA	0.1±0.01	0.13±0.02	0.14±0.02	0.09±0.01	0.11±0.01	0.1±0.02	0.11±0.01	0.331

Suppl. Table 19. Continued II.

	CTRL	SAA	n-3 LC-PUFA	PL	P	Min	Vit	*P*-value[1]
IL-10RB	4.96±0.93	4.45±0.64	3.95±0.23	4.82±0.37	4.2±0.44	4.97±0.57	5.02±0.45	0.720
TNF-α	0.14±0.02	0.12±0.02	0.13±0.02	0.17±0.01	0.11±0.01	0.14±0.01	0.13±0.01	0.325
TRADD	0.96±0.06	0.83±0.11	0.92±0.04	0.91±0.09	0.87±0.05	0.93±0.13	1.02±0.04	0.714
SIRT1	0.58±0.04	0.64±0.11	0.56±0.02	0.65±0.05	0.63±0.04	0.54±0.06	0.58±0.03	0.715
SIRT2	1.83±0.08	1.56±0.20	1.54±0.07	1.94±0.15	1.74±0.15	1.73±0.21	1.71±0.09	0.528
SIRT3	0.22±0.02	0.28±0.03	0.2±0.02	0.3±0.04	0.2±0.02	0.26±0.04	0.3±0.03	0.060
SIRT4	0.10±0.01^{a}	0.10±0.01^{a}	0.11±0.01^{ab}	0.12±0.02^{ab}	0.15±0.01^{b}	0.12±0.01^{ab}	0.10±0.01^{a}	0.017
SIRT5	1.7±0.08	1.82±0.16	1.59±0.15	1.92±0.15	1.81±0.15	1.48±0.14	1.96±0.17	0.266
PGC1α	0.45±0.14	0.58±0.08	0.49±0.1	0.65±0.08	0.88±0.15	1.03±0.1	0.78±0.19	0.042
CPT1A	2.41±0.14^{ab}	2.41±0.27^{ab}	5.29±0.69^{c}	3.16±0.53^{ab}	1.73±0.20^{a}	3.33±0.38^{ab}	3.50±0.39^{b}	<0.001
CS	5.58±0.26	5.85±0.94	6.81±0.72	5.51±0.44	7.49±0.86	6.17±0.47	5.54±0.45	0.221
ND2	180.27±12.73	131.02±17.47	148.43±11.31	187.7±32.25	264.63±48.47	191.83±31.07	162.34±8.53	0.054
NDUFAF2	1.6±0.12	1.46±0.14	1.37±0.1	1.84±0.17	1.78±0.15	1.61±0.14	1.76±0.1	0.182
COXI	463.51±43.36	305.52±44.29	405.67±38.81	366.53±41.55	521.73±86.17	359.45±45.96	509.48±50.46	0.096
SCO1	0.36±0.01^{a}	0.43±0.06^{a}	0.40±0.03^{a}	0.47±0.09^{a}	0.65±0.06^{b}	0.40±0.05^{a}	0.42±0.04^{a}	0.009
UCP1	81.02±3.9^{ab}	61.22±10.60^{a}	90.54±10.03^{ab}	77.84±9.07^{ab}	107.3±12.64^{b}	67.12±6.27^{a}	57.62±7.99^{a}	0.005
LXRα	5.48±0.57	3.73±0.74	5.58±0.24	4.6±0.39	5.24±0.6	4.56±0.63	4.79±0.69	0.358
PPARα	18.17±1.74	15.83±2.48	14.57±0.62	19.4±2.55	22.67±3.55	19.6±1.74	17.42±1.39	0.225
PPARγ	3.66±0.59	4.11±1.00	2.93±0.17	3.5±0.13	3.8±0.32	3.82±0.43	3.7±0.44	0.805

[1]Result values from one-way analysis of variance

Supplemental Table 20. Effect of nutrient deficiencies on the relative mRNA expression of growth-related genes in white muscle of GSB in trial 3. Data are the mean (SEM) of 6 fish. Different superscript letters in each row indicate significant differences among dietary treatments (SNK test, *P*<0.05).

	CTRL	SAA	n-3 LC-PUFA	PL	P	Min	Vit	P-value[1]
GHR-I	6.96±0.72^{ab}	6.88±0.87^{ab}	5.60±0.31^{a}	10.02±1.31^{b}	8.20±1.11^{ab}	8.13±1.03^{ab}	7.17±0.94^{ab}	0.077
GHR-II	2.00±0.24^{a}	3.47±0.64^{ab}	6.13±0.63^{ab}	3.25±0.84^{ab}	8.05±1.61^{b}	4.04±0.92^{ab}	6.61±2.29^{ab}	0.006
IGF-I	0.89±0.06	0.79±0.06	0.70±0.05	0.90±0.12	0.68±0.06	0.92±0.13	0.63±0.07	0.127
IGF-II	3.92±0.48^{a}	4.12±0.31^{a}	3.65±0.19^{a}	3.65±0.27^{a}	3.85±0.33^{a}	3.77±0.15^{a}	5.14±0.40^{b}	0.038
IGFBP1	0.58±0.12	0.34±0.07	0.35±0.02	0.47±0.11	0.39±0.04	0.31±0.04	0.49±0.04	0.139
IGFBP4	1.11±0.12	0.82±0.10	0.72±0.09	0.88±0.22	0.67±0.09	0.78±0.09	0.78±0.12	0.262
IGFBP7	5.18±0.54	5.10±0.60	4.70±0.79	5.16±0.65	3.63±0.48	5.20±0.40	4.22±0.35	0.381
INSR	1.94±0.16	1.96±0.17	2.37±0.19	2.13±0.23	2.65±0.25	2.19±0.17	1.92±0.2	0.140
IGFR1	1.38±0.10	1.30±0.15	1.41±0.09	1.66±0.09	1.21±0.12	1.41±0.11	1.52±0.18	0.270
IGFR2	1.02±0.07^{ac}	0.88±0.07^{abc}	0.79±0.05^{ab}	1.06±0.09^{ac}	0.69±0.07^{b}	0.88±0.07^{abc}	1.12±0.07^{c}	0.001
MyoD1	18.04±2.06	17.88±1.54	18.64±1.4	23.27±1.14	23.81±2.52	20.02±1.60	23.62±2.66	0.087
MyoD2	9.47±0.84^{ab}	11.4±0.88^{b}	10.92±1.38^{b}	10.47±1.03^{ab}	12.92±1.15^{b}	10.28±0.86^{ab}	6.81±0.37^{a}	0.009
Myf5	1.68±0.08	1.44±0.13	1.39±0.10	1.22±0.07	1.61±0.10	1.50±0.12	1.52±0.11	0.081
Myf6	1.37±0.22	1.22±0.15	1.24±0.11	1.38±0.11	1.34±0.12	1.12±0.07	1.08±0.11	0.541
MSTN	6.43±1.23^{a}	8.01±1.93^{a}	7.02±1.04^{a}	5.61±0.84^{a}	20.60±2.05^{b}	8.25±1.22^{a}	12.02±2.02^{a}	<0.001
MEF2A	35.83±3.83^{a}	32.75±4.17^{a}	51.95±4.13^{b}	40.00±4.30^{a}	36.65±3.31^{a}	30.92±3.65^{a}	32.55±3.98^{a}	0.011
MEF2C	12.28±1.20	10.68±1.02	14.32±0.93	12.50±0.55	12.48±0.65	11.15±0.43	12.49±0.77	0.097
FST	1.67±0.22^{a}	1.22±0.14^{ab}	0.92±0.13^{b}	0.97±0.10^{b}	1.47±0.14^{ab}	1.44±0.17^{ab}	1.62±0.08^{a}	0.004
CAV3	81.83±7.70	77.51±9.76	82.54±5.74	83.68±6.88	92.45±7.20	81.44±3.15	85.56±9.59	0.886
DES	259.8±33.90	238.0±33.18	232.7±21.44	255.6±21.21	191.59±20.8	226.01±18.77	270.25±40.82	0.545
VIM	1.63±0.20	1.68±0.25	1.18±0.09	1.48±0.13	1.49±0.05	1.55±0.14	1.35±0.2	0.350
CDH15	2.31±0.22	2.13±0.21	2.16±0.25	1.86±0.21	2.16±0.33	2.13±0.18	1.97±0.12	0.860
PCNA	3.06±0.32	3.59±0.37	2.89±0.33	3.18±0.61	3.20±0.37	3.42±0.29	3.21±0.16	0.875
PAX7	0.23±0.02	0.17±0.01	0.18±0.03	0.19±0.02	0.21±0.03	0.18±0.02	0.16±0.02	0.257
MET	0.47±0.03	0.37±0.03	0.36±0.05	0.38±0.04	0.45±0.03	0.39±0.01	0.45±0.03	0.127
CAPN1	4.80±0.33	4.70±0.49	4.18±0.43	4.75±0.34	4.35±0.38	4.58±0.37	5.21±0.38	0.641
CAPN2	6.95±0.59	7.08±0.83	4.83±0.40	6.43±0.70	5.96±0.59	7.13±0.70	6.94±0.45	0.140

Suppl. Table 20. Continued I.

	CTRL	SAA	n-3 LC-PUFA	PL	P	Min	Vit	P-value[1]
CAPN3	13.63±1.93^{ab}	10.18±1.29^{a}	12.18±1.09^{ab}	15.74±2.37^{b}	10.77±1.44^{ab}	9.00±1.05^{ab}	15.92±1.26^{b}	0.017
CAST	14.55±1.06^{a}	12.79±1.06^{a}	17.65±1.32^{ab}	14.23±1.42^{a}	19.95±1.15^{b}	15.15±1.08^{a}	17.05±1.22^{ab}	0.003
CTSB	7.22±0.26^{a}	9.05±2.45^{a}	6.89±0.68^{a}	6.67±0.40^{a}	6.32±0.38^{a}	9.97±2.31^{a}	21.2±2.72^{b}	<0.001
CTSD	1.01±0.08^{a}	0.89±0.07^{a}	0.92±0.05^{a}	0.96±0.07^{a}	1.16±0.08^{a}	0.90±0.07^{a}	1.60±0.13^{b}	<0.001
CTSL	15.26±2.15	12.15±1.26	11.66±0.80	13.46±1.09	15.10±1.22	13.77±0.77	15.01±1.01	0.281
CTSS	1.94±0.31^{a}	1.97±0.47^{a}	1.61±0.16^{a}	1.84±0.33^{a}	1.63±0.10^{a}	2.42±0.53^{a}	7.85±1.66^{b}	<0.001
PSMD4	2.61±0.14	2.45±0.22	2.48±0.21	2.95±0.14	2.39±0.20	2.23±0.15	2.83±0.09	0.066
PSD12	7.85±0.55	7.21±1.33	6.51±0.64	7.46±0.82	7.26±0.66	5.74±0.51	8.11±0.27	0.285
PSMA5	4.13±0.26	4.05±0.50	4.11±0.51	4.72±0.60	4.20±0.34	3.40±0.32	4.87±0.39	0.284
PSMB1A	8.91±0.69	6.72±0.49	7.37±0.49	8.61±1.11	8.27±0.70	7.01±0.68	8.3±0.46	0.218
UCHL3	4.92±0.60^{ab}	3.69±0.15^{a}	4.54±0.50^{ab}	4.71±0.43^{ab}	5.12±0.37^{ab}	3.69±0.32^{a}	5.77±0.34^{b}	0.021
UBE2A	4.91±0.49	4.05±0.66	4.20±0.33	5.06±0.34	5.00±0.59	4.15±0.37	4.73±0.34	0.499
UBE2D2	2.70±0.21	2.57±0.25	2.38±0.20	2.53±0.24	2.35±0.15	2.59±0.13	2.77±0.16	0.691
UBE2L3	23.33±1.86	19.60±1.27	22.26±2.36	24.22±1.75	22.18±1.67	20.56±1.49	21.06±1.13	0.552
UBE2N	17.67±1.52	16.36±1.54	17.95±2.66	19.03±1.82	17.37±1.13	15.29±1.25	16.13±0.84	0.751
CUL2	2.27±0.16	2.07±0.27	2.10±0.16	2.52±0.14	2.17±0.18	1.88±0.10	2.13±0.19	0.286
CUL3	3.08±0.29	2.94±0.32	2.85±0.18	3.46±0.35	3.45±0.29	2.69±0.08	2.78±0.14	0.192
CUL5	0.71±0.04	0.79±0.13	0.75±0.06	0.87±0.09	0.86±0.07	0.64±0.03	0.76±0.05	0.364
mtHsp10	8.34±1.57	5.73±0.94	7.36±0.83	9.27±1.93	5.85±0.79	6.07±0.45	8.69±0.98	0.203
mtHsp60	2.97±0.47	2.22±0.38	2.72±0.34	3.22±0.89	2.51±0.31	2.06±0.17	3.11±0.21	0.429
mtHsp70	6.36±0.80	4.69±0.39	5.60±0.41	6.31±0.95	6.70±0.65	4.92±0.36	6.91±0.55	0.097
Hsp90α	117.6±26.02	81.00±10.70	124.1±9.90	101.8±14.71	101.8±8.85	84.9±6.91	132.21±12.84	0.154
Hsp90β	44.20±1.21	40.54±3.22	41.87±3.56	45.43±6.23	43.11±2.58	46.2±3.49	56.66±4	0.088
GRP-170	1.89±0.12^{ab}	1.93±0.25^{ab}	1.71±0.14^{a}	1.92±0.22^{ab}	1.92±0.18^{ab}	1.81±0.15^{ab}	2.53±0.15^{b}	0.059
GRP-94	4.91±0.86	4.62±0.45	5.25±0.87	4.32±0.39	4.59±0.43	5.01±0.47	6.01±1.06	0.741
DER-1	9.71±0.64	9.49±0.89	9.43±0.87	10.58±0.84	10.33±0.90	8.96±0.47	11.81±0.48	0.168
IL-1β	0.10±0.02^{ab}	0.04±0.01^{a}	0.06±0.01^{ab}	0.17±0.07^{b}	0.10±0.01^{ab}	0.06±0.01^{ab}	0.11±0.01^{ab}	0.049
IL-1R1	0.75±0.06^{a}	0.68±0.05^{a}	0.63±0.04^{a}	0.73±0.05^{a}	0.68±0.06^{a}	0.76±0.06^{a}	1.29±0.13^{b}	<0.001

Suppl. Table 20. Continued II. [1]Result values from one-way analysis of variance.

	CTRL	SAA	n-3 LC-PUFA	PL	P	Min	Vit	*P*-value[1]
IL-1R2	0.02±0.01^{a}	0.01±0.01^{a}	0.01±0.01^{a}	0.01±0.01^{a}	0.01±0.01^{a}	0.02±0.01^{a}	0.09±0.03^{b}	<0.001
IL-6	0.03±0.01	0.03±0.01	0.03±0.01	0.02±0.01	0.03±0.01	0.02±0.01	0.05±0.02	0.287
IL-6RA	0.54±0.08	0.37±0.03	0.37±0.02	0.52±0.05	0.43±0.03	0.40±0.03	0.58±0.09	0.028
IL-6RB	3.03±0.22^{a}	3.17±0.35^{a}	3.23±0.19^{a}	3.91±0.35^{ab}	4.03±0.46^{ab}	3.37±0.26^{a}	4.77±0.22^{b}	0.002
IL-8	0.06±0.02	0.03±0.01	0.03±0.01	0.12±0.09	0.03±0.01	0.06±0.01	0.07±0.01	0.492
IL-10	0.05±0.01^{a}	0.06±0.01^{a}	0.05±0.01^{a}	0.05±0.01^{a}	0.05±0.01^{a}	0.07±0.01^{a}	0.15±0.02^{b}	<0.001
IL-10RA	0.06±0.01^{a}	0.05±0.01^{a}	0.04±0.01^{a}	0.06±0.01^{a}	0.04±0.01^{a}	0.06±0.03^{a}	0.19±0.05^{b}	<0.001
IL-10RB	0.81±0.08^{a}	0.83±0.06^{a}	0.86±0.06^{a}	0.95±0.08^{a}	0.97±0.08^{a}	0.97±0.05^{a}	1.42±0.10^{b}	<0.001
TNF-α	0.14±0.02	0.13±0.01	0.11±0.01	0.13±0.02	0.13±0.02	0.13±0.02	0.11±0.01	0.892
TRADD	0.43±0.06	0.36±0.05	0.42±0.05	0.32±0.03	0.46±0.04	0.32±0.05	0.5±0.03	0.064
SIRT1	0.75±0.06	0.74±0.06	0.73±0.05	0.77±0.06	0.83±0.07	0.79±0.06	0.84±0.06	0.807
SIRT2	1.39±0.13	1.42±0.13	1.24±0.09	1.55±0.08	1.56±0.16	1.48±0.07	1.46±0.09	0.474
SIRT3	0.18±0.02^{a}	0.22±0.03^{ab}	0.19±0.02^{a}	0.21±0.03^{ab}	0.17±0.02^{a}	0.22±0.02^{ab}	0.28±0.03^{b}	0.041
SIRT4	0.14±0.02	0.13±0.03	0.12±0.01	0.14±0.02	0.18±0.03	0.13±0.02	0.16±0.02	0.393
SIRT5	1.99±0.23	2.19±0.2	2.22±0.22	2.91±0.24	2.27±0.25	2.01±0.17	2.26±0.26	0.127
PGC1α	0.42±0.10	0.45±0.16	0.54±0.12	0.79±0.26	0.33±0.12	0.32±0.03	0.30±0.08	0.176
CPT1A	7.98±1.88	6.34±1.03	7.36±0.25	9.27±1.19	6.72±0.85	7.04±0.62	6.65±0.88	0.574
CS	48.1±10.94	40.18±5.59	47.53±2.93	50.32±3.31	45.57±3.06	40.22±2.68	43.96±3.61	0.812
ND2	403.5±76.35	301.13±31.81	363.02±70.5	437.27±42.21	285.8±16.09	314.7±52.11	414.0±71.68	0.400
NDUFAF2	2.29±0.29	2.27±0.32	2.05±0.14	2.52±0.18	2.34±0.13	2.14±0.11	2.38±0.23	0.768
COXI	824.0±112.6	642.83±95.42	704.02±73.29	776.15±50.83	862.9±45.64	553.3±37.06	744.6±61.82	0.073
SCO1	0.36±0.07^{a}	0.38±0.07^{ab}	0.38±0.04^{ab}	0.40±0.04^{ab}	0.40±0.04^{ab}	0.30±0.03^{a}	0.60±0.08^{b}	0.031
UCP2	0.85±0.14^{ab}	0.60±0.12^{a}	0.35±0.04^{a}	0.48±0.06^{a}	0.72±0.07^{ab}	0.75±0.10^{ab}	1.24±0.33^{b}	0.006
UCP3	21.11±3.10	14.78±2.02	14.62±2.43	23.65±4.84	20.87±1.48	21.99±2.63	24.95±4.00	0.165
LXRα	1.34±0.12^{a}	0.83±0.06^{b}	0.95±0.08^{bc}	0.90±0.06^{bc}	1.21±0.05^{ac}	0.99±0.06^{bc}	1.29±0.07^{a}	<0.001
PPARα	2.71±0.29	2.35±0.16	2.27±0.29	2.43±0.32	3.24±0.37	2.73±0.10	2.75±0.26	0.214
PPARγ	1.71±0.19	1.35±0.29	0.97±0.08	1.52±0.40	1.34±0.12	1.60±0.21	1.45±0.20	0.319

Annex 2 - Salmon

Supplemental Table 1. Formulation of AS experimental diets.

Ingredient	S0	S10	S20	S30
Fish Meal NA LT 70	420.10	368.00	344.00	291.00
Soya cake 48 Hi-Pro Solvent Extr.	0.00	100.00	200.00	299.50
Corn gluten 60	77.00	77.00	33.00	23.00
Wheat gluten	0.00	0.00	0.00	0.00
Sunflower cake	125.00	104.70	95.80	70.60
Horsebeans	160.00	135.60	105.30	85.30
Fish oil std 18	154.00	158.00	164.00	170.00
Rapeseed oil	40.00	40.00	40.00	40.00
Additives - Amino acids	5.70	6.40	7.30	12.10
Additives - Vitamins and Minerals	31.90	31.90	31.90	31.90
Total	**1000.00**	**1000.00**	**1000.00**	**1000.00**
Protein - crude (%)	44.06	44.18	43.83	43.59
Fat - crude (%)	25.97	25.96	25.96	26.02
Ash (%)	7.28	7.47	7.75	7.42
Energy - gross (MJ/kg)	23.65	23.78	23.70	23.75

All values are represented as g/kg.

Supplemental Table 2. RT-qPCR primers used for validation of the salmon experiment.

Tissue	Name	Abbreviation	Forward Primer	Reverse Primer
Liver	Trypsin	TRY1a	ATGTTCTGTGCTGGATACCT	GGATGTTGTAGAGTTGTGGG
Liver	Diphosphomevalonate decarboxylase	DDC	CCGCTATAACCGTCACTACAG	AGACCCTTTAGAAACTGTCCT
Liver	2-oxoglutarate dehydrogenase E1 component	OXOD	CCCAACACCCTTAATCCTACTC	ATTTCCCTCCATTGCTCAACAG
Liver	Bile salt-stimulated lipase	BSSL	CAATCGCTAACCTCCCTCTG	CAACAGTCTTCTTAATGGTCTCCT
Liver	Biotinidase	BIO	TATGTTTACCCGTCGTTGCT	CTCTCACACTTACACTCACAC
Intestine	Receptor-interacting serine/threonine-protein kinase 3	RIST	TACGAGAAACACAAACAAGGGA	TGCTGAACGGATGGATACTC
Intestine	Growth factor receptor-binding protein 2	GFRBP	GACTCTACAGTACCCTAAACCCA	GTTCAACATCTCCTCTGCCT
Intestine	Transferrin receptor (p90, CD71)	TRANSF	ATCCGTCTCATTCCGTTTCAC	CGACTTAGGCAACATCTGGG
Intestine	Interleukin 18	IL-18	CATAAGGATGTGGATGAGAACTG	AGAGCATATACAGAGGACGG
Intestine	Aquaporin-8	AQUA8	GATGACAGTACAGCCTACCA	TCCCATACCTTATCAGCCAG
Intestine	Transcobalamin-2	TRCOBAL2	CTCTCACGTCAGCAAGAAACTC	GTAGAACACTCCTGCACCTG
Intestine	Fatty acid-binding protein 2, intestinal	FABP2	CGACAGTATCTAATCTCAACGCA	TTTACCCTTCAACACATCTCCA

Primers were designed on AS sequences available from the sequence library used to design the array. All primers had an annealing T of 60°C.

Annex 3 - Rainbow trout

Supplemental Table 1. Formulation and composition of diets differing in protein and/or methionine levels fed to rainbow trout for 12 weeks. Diet MP1 serves as a control diet (Trial 1).

Ingredient (% diet)	MP1	MP0	LP1	LP0
Protein blend	44.5	44.5	27.7	27.7
Basal AA mix	*9.6*	*10.0*	*6.0*	*6.2*
Starch	13.5	13.5	26.0	26.0
Fish oil	15.0	15.0	15.3	15.3
Cellulose	7.9	7.9	15.7	15.7
Other (vit, min, binder)	9.0	9.0	9.0	9.0
Methionne	0.38	0.07	0.24	0.04
Cysteine	0.08	0.00	0.05	0.00
Analysed composition (% DM)				
Crude protein (CP)	38	37.9	24.0	24.1
Met (% CP)	2.2	1.4	2.3	1.5
Cys (% CP)	1.1	1	1.3	1.1
Met (% diet DM)	0.8	0.5	0.5	0.4
Cys (% diet DM)	0.4	0.4	0.3	0.3

Supplemental Table 2. Formulation and composition of diets differing in basal composition (V vs M) to which a mineral premix was added (V1 and M1) or not (V0 and M0). Diets were fed to rainbow trout for 12 weeks (Trial 2).

Ingredients (g/kg diet)	**M**	**V**
Norwegian herring meal, (CP 70; Sopropêche, France)	625.7	-
Corn Gluten meal (CP 60; Inzo, France)	-	180.0
Wheat Gluten (CP 70; Roquette, France)	-	200.0
Soybean meal (CP 48; Inzo, France)	-	50.0
Soy protein concentrate (Estrilvo ; CP 70; Sopropêche, France)	-	170.0
White lupin meal (Terrena, France)	-	50.0
Extruded peas (Aquatex, Sotexpro, France)	-	30.0
Rapeseed meal (Primor 00; Sud Ouest Alimants, France)	-	40.0
Whole wheat	245.6	31.8
Soy lecithin (Louis François, France)	-	20.0
L-Lysine (Eurolysine)	-	13.4
L-methionine (Evonik, Germany)	-	3.0
CaHPO4.2H20 (18%P; 22% Ca)	-	21.7
Attractant Mix§	-	15.0
Trace mineral premix¶	0 or 10	0 or 10
Vitamin premix INRA	10	10.0
Yttrium oxide (Sigma-Aldrich, USA)	0.1	0.1
Fish oil (southern hemisphere, Sopropêche, France)	118.6	-
Rapeseed Oil (Daudruy, France)	-	66.0
Linseed Oil (Daudruy, France)	-	66.0
Palm Oil (Daudruy, France)	-	33.0
Analytical composition		
Dry matter (DM), g/kg	948	949
Crude protein, g/kg DM	494	500
Crude lipid, g/kg DM	221	227
Crude ash, g/kg DM	82	40
Energy, kJ/g DM	23.8	25.1

§Attractant premix: glucosamine, 5g; taurine, 3g; betaine, 3g; glycine, 2g and alanine, 2g.
¶ Trace mineral premix (g/kg premix): FeSO4.7H2O (21% Fe; 11.5% S), 25 g; CuSO4.5H2O (25.45% Cu; 12.8% S), 3 g; MnSO4.H2O (33% Mn; 19% S), 3 g; ZnSO4.H2O (36% Zn; 18% S), 4 g; Na2SeO3 (46% Se; 27% Na), 0.03 g and α-cellulose, 964.93 g.

Supplemental Table 3. Gene name and primer sequences used for PCR analysis in brain of RT challenged to eat diets deficient in protein and/or methionine (Trial 1).

Gene	Full gene name	Primer sequence (5′ → 3′)	Annealing Temp (°C)
ASNS	Asparagine synthetase	F: CTGCACACGGTCTGGAGCTG R: GATCTCGTCTGGGATCAGGTT	62°C
ATF4	Activating transcription factor 4	F: AGCTATGACCATGATGAG R: CAGCCATGAGAGAGGAAG	60°C
CCK	Cholecystokinine N (asparagine) Cholecystokinine T (leucine)	F: TACCATATACGGCAGAAG R: CGTGAAGAGATGAGTCTA F: AGACATACTCACTCCTCTCC R: CTGGCTCTGCTGTTCACT	60°C 60°C
EF1α	Elongation factor	F:TCCTCTTGGTCGTTTCGCTG R: ACCCGAGGGACATCCTGTG	60°C
NPY	Neuropeptide Y	F: CTCGTCTGGACCTTTATATGC R: GTTCATCATATCTGGACTGTG	60°C
SLC7A1 (CAT)	Cationic amino acid transporter	F: ATCGCCACTACAAGCGAAGA	62°C
SSTR1B	Somatostatin receptor type 1 subtype B	R: CTGCCATGGCGTAGATAACG F: TGGTCATCTATGTCATCCTCAA R: CCAAGAACGGAACACTCAAC	60°C
SSTR2	Somatostatin receptor type 2	F: TGGAGAGGTGTTTGAGAATG R: CAAGGAACTCGGACTATGAC	60°C

Supplemental Table 4. Gene name and primer sequences used for PCR analysis in intestine and liver of RT in order to monitor the dietary regulations of iron balance.

Gene name	Accession no. (GenBank or INRA-SIGENAE)	Primer sequence (5′ → 3′)	Annealing temp. (°C)
EF1α	AF498320.1*	F: TCCTCTTGGTCGTTTCGCTG R: ACCCGAGGGACATCCTGTG	59
HAMP	BX088223.s.om.10	F: GGAGGAGGTTGGAAGCATTG R: GATGGTTTTAGTGCAGGCAGG	59
HO1	CA387878.s.om.10	F: ACTCTTCCGCAGTACAAGCT R: CTGTGTGTTGCAGCAGGAAT	59
FPN1	CA351776.s.om.10	F: GTCCTCTTACTGGGCGCTAT R: GCCAGGTTAGCGATGTTAGC	59
Nramp-β	AF048761.1*	F: CACCTCCCCTCCGGCTT R: CCTGGGTCAAGATAGGCGAT	60
Nramp-γ	EF495162.1*	F: GCCATCCTCAACAGTGTCT R: TTAGCTCCAGACTGTAGATCA	57

F, forward primer; R, reverse primer; EF1α, elongation factor 1α; HAMP, Hepcidin anti-microbial peptide; HO1, heme oxygenase 1; FPN1, ferroportin1; Nramp-β, Natural resistance associated macrophage protein beta polypeptide; Nramp-γ, Natural resistance associated macrophage protein gama polypeptide ;

Annex 4 - Publications

1. Antony Jesu Prabhu P, Geurden I, Fontagné-Dicharry S, Veron V, Larroquet L, Mariojouls C, Schrama JW, Kaushik SJ. Responses in trace mineral metabolism in rainbow trout to change in dietary ingredient composition and inclusion of a trace mineral premix (submitted)
2. Bermejo-Nogales A, Calduch-Giner JA, Pérez-Sánchez J. 2015. Unravelling the molecular signatures of oxidative phosphorylation to cope with the nutritionally changing metabolic capabilities of liver and muscle tissues in farmed fish. PLoS One (in press).
3. Calduch-Giner JA, Echasseriau Y, Crespo D, Baron D, Planas JV, Prunet P, Pérez-Sánchez J. 2014. Transcriptional assessment by microarray analysis and large-scale meta-analysis of the metabolic capacity of cardiac and skeletal muscle tissues to cope with reduced nutrient availability in gilthead sea bream (*Sparus aurata* L.). Marine Biotechnology 16:423–43.
4. De Santis C., Bartie K, Olsen RE, Taggart JB, Tocher DR. Nutrigenomic profiling of liver and distal intestine in response to a soybean meal-induced nutritional stress in Atlantic Salmon (*Salmo salar*) . Comp. Biochem. Physiol. D (submitted).
5. Geurden *et al.* How does the trout brain sense an essential amino acid (methionine) deficiency (in preparation).
6. Pérez-Sánchez *et al.* Molecular signatures of liver and muscle tissues in sea bream with nutritional deficiencies (in preparation).
7. Pérez-Sánchez J, Borrel M, Bermejo-Nogales A, Benedito-Palos L, Saera-Vila A, Calduch-Giner JA, Ballester-Lozano GF. 2013. Dietary oils mediate cortisol kinetics and the hepatic expression profile of stress responsive genes in juveniles of gilthead sea bream (*Sparus aurata*) exposed to crowding stress. Comparative Biochemistry and Physiology 8D: 123-130.

Deliverable Check list (to be completed by Deliverable leader)

	Check list		Comments
BEFORE	I have checked the due date and have planned completion in due time	☺	*Please inform Management Team of any foreseen delays*
	The title corresponds to the title in the DOW	☺	*If not please inform the Management Team with justification*
	The dissemination level corresponds to that indicated in the DOW	☺	
	The contributors (authors) correspond to those indicated in the DOW	☺	
	The Table of Contents has been validated with the Activity Leader	☺	*Please validate the Table of Content with your Activity Leader before drafting the deliverable*
	I am using the AQUAEXCEL deliverable template (title page, styles etc.)	☺	*Available in "Useful Documents" on the collaborative workspace*
The draft is ready			
AFTER	I have written a good summary at the beginning of the Deliverable	☺	*A 1-2 pages maximum summary is mandatory (not formal but really informative on the content of the Deliverable)*
	The deliverable has been reviewed by all contributors (authors)	☺	*Make sure all contributors have reviewed and approved the final version of the deliverable. You should leave sufficient time for this validation.*
	I have done a spell check and had the English verified	☺	*Ask a colleague with a good level of English to review the language of the text and do a spell-check too.*
	I have sent the final version to the Activity Leader and to the 2nd Reviewer for approval	☺	*Send the final draft to your Activity Leader and the 2nd Reviewer and leave 2 weeks for feedback and final changes before the due date. Once validated by the 2 reviewers, the draft is ready to be sent to the Management Team that will ask for the Coordinator validation and then transfer it to the EC.*